Multi-objective microgrid storage planning problem using plug-in electric vehicles

Vitor Nazário Coelho
Universidade Federal de Minas Gerais

Orientador: Frederico Gadelha Guimarães
Co-Orientador: Marcone Jamilson Freitas Souza

Tese submetida ao
Programa de Pós-Graduação em Engenharia Elétrica
da Universidade Federal de Minas Gerais
como requisito para obtenção do título de Doutor em Engenharia Elétrica

Dedico este trabalho aos meus pais, Papy e Mamy, João e Gessi, pela eterna energia direcionada para motivar meus estudos. Aos meus irmãos, Bruno, Igor, Mateus e Vinicius, dedico esse trabalho para exaltar a grande harmonia e amizade que vivemos dentro de casa. A minha amada, Thays, pelo companheirismo e apoio durante os últimos 10 anos que estivemos juntos, irmãos de amor e paixão.

Obrigado por tudo. Amo vocês!

Multi-objective microgrid storage planning problem using plug-in eletric vehicles

Abstract

Energy storage has been evolving towards a dynamic scenario with bidirectional communication between several autonomous agents. Efficient power dispatching systems have been mainly assisted by the use of Information and Communication Technologies, Distributed Systems and Artificial Intelligence. This thesis describes a Multi-objective Storage Planing Problem considering Plug-in Electric Vehicle (PEV) as storage units. The problem involves several PEVs and a Microgrid (MG) community, composed of small houses, residential areas, and different Renewable Energy Resources. The energy storage planning is formulated as a Mixed-Integer Linear Programming (MILP) problem, considering PEVs' users requirements, minimizing three different objectives and analyzing three different criteria. Two novel cost-to-variability indicators, based on Sharpe Ratio, are introduced for measuring energy storage schedules volatility. By adding these additional criteria, energy storage planning is optimized seeking to minimize the following: total MG costs; PEVs batteries usage; maximum peak load; difference between extreme scenarios and two Sharpe Ratio indices.

Since prediction involves inherent uncertainty, the use of probabilistic forecasting is proposed. Probabilistic forecasts of wind and solar power production, energy consumption and prices are used in order to perform smart energy storage, checking storage plan robustness. A novel Hybrid Forecasting Model (HFM) with automatic parameter optimization, done by metaheuristic procedures, is proposed for handling the different MG forecasting problems, generating probabilistic quantiles. Finding optimal values for the HFM fuzzy rules and weights is a highly combinatorial task. Thus, parameter optimization of the model is tackled by a bio-inspired optimizer, namely GES, which combines two heuristic approaches, namely the GRASP and the Evolution Strategies metaheuristics. The proposed forecasting model is applied to forecasts different mini/microgrid

time series. In particular, its results are highlighted for load forecasting in residential and commercial areas, which are typical microgrid scenarios. Due to the quick training phase done by the proposed metaheuristic calibration algorithm, the proposed model is suggested to be embedded into Smart Meters (SM) and other future SG devices.

Storage planning is scheduled for different time horizons, according to information provided by lower and upper bounds extracted from those probabilistic forecasts. In order to find sets of non-dominated solutions, a matheuristic black box solves several weighted-sum MILP subproblems. Candidate non-dominated solutions are searched from feasible solutions obtained during the searching process over the branches of a Branch-and-Bound tree. Pareto fronts are discussed and analyzed for different energy storage scenarios. The sets of non-dominated solutions and their conflicts and harmonies indicate that only minimizing system costs goes against the system robustness, increasing the risk of having higher peak loads as well as more fluctuations over the expected costs. It was also noticed the trade-off between grid maximum peak load and the MG total costs.

Declaration

This thesis is result of my own work, except where explicitly referred to other works, and it was not submitted to any other institution.

Vitor Nazário Coelho

Agradecimentos

Obrigado Mãe, pelos ensinamentos ao longo desta vida. Obrigado Pai, pela honestidade, exemplos e valores que você sempre cultivou. Papy, você é um exemplo de um grande homem, honesto, humilde, justo, simples, singelo, sutil e alegre. No meio de um mundo tão conturbado, vocês escolheram ter 5 filhos. Obrigado, Mamy, por ter me ensinado a ler e, Papy, por ter, implicitamente, nos ensinado inglês. Os seus exemplos estarão guardados na minha memória por toda minha vida. Mãe, o seu amor flui em meu corpo e motiva-me a seguir em frente, misturando a minha lucidez com um pouco de insensatez. Lembro-me do momento em que emergi nesse mundo e respirei livremente pela primeira vez, obrigado por me proporcionar tão agraciada boas-vindas ao mundo.

Irmãos, Bruno, Igor, Mateus e Vinicius, obrigado pelo companheirismo e motivação. Igor, mestre da programação e da paciência, valorizo incrivelmente os ensinamentos que você vem me passando ao longo da minha vida. Bruno, obrigado pelas dicas espirituais e equilíbrio, bem como, ter guiado meus caminhos pelo curso de Engenharia de Controle e Automação. Ao Mateus e Vinicius, vos agradeço por acompanharem a minha adolescência e respeitaram as minhas diversas mudanças, vocês são o futuro!

Obrigado Thays, irmã, minha companheira de mais de 10 anos, pelo amor, compreensão, amizade e aventuras. Sem dúvidas, você foi o meu pilar em vários momentos da minha vida. Obrigado Acácio e Sãozinha, minha segunda família, pela confiança, amizade e bons momentos e viagens juntos.

Aos meus grandes tutores Fred e Marcone, além de amigos, os considero exemplos de caráter e ética na pesquisa. Agradeço a motivação e conselhos. Ao Marcone, serei eternamente grato pela paciência durante minha graduação. Você é o exemplo de um grande Pai da ciência, sempre disposto a ajudar a todos, justo, honesto e humilde. Ao Fred, por ser esse amigo que você é, alegre, aberto e sempre disposto a ajudar de

uma forma sutil. Em especial, por ter desbravado o modelo fuzzy descrito nessa tese, acreditado e apoiado as ideias aqui descritas, bem como, outras conversas filosóficas. Agradeço, também, ao Agnaldo, por ter iluminado os caminhos futuros, ensinando-me redes neurais.

Em especial, ao amigos Titherme e Zezera Titini, André Bolinho, e Buenísima Onda, por me acolherem em BH city durante parte do meu doutorado. Serei eternamente grado por ter e estar convivendo com vocês. Aos reis, amigos e mestres Alexandre Barbosa, Rei do Conhecimento, Allyson, Prof. Teacher Babylon, Alex Figueiredo, Bresko Dredslock Rasta, Cristiane Tavares, Crisssssss cunha incrível, Deiberson Gomes, Klitz Bacon King, Carina Alves, Carlos Niquini, Charles Darwin, Diógenes Viegas, JowJow, Dalton César, exemplar Daltits, Fátima, Tîmas, Igor Bispo, Paladino, Jéssica Aquino, Jonas Oliveira, Johny Tavares, Karina Tavares, Kledder Hugo, Derugo, Ludmila Pedrosa, Luiz Knorst, Bileko, Lucas Carvalho, Lucão, Lucas Savoi, Luiz Paulo, L.P. the master, Luiz Gustavo, Guzera, Luciana Brandão, Mihai Damian, Georgia Toffolo, Gabriel Pitchioni, Guilherme Machado, Gustavo Albergaria, Gustavo Oliveira, Higor Martins, Henrique Afonso, Iara Veloso (Iariiitcha), singela, simples e humilde, Marcelo Versiane, O Babilônia, Nina Alkmim, Paola Villaschi, Pedro Borges, Bujabas, Raphael Camargo, Dúnior Dugo, menino sagaz, Raphael Cruz, Roldolfo Bisi, Rodrigo Chaves, Samuel Alves, Sávio Ribas, Ribaço, Sara Jemima, Irmã, Thiago Loureiro, T. Pinheiro 23 :D, Vitor Lagoeiro, Vinicius Lages, Ygor Coelho, Isacó Perez, ao PCA, a todos amigos e irmãos da Automação e Para Facilitar. Sem sombra de dúvidas, vocês foram a luz do meu conhecimento e paz. Obrigado por todos os momentos vívidos.

Em especial, as ideias aqui enviosionadas são partes de diversas conversas filosóficas com meus amigos intrinsecamente ligados a Natureza. Sem dúvidas, passamos vários momentos espirituais juntos que me deram luzes para seguir em frente e acreditar nas nossas ideias. Vocês são parte desse trabalho!

Em especial, eu não poderia deixar de agradecer ao povo Brasileiro, irmãos, irmãs e amigos! Eu tenho um orgulho imenso de ter recebido o apoio de vocês durante a minha vida. Sempre estudei em escola pública e desde o meu ensino médio fui agraciado com a oportunidade de cursar o mestrado em Matemática junto a minha graduação. Recentemente, tive o apoio de vocês pelo programa CsF, no qual, vivi momentos únicos na minha vida, viajando e conhecendo pessoas espetaculares. O meu amor pelo ser humano e pelo bem que as ações em comum podem proporcionar é memorável. Espero um dia retribuir à nossa nação, apesar de eu não me considerar patriota, o investimento que vocês têm feito em mim.

Agradeço ao CNPq, FAPEMIG e CAPES e outras instituições que financiaram projetos dos meus amigos, orientadores e apoiaram minhas pesquisas ao longo da minha vida. Agradeço imensamente o apoio do PPGEE para que eu pudesse participar do WCCI 2014, na China, e REM 2016, nas ilhas Maldivias. Vivenciar um pouco da cultura milenar chinesa mudou e me fez crescer como ser humano e humanista. Agradeço a União Europeia, ao FP7 Marie Curie, que proporcionou-me seguir com as ideias descritas aqui nesta tese, apresentando-as para pesquisadores na Inglaterra e em Israel. Além disso, dando-me a oportunidade de estar com minha amada e visitar terras maravilhosas, como a Islândia e a Rússia. Aproveito a oportunidade e agradeço aos povos os quais tive a oportunidade de conhecer e me apaixonar pelas suas culturas. O mundo é incrível e os seres vivos ainda mais!

Agradeço o apoio dos pesquisadores Nian Liu, James W. Taylor, J. Zico Kolter and Matthew J. Johnson por providenciarem parte dos dados utilizados aqui nesta tese.

Agradeço a harmonia e a perfeição do universo, repleto de incertezas e imperfeições. Ao mundo dos esportes, a maior caixa de brinquedos da vida. A todos seres vivos de Ouro Preto, Minas Gerais, maravilhoso mar de montanhas magnéticas, do Brasil e do Mundo.

A uma das maiores redes de comunicação do mundo, composta por vibrações das plantas, as quais purificam o mundo (a minha alma), alegrando os meus dias com uma dança sem fim.

Preface

This thesis introduces different aspects that I have been envisioning during my PhD and a some months before starting it. Thus, it comprises free optimization knowledge taught to me, mainly by my brother, my family and Marcone, since the beginning of my undergraduate course and during my childhood.

In the beginning, the forecasting model was only a simple matrix of rules, done for the final project of an undergraduate guided by Agnaldo. At that time, my brother Bruno gave me some ideas for using derivatives, integrals and playing with model's inputs. Thus, I realized that it might be simple to extend and adapt this model for other applications. Personally, I really do not think that the proposal is better than any other forecasting model. However, due to the background given by Igor, the code used in this thesis is implemented in the core of the OptFrame. The important part of this is that it is, at least, easy to be used by me! :)

Based on the shoulders and support given by Fred, advisor of this thesis, we extended the initial model, participating in a forecasting competition and presenting the ideas in the 2014 WCCI. The real motivation that moves me to keep improving the forecasting model are manifold. One of them goes back to a day when my girlfriend's grandmother was feeling pain and I started to realize the importance of understanding neural signals (basically, a special type of time series). Emerged in my dreaming world, I thought that with assistance of this model, or other well-known forecasting models, it might be possible to learn brain or magnetic fingerprints. Furthermore, hear the plants and the animals, as I can hear in my inspired moments, is something that I believe that will become more real to the humans beings. Specially, I should mention that my brother Igor has just, with few hours of programming, implemented the evaluation function in CUDA threads. The latter can open a wide range of possible applications. Flexibility and power of the new generation computers and devices can scare those how think life is

only what we see. Each of our senses might be able to catch an specific range of waves, frequency and shapes. It is also expected that some of us can not even catch all sorts of energy that are moving around the universe. However, I believe that we can fell it even without knowing what it is. In this sense, computers might assist our understanding in relation to the electromagnetic spectrum.

Finally, about the multi-objective Microgrid Storage Planning Problem itself, I have been realizing that minimizing only costs is what the industry and capitalism has been doing. Thus, why not consider other objective functions, such as energy quality and environmental impacts? The latter motivates me to keep working with this research and guiding the transformation that the power grid is passing through. This current thesis opens possibilities in my mind, thinking about a beautiful and incredible scenario fulfilled of electric cars, equipped with distinct energy storage systems, moving around the world and spreading good energies to mother Nature. My brother Bruno has just been realizing how the ideas described here could be extended to the new generation of drones and VANTs. Recently, a woman hailed the wind to be stored, here, I wonder if batteries have already evolved so that it may be a solution.

Dream, dream, dream, it is what moves our actions in the present, taking into account experiences from the past. Out of this life, our physical body, everything is infinity.

Contents

List of Figures

List of Tables

List of Algorithms

"Apreciar a vida como ela é, viver o presente e aprofundar-se na imensidão dos sentidos. Imaginar o passado e projetá-lo no futuro. Vislumbrar tudo que existe, a vida de todos os seres, em sua magnífica forma de processar energia. Amar ao próximo e disseminar o bem. "

— Anônimo

Nomenclature

ACF	Autocorrelation function
AI	Artificial Intelligence
AT	Aggregation Trees
BB	Branch-and-Bound
ANN	Artificial Neural Networks
CAES	Compressed Air Energy Storage Systems
CI	Computational Intelligence
DER	Distributed Energy Resources
DG	Distributed Systems
DoD	Depth of Discharge
EA	Evolutionary Algorithms
EC	Evolutionary Computing
ES	Evolution Strategy
ESS	Energy Storage Systems
FIS	Fuzzy Inference Systems
FTS	Fuzzy Times Series
FLRs	Fuzzy Logical Relationships
GES	**G**RASP + **ES**
GRASP	Greedy Randomized Adaptive Search Procedure
GHG	Greenhouse Gas
ICT	Information and Communication Technologies
LTF	Long-Term Forecasting

LG	Large Grid
HFM	Hybrid Forecasting Model
HV	Hypervolume
MAS	Multi-agent systems
MSPP	Microgrid Storage Planning Problem
MOMSPP	Multi-Objective Microgrid Storage Planning Problem
MOOP	Multi-Objective Optimization Problem
MILP	Mixed-integer linear programming
MG	Microgrid
PCA	Partial Autocorrelation Function
PDP	Probability Distribution Function
PEV	Plug-in Electric Vehicles
RER	Renewable Energy Resources
RVNS	Reduced Variable Neighborhood Search
SOC	State of Charge
SVM	Support Vector Machines
SG	Smart Grid
SM	Smart Meters
SMES	Superconducting Magnetic Energy Storage
STF	Short-Term Forecasting
STLF	Short-Term Load Forecasting
SR	Sharpe Ratio
SPSMH	Smart Pool Search Matheuristic
VND	Variable Neighborhood Descent
VNS	Variable Neighborhood Search

Chapter 1

Introduction

"Quando a última árvore tiver caído, quando o último rio tiver secado, quando o último peixe for pescado, vocês vão entender que dinheiro não se come."

— Greenpeace

Electric grids are changing from a centralized single supply model towards a decentralized bidirectional grid of suppliers and consumers. In this new environment, so-called Smart Grid (SG), the reality becomes a more dynamic scenario involving uncertainty in energy production, consumption and distribution. The development of efficient algorithmic techniques that deal with these scenarios is crucial for supporting this important economical and environmental activity.

The choice of Renewable Energy Resources (RER) by the future power grid is being expected, and this growth is also motivated because of the need of reducing environmental impacts, such as emissions of Greenhouse Gas (GHG) (Pereira Jr. et al. 2013, Welsch et al. 2013). This process leads to an increasing use of renewable energy systems (primarily wind and photovoltaic units) (Batista et al. 2013). The potential for RER is growing quickly and it is expected that it will, in principle, exponentially exceed the world's energy demand (Ellabban et al. 2014). SG infrastructure should also provide new opportunities for the grid and its customers for information exchange regarding real-time electricity rates and demand profiles (Kahrobaee et al. 2014). The massive insertion of these RER motivates the development of management systems able to integrate these Distributed Energy Resources (DER) to the SG.

One of the first steps of these changes was highlighted by Rogers, Ramchurn & Jennings (Rogers et al. 2012), emphasizing that the demand side, the consumers, will have to adapt to the available resources, in contrast to the current model in which the supply should always match the demand.

In special, Microgrid (MG) systems aggregate many Distributed Energy Resources (DER) and loads together as an autonomous entity (Zheng & Cai 2010). Additional components added by MG consumers, summed to those that are already installed, are being integrated to the SG, imposing new frontiers for control and management of combinations of several mini/microgrids. For example, Plug-in Electric Vehicles (PEV) (Romo & Micheloud 2015) are being integrated to the power grid (specially with the rise of smart charging parks, namely SmartPark (Mwasilu et al. 2014)), imposing new grid constraints, requirements and goals, settled by its users. This massive integration of DER may cause lack of efficient control and problems in stability, reliability, power quality and security over MG. However, if these components are used in effective ways and tried to be understood, their potential will benefit the grid. This new class of components, such as PEV, has intrinsic elements for enhancing energy quality and reducing costs and environmental impacts.

It is expected that energy storage systems will improve MG performance, leading to higher profits and better use of the RER. Especially in MG systems, its use has important benefits. The use of storage allows both sides, demand and production, to optimize the power exchanged with the main grid, in compliance with the electricity market and forecasts. Renewable energy generators associated with storage units are considered as active distributed generators, one of the fundamental elements of power management in MG systems. Current smart-microgrid scenarios may include different renewable energy resources and different storage units. In this regard, storage increases renewable energy self-consumption and independence from the grid. A wide range of applications exist for Energy Storage Systems (ESS). Tan et al. (2013) refer to the following: power quality enhancement, microgrid isolated operation, active distribution systems and PEVs technologies. ESS ensembled with nondispatchable renewable energy generation units, such as wind and solar energy, can be molded into dispatchable units. Their use may improve dynamic stability, transient stability, voltage support and frequency regulation (Ribeiro et al. 2001). Furthermore, they can also be used for minimizing global cost and environment impact.

In this thesis, a new Microgrid Storage Planning Problem (MSPP) is introduced, aiming to minimize global MG costs while considering grid maximum peak load and

batteries wear and tear. Understanding the contributions of batteries as an objective function does not provide profits only for the PEVs owners, but also for the community linked to that grid. Optimizing its use not only reduces battery replacement costs for the PEVs owners but is also beneficial for the environment, since they are going to be used only when needed. The proposed model tries to obtain energy storage planning scenarios which minimize maximum power flow between the smart-microgrid and the main grid. Furthermore, additional criteria are taken into account, such as: volatility between extreme scenarios and schedule total cost and maximum peak load volatility. The two latter evaluate the schedule compared to its extreme scenarios and also to a wide range of possible scenarios. This is done by measuring the current expected cost compared to other possible costs using Sharpe Ratio (Sharpe 1994). Sharpe ratio is a useful index tool for analysis, used by investors facing alternative choices under uncertainties (Chow & Lai 2015).

A smart storage scheduling model based on a Mixed-Integer Mathematical formulation is designed. Non-dominated solutions are obtained from feasible solutions found over branches of the Branch-and-Bound (BB) (Land & Doig 1960) optimization tree, searched with a smart matheuristic black-box algorithm. Examining suitable schedules to be applied in extreme scenarios is explored by the use of probabilistic forecasts. The multi-objective energy storage management problem considers PEVs as main storage units, located at SmartParks. Power dispatching schedule is planned attending PEV operational requirements, settled by its users, and trying to charge PEVs batteries when energy price is cheaper.

Focusing on reliable forecasts for feeding the proposed multi-objective energy storage optimizer, a new Hybrid Forecasting Model (HFM) is also introduced in this thesis. The use of a class of bio-inspired metaheuristics to optimize the parameters of a model based on fuzzy rules is discussed. Furthermore, we propose an expert input selection that enhances models input during the training phase. By incorporating the power of evolutionary algorithms to optimize the fuzzy rules and calibrate them, an improvement of the forecasting performance of the proposed model is expected. In this context, Evolution Strategies (ES) (Beyer & Schwefel 2002a) stands out as a robust and flexible framework, which has been effectively applied to solve many combinatorial optimization problems (Chen & Chen 2009, Costa & Oliveira 2001). However, up to the moment, with only sparse/none results reported over forecasting problems. Thus, a hybrid heuristic algorithm based on Greedy Randomized Adaptive Search Procedures (GRASP) (Resende & Ribeiro 2010) and ES metaheuristics is proposed. The GRASP is used to generate the

initial population of the ES procedure. Each solution, initialized as a different forecasting model, is generated according to a randomized solution generator in connection with a feature extraction technique.

1.1 Motivation

Coordination and integration of DER in MG systems have been the focus of different researches and remain a complex task (Logenthiran et al. 2008), along with smart energy storage. The latter has been studied over the last decades and also remains a great challenge (Colson & Nehrir 2009). Efficient power dispatching schedules are able to reduce MG stability problems, limitations and uncertainties associated with the use of RER.

In most countries, the migration to this future power grid model, the implementation of the SG, has as its starting point the installation of smart meters (McHenry 2013) and sensors in residences and commercial buildings. Considering measurement systems with high sampling rates over years of data acquisition (Monacchi et al. 2014), one can expect a large amount of detailed data. In the case of electrical network metering, this data can be converted into valuable and useful information, which is crucial for the success of a wide range of SG applications. A task that has been left to the researchers is the one related to the selection and analysis of parts of these datasets. From such data treatment, those huge datasets become available in different ways in order to allow researchers from distinct areas to develop smart solutions for multifunctional and highly complex problems.

In this context, the use of Computational Intelligence (CI) and Artificial Intelligence (AI) techniques embedded into autonomous agents might provide interesting tools for assisting data processing. The different components of the SG will be able to process real-time information and participate in the decision making process. In particular, an efficient mathematical formulation is able to provide optimal solutions for small problems, whereas metaheuristics based models offer flexibility for using the methodology on standard computers or embedded terminal devices.

The development of metaheuristic models for assisting the power dispatching system with probabilistic forecasts is a suitable approach. Dealing with MG forecasting problem in RER real databases, involving short-term forecasts poses a great challenge. Thus, the new proposed forecasting framework tackles this issue by proposing a flexible open-source model able to forecast different MG components. Furthermore, understanding the differ-

ences between energy storage schedules regarding multiple views (objectives functions) is also important for the companies and industries that will assist SG implementation.

1.2 Objectives

The main goal of this thesis is to improve the ability of MG management by designing a multi-objective power energy dispatching system. Additionally, it has the goal of filling the gap of the lack of robustness indicators according a given energy storage planning, which might be a very useful feature for SG implementation and for the integration of mini/microgrid systems. Thus, this thesis addresses a power dispatching problem regarding the minimization of different objective functions.

Specific objectives can be divided into five parts:

- Prepare a review of the main approaches presented in the literature regarding energy storage, highlighting their advantages and disadvantages;
- Understand typical probabilistic forecasts for different MG components, from RER to energy consumption.
- Introduce a forecasting model based on metaheuristic in order to facilitate the achievement of efficient forecasts;
- Design a MG scenario composed of different RER with a SmartPark able to accommodate different PEVs;
- Implement an approach for solving the Multi-Objective MSPP (MOMSPP), providing useful sets of non-dominated solutions.

1.3 Contributions

The major contributions of the current work are:

- A novel multi-objective microgrid storage planning problem:
  - Handle the minimization of three different objective functions and three additional criteria: MG total costs; usage of PEV batteries, maximum grid peak load, volatility behavior in extreme scenarios and two different objective functions based on the Sharpe Ratio index.

  - Consideration of PEVs located at SmartParks as storage units while respecting the operational constraints required by their users;
  - Analysis the upper and lower bounds provided by the probabilistic forecasts in order to test best-case and worst-case energy storage scenarios;

- Development of a Hybrid forecasting model:
  - propose a self-adaptive forecasting model with real-time parameter optimization during the learning process;
  - Introduce a GRASP solution generator that selects inputs based on values from feature extraction techniques;
  - An expert mechanism for refining the model's inputs during the supervised learning phase using Neighborhood Structures (NS), which can add, remove and adapt model's input;

- Design of a new self-adaptive evolution strategy for combinatorial optimization problems:
  - Using and adapting a population-based algorithm for combinatorial optimization problems, combining it with trajectory search techniques, which is able to:
    * Walk through the search space by using discrete moves, following a trajectory provided by random moves in a Reduced Variable Neighborhood Search;
    * Combine neighborhood structures in order to guide the search for new solutions using self-adaptive mutation operators;
  - Introduce a flexible self-adaptive search framework implemented in the core of the open-source optimization framework OptFrame;
  - Apply the proposed methodology for solving different $\mathcal{NP}$-Hard combinatorial optimization problems, including two large scale real case problems (OPMOP and HFVRPMT).

Minor contributions are related to:

- Design a smart pool search matheuristic algorithm for handling the weighted-sum MILP in order to solve the MOMSPP;

- Consider the use of different exogenous variables as input of the forecasting model, adapted or included during the evolutionary process;
- Use of a bio-inspired optimizer based on the concepts of the ES.
- Apply the model over real load databases composed of different typical MG consumers and large grids;
- Quick training strategy for forecasting in online MG scenarios;
- Use of a metaheuristic based framework suitable to be applied for different forecasting horizons, generating h-steps-ahead forecasting.
- Tackles rainfall and wind power generation with probabilistic forecasts;

As s result of this current thesis, the following papers are highlighted:

Published in conferences:

- A General Variable Neighborhood Search heuristic for short term load forecasting in Smart Grids environment (Coelho et al. 2014b). Presented in 2014 Power Systems Conference;
  - This first conference paper introduced the metaheuristic forecasting model, using a trajectory search algorithm for calibrating a matrix of rules.
- A heuristic fuzzy algorithm bio-inspired by Evolution Strategies for energy forecasting problems (Coelho et al. 2014a). Presented in the 2014 IEEE World Congress on Computational Intelligence, held in China;
  - The training algorithm presented in Clemson was improved, as well as a better interpretation of the proposed hybrid forecasting model.
- A hybrid deep learning forecasting model using GPU disaggregated function evaluations applied for Household Electricity Demand Forecasting. Presented in the Applied Energy Symposium and Forum, REM2016: Renewable Energy Integration with Mini/Microgrid.
  - The hybrid forecasting function evaluation was disaggregated and can now handle big data time series.

- A smart pool search matheuristic for solving a multi-objective objective microgrid storage planning problem. Presented in the Applied Energy Symposium and Forum, REM2016: Renewable Energy Integration with Mini/Microgrid.
  - The mathematical programming model was improved, as well as the metaheuristic searching strategy.
- An automatic calibration framework applied on a metaheuristic fuzzy model for the CIF competition. To be presented in the 2016 IEEE World Congress on Computational Intelligence, to be held in Vancouver;
  - A flexible and automatic framework has been extended to be applied for different types of time series. Thus, it can easily compete in the competition without an exhaustive calibration phase. It will participate in the forecasting competition of the 2016 WCCI.
- A hybrid evolutionary probabilistic forecasting model applied for rainfall and wind power forecast. To be presented in the 2016 IEEE Conference on Evolving and Adaptive Intelligent Systems, to be held in Natal;
  - We extended the hybrid forecasting model in order to apply it for generating probabilistic forecasting. Probabilistic rainfall and wind power generation forecasting were tackled.

Published in journals:

- Multi-objective energy storage power dispatching using plug-in vehicles in a smart-microgrid (Coelho, Coelho, Coelho, Cohen, Reis, Silva, Souza, Fleming & Guimaraes 2016). Published in Renewable Energy special issue on integrated Energy systems, with impact factor 3.476 and 3.982 5-year impact factor.
  - The first accepted journal paper related to this thesis. It comprises the use of the hybrid forecasting model, generating probabilistic forecasts and using its information in order to analyze different possibilities for storing energy into the batteries.
- A self-adaptive evolutionary fuzzy model for load forecasting problems on smart grid environment (Coelho, Coelho, Coelho, Reis, Enayatifar, Souza & aes 2016). Published in Applied Energy, with impact factor 5.613 and 6.330 5-year impact factor.

  - The hybrid forecasting model was formally detailed and applied for load consumption forecasting. In special, the flexibility of the model was highlighted.

- Hybrid self-adaptive evolution strategies guided by neighborhood structures for combinatorial optimization problems. Accepted, to appear, in a special issue of Combinatorial Optimization Problems in the Evolutionary Computation journal.

  - In this paper, the hybrid fuzzy model used in this thesis is calibrated using a discrete evolution strategies. Neighborhood structures are used for adapting rules values.

- Low risk targeted customers in direct marketing campaigns using a hybrid multi-objective metaheuristic. In the second round of revisions in a special issue of Variable Neighborhood Search applications in the Computers & Operations Research journal.

  - The idea of using Sharpe Ratio index came from this first application described in this paper.

1.4 Work structure

The topics presented in this thesis are organized as follows:

Chapter 2 – Literature Review: discusses the literature surrounding the emerging SG technology and current state-of-the-art applications related to energy storage. A brief introduction related to point and probabilistic forecasts, as well as a literature review, is also presented.

Chapter 3 – Hybrid self-adaptive fuzzy model: introduces the self-adaptive fuzzy model proposed in this thesis. The model and its expert adaptive mechanisms are detailed and calibrated using load historical time series from real MG residences.

Chapter 4 – Hybrid self-adaptive evolution strategies: introduces an Evolution Strategy (ES) based algorithm, designed to self-adapt its mutation operators, guiding the search into the solution space using a Self-Adaptive Reduced Variable Neighborhood Search procedure.

Chapter 5 – Multi-objective power dispatching problem: describes the proposed multi-objective power dispatching problem with six objective functions. The mathematical formulation and the objective functions are detailed. The optimization

algorithm designed for optimizing the linear combination of the objective functions is also described.

Chapter 6 – Computational Experiments: introduces the MG scenario used as cases of study. Different sets of non-dominated solutions are described and the behavior of the solutions is described and analyzed.

Chapter 7 – Conclusions and future works: draws the final considerations and possible extensions of this thesis.

Chapter 2

Literature Review

"Nunca devemos perder o fascínio pela beleza do mundo natural."
— Marcelo Gleiser

2.1 Smart grid

Smart Grid is considered as the future of a power grid able to manage production, transmission and electricity distribution. The task involves the use of Information and Communication Technologies (ICT), Distributed Generation (DG) and AI. Due to the need of consistently adapting and integrating new tools to the current grid, SG has become a major challenge for developed and developing nations in both research and utilization aspects (Tugcu et al. 2012). Investing on SG infrastructure is a key enabler for public goods, such as decarbonisation and energy security (Hall & Foxon 2014). SG are expected to play an important role in the resolution of many issues of current power grid systems (Fadaeenejad et al. 2014). The latter will be composed of a mesh of networked MG collaborating to deliver electricity to consumers and, occasionally, assisting stand-alone systems (Zhao et al. 2015), specially in developing countries (Pereira et al. 2012, Díaz & Masó 2013, Pao & Fu 2013, Pereira Jr. et al. 2013, Alemán-Nava et al. 2014, Yuan et al. 2014, Lin et al. 2013, Welsch et al. 2013, Acharjee 2013, Mahmood et al. 2014).

The term Smart Grid has been used to represent the entire electrical system including generation, transmission and distribution (Ekanayake et al. 2012). Regarding the distribution system, several efforts target the increase of manageability and efficiency by dividing the smart distribution grid into sub-systems. Figure 2.1 presents a

future envisioned SG system, adapted from the European Commission report on SG (Commission 2006).

Figure 2.1: Adaptation from the Future Network Vision of the European Commission report on SG

Different sub-systems will compose the future SG, as can be imagined through Figure 2.1. These sub-systems are called "Smart-Microgrids", "Mini/Microgrid", or just "Microgrids", and consist of energy consumers and producers at a small scale, which are able to manage themselves, being self-sustainable or in a stand-alone state. The environment depicted involves different components idealized for the future power grids, such as: Hydro power stations (medium and small); Low emission power plants; Solar power plant; Wave energy generation (a brief view of these last five RER can be seen in (Ellabban et al. 2014)); Offshore wind farms (Ederer 2015); Residential photovoltaic generation (Dávi et al. 2016); Energy storage systems (Ribeiro et al. 2001); PEVs (García-Villalobos et al. 2014); Distribution and management: Transformers, links, underground systems and power transmission, control and communication center and satellites. Small wind turbine on buildings rooftops (Tabrizi et al. 2015) and Smart Parks (Venayagamoorthy & Chakravarty 2014) could be also envisioned for this future system.

Literature works have demonstrated the technical and economical feasibility of greener

generation technologies based on wind, solar, hydrogen and hydro power. Integrating these technologies has become a priority in MG (Olivares et al. 2014a), not only because of insertion of these Renewable Energy Resources (RER) but also because extra elements have been required (Farhangi 2010): sensor and metering network; network nodes with computation capabilities; switches or actuators that allow the grid setup to be changed and the capability of plug-in or plug-out new devices. Future MG may equip customers with distributed energy generation and storage systems that can change their overall demand behavior, promoting the development of several smart-microgrids. These tools will provide users with the ability of taking profit of their generated energy as an important economic factor (Xenias et al. 2015) or even aiding them to turn into stand-alone systems and self-sustainable users. Providing autonomous assistance in order to assist complex decision making tasks will be required by an increasing number of MG users.

Coordination and control of these new emerging grid components remains a great challenge (Rogers et al. 2012). Advanced networking, as well as ICT, have been assisting the integration of the conventional power grid in smarter ways (Nguyen & Flueck 2012), inspiring the use of distributed Multi-Agent Systems (MAS). Autonomous control of SG systems allows placing additional DGs without reengineering the whole system, and using it in the peer-to-peer model eliminates the requirement of a complex central controller and associated telecommunication facilities (Lidula & Rajapakse 2011).

Brown (2008) emphasized bidirectional communication between devices as the most important characteristic for integrating new DER into the energy systems. From this communication process and standards (for example IEC61850, as can be seen in Figure 2.2, or ZigBee based protocols (Batista et al. 2013)), a process of decision making is taken by different SG components. In this sense, MAS, using agent peer-to-peer interaction instead of client-server, will face an open field of applications in the next years. The migration to this paradigm and its implementation in the SG has as its starting point the installation of Smart Meters (SM), which improve access to electricity consumption information, and sensors in residences or commercial buildings. SM are a key enabler for communication between SG devices.

2.2 Energy Storage

MG systems require smarter operations to well-coordinate the emerging decentralized sources of energy. Optimization methods justify the cost of investing in a MG system by enabling economic and reliable utilization of resources (Fathima & Palanisamy 2015). Olivares et al. (2014a) observed that the microgrid optimal energy management prob-

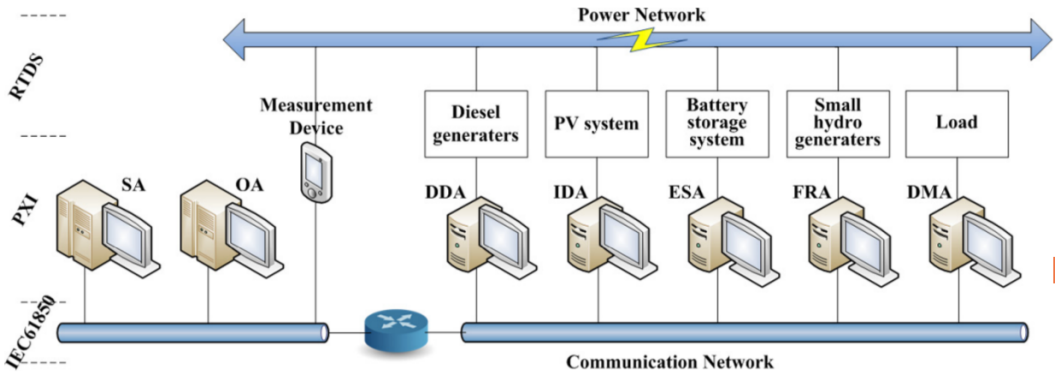

Figure 2.2: Real-time PXI-RTDS MAS simulation platform for a PV-small hydro hybrid microgrid.

lem falls, generally, into the category of mixed integer nonlinear programming problems, because, in general, objective functions may include higher polynomial terms and operational constraints. Levron et al. (2013) presented a methodology for solving the optimal power flow in MG. The model solves small systems containing up to two renewable generators and two storage devices. The proposed approach grows in complexity exponentially, since each storage device contributes extra dimensions to the solution space. Recently, a mathematical formulation proposed by Macedo et al. (2014) extended the approach of Levron et al. (2013). Their formulation uses a convex equivalent model which obtains an approximate optimal solution for the same microgrid system. Rigo-Mariani et al. (2014) researched the power dispatching problem seeking to minimize system global energy costs. A smart-microgrid DC system with flywheel energy storage was analyzed. By considering forecasts for a MG residence and solar PV production, an off-line power dispatching was performed in the search for storage planning schedules. Mohammadi et al. (2014) considered uncertainties over the forecasting of consumption and renewable energy generation. A stochastic operation management of one day ahead was performed using a Heuristic Algorithm. At the initial state 2000 storage planning scenarios were generated, using a Probability Distribution Function (PDF) to represent the uncertainty of the forecasts. Those scenarios were generated and later reduced to 20 and sorted in ascending order of probability of occurrence.

Some approaches in the literature incorporated the reduction of GHG emissions as part of a Multi-Objective Optimization Problem (MOOP) (Colson et al. 2009, Alvarez et al. 2009, Kanchev et al. 2010). Other applications spotlighted on finding the energy and power capacities of the storage system that minimize the operating costs of the MG, as can be verified in Fossati et al. (2015).

Different ESS have been adapted to be used over MG, some examples are: Battery Energy Storage System (Levron et al. 2013), Compressed Air Energy Storage (CAES) systems (Manchester et al. 2015), Flywheels (Rigo-Mariani et al. 2014), Thermal Energy Storage (Comodi et al. 2015), Pumped-storage hydroelectricity (Zakeri & Syri 2015), Superconducting Magnetic Energy Storage (SMES) (Tinador 2008). On the other hand, the use of energy storage in connection with SmartParks is becoming a crucial demand as the number of PEVs, such as electric cars and plug-in hybrids, in the market is increasing (Venayagamoorthy & Chakravarty 2014). Smart Grid application being developed are still analyzing the benefits of this growth (Kempton & Tomić 2005). Power dispatching systems are incorporating vehicle-to-grid (V2G) power transactions over their schedule. Bidirectional power flow between PEVs and the grid will become essential (Venayagamoorthy & Chakravarty 2014, Saber & Venayagamoorthy 2010). As emphasized by Romo & Micheloud (2015), penetration of PEVs will increase significantly in the next 20 years. As a conclusion, smart parking lots with large fleets of electric cars can provide a flexible storage reserve for a MG system, reducing energy production needs.

Most of the works in the literature dealt with the concept of parameters uncertainties of ESS management. In Papadopoulos et al. (2012), results from a deterministic storage planning model showed that voltage violations would be quite high without the consideration of errors in the forecasts. From a probabilistic model with uncertainties, it was concluded that the integration of micro-generation in each MG household might reduce such violations. Previous works in ESS have focused on obtaining deterministic storage scenarios. This task was mainly done by the introduction of uncertainty over forecasts and identifying the most likely scenarios (Comodi et al. 2015, Rigo-Mariani et al. 2014, Mohammadi et al. 2014). In this thesis, uncertainties are considered through the use of probabilistic forecasts, analyzing scenarios provided by their upper and lower bounds.

2.3 Forecasting in MG scenarios

"The future lies under uncertainties", recently published in Science by Spiegelhalter (2014), emphasized the importance of forecasting over decision making problems. Scientific problems are requiring smart tools for handling with complex situations, and the need of quantifying uncertainty of future events has been investigated for several real-world applications.

Lee & Tong (2011) underscore the importance of energy consumption forecasting in the context of economic development of a country due to the large and rapid changes

in the industry, which have strongly affected energy consumption. Taylor & McSharry (2007) emphasized that electricity demand forecasting is of great importance for the management of power systems. Nowadays, it is a consensus that electrical load forecasting assisted by AI tools plays a vital role for the effective success of the SG (Raza & Khosravi 2015).

Long-Term Forecasting (LTF) is, usually, required for capacity planning and maintenance scheduling. LTF has been performed for decades and remains a challenge, as can be verified in Javed et al. (2012), where a twenty-year load forecast background is studied. However, classical approaches to deal with long term load forecasting are often limited to the use of load and weather information occurring with monthly or annual frequency. The modern approaches take advantage of the advanced metering infrastructure presented in the SG and the hourly information to create more accurate and conservative forecasts (Hong et al. 2014). For instance, the Energy Information Administration of the United States has forecasted that global energy consumption will increase by 49% from 2007 to 2035 (Administration. 2015). Furthermore, the need for Short-Term Forecasting (STF) for control and scheduling of power systems is increasing, a task that is also required by transmission companies when a self-dispatching market is in operation. Commonly, in Short-Term Load Forecasting (STLF) studies, one is interested in predictions for the next 1-24 hours ahead, sampling data every half hour or one-hour (Javed et al. 2012). Nowadays it is also possible to find research reporting shorter time periods, such as Gangui et al. (2012), who studied wind power energy forecasting with 15 minutes of forecasting horizon. Real-time forecasts will not be useful only for wind or solar forecasts, as it is already a need when considering Microgrids (MG) control and efficient management (Pascual et al. 2015).

In terms of STLF, MG should be taken into account, since they are more difficult to be monitored and predicted than large power grids due to their higher randomness and lower autocorrelation factors (Liu et al. 2014). MG had become a basic and fundamental infrastructure in the SG environment and have been receiving attention in recent literature works. For instance, Sun et al. (2013) used a backpropagation neural network to perform forecasts over a MG environment, however, the accuracy of their results had been compromised due to large load variations in the small office building that they analyzed. A problem that does not happen in Large-Grid and Medium-Grid environments, as can be verified in Taylor & McSharry (Taylor & McSharry 2007), where STLF was performed over a huge European data set from 10 different countries. Forecasts and, in particular, probabilistic forecasts will assist decision making in MG, guiding

and assisting suitable and profitable energy storage. Forecasts of load and prices are also being considered for auction-based market, where the length of a market period has been modeled as an interval between 15 min and one hour, which is included in the category of STLF (Stadler et al. 2016). Hernández et al. (2014) focus on Artificial Neural Networks (ANN) approach for STLF in order to provide useful information for MG intelligent elements, in case they can adapt their behavior depending on the future generation and consumption conditions.

Recent works have proposed various AI techniques for tackling forecasting problems in applications where traditional forecasting methods have many limitations to tackle big time series data with high fluctuations (Amjady et al. 2010), such as: ANN (Reis & Alves da Silva 2005), Fuzzy Inference Systems (FIS) (Mastorocostas et al. 1999, Wai et al. 2011) and Fuzzy Times Series (FTS) (Chakrabarty et al. 2013, Enayatifar et al. 2013), Support Vector Machines (SVM) (Selakov et al. 2014) and Hybrid models (Huarng 2001, Lee & Tong 2012)

Most forecasting models require feature extraction in pursuance of selecting good quality inputs (Buzug & Pfister 1992). Different works in the literature have already tried to obtain such features to improve forecasting performance, specially for ANN (Drezga & Rahman 1998). Enayatifar et al. (2013) obtained the Fuzzy Logical Relationships (FLRs) by analyzing the Autocorrelation Function (ACF). Lahouar & Slama (2015) proposed the use of ACF to assist a mechanism for input selection of a random forecasting model. However, feature extraction from the time series is not the only viable solution to selecting possible sets of model's inputs, this problem has been also approached with the use of bagging (Khwaja et al. 2015).

Driven by theoretical and real world applications, extracted from the literature, the purpose of this thesis is to use a class of bio-inspired metaheuristics for calibrating the parameters of a Hybrid Forecasting Model (HFM), which is mainly based on *if-then* fuzzy rules. We incorporated the power of the evolutionary algorithms for optimizing the fuzzy rules and calibrating their parameters, while Neighborhood Structures (NS) are used for searching for a prominent set of lags. The expert input selection done by the NS, along with the evolution process, modify and adjust the model inputs during the training phase.

2.3.1 Probabilistic forecasts

Several works in the literature so far have been focused on deterministic point forecasts, which, usually, indicate the conditional mean of future observations. An increasing need for generating the entire conditional distribution of future observations has been required for the new generation of soft sensors. Thus, point forecasts are being suppressed by a new class of forecasts, called probabilistic forecasts, which are able to provide additional quantitative information on the uncertainty associated to future time series data. As discussed in the beginning of this chapter, the energy sector has been changing quickly and dramatically. With the growing amount of data from the SG associated to energy systems, there is a need for utilities to generate the entire conditional distribution of future observations. In special, given the inherent uncertainties associated with RER, probabilistic forecasts of MG components have been researched in the following areas: load (Hong et al. 2014), electricity prices (Kou et al. 2015) (Weron 2014), wind (Zhang et al. 2014) and photovoltaic power (Bessa et al. 2015, Zamo et al. 2014, Monache & Alessandrini 2014).

Compared to currently widely used deterministic forecasts, probabilistic forecasts are able to supplement point forecasts with probability information about their likely errors. This kind of forecasts can be used in order to effectively quantify the uncertainty in time series data. Another advantage of using a probabilistic forecasting model is that they are able to quantify non-Gaussian uncertainties in wind and solar power forecasts. As analyzed by Zhang et al. (2014), probabilistic forecasts are more appropriate inputs for decision-making in uncertain environments. It is expected that the use of probabilistic forecasts as inputs for energy storage management and power dispatching systems will become more widespread. The probabilistic forecasts provide reliable lower and upper bounds for each predicted time step, and their use for analyzing schedules in extreme scenarios is addressed within this study.

As example, Section 3.5 tackles two different forecasting problems composed of time series with high fluctuations and low ACF values. Both problems are introduced in the following Sections.

Rainfall forecast

Water is the most abundant natural resource on the planet. Nearly ubiquitous way, it is in the daily lives of seven billion people inhabiting the planet. However, it have been experienced severe changes regarding its supply (Lutzenberger 1980). Currently the

management of water resources is undergoing a paradigm shift, which has a strong tradition in controlling the environmental problems assisted by engineering based technical solutions.

Risk management involving tools for predicting extreme scenarios is of great importance due to the limits of current implemented technologies, such as dams and reservoirs. In this sense, the need of novel rainfall forecasting models has been increasing in recent years (Pahl-Wostl et al. 2008). It is noteworthy that this topic can be carried out in a sustainable manner, based on the trade-off between social, environmental and economic interests.

Much of the need to forecast hydrological events is linked to global warming and possible adverse effects to humans. A study presented at the 2007 International Panel on Climate Change pointed a variation in climate that occurs due to increased carbon dioxide concentration, largely irreversible for a thousand years after emissions stop (Solomon et al. 2009). Thus, it is expected that extreme events, with higher fluctuations at its time series, are likely to be more frequent in the future.

In particular, rain is one of the most complex and difficult elements of the hydrological cycle to be understood and modeled. The complexity of atmospheric processes, the effects of the solar rain (the current phenomenon of El Niño), forms huge range of variation over a wide range of scales in space and time (French et al. 1992). French, Krajewski & Cuykendall (French et al. 1992) felt this need of forecasting this complex time series and developed a neural network model for rainfall forecasting based on data from a space-time mathematical rainfall simulation model. Gwangseob & Ana (Gwangseob & Ana 2001) emphasized that rainfall forecasting is one of the biggest challenges of operational hydrology, despite many advances in climate predictions in recent decades. For these reasons, any attempt to predict rainfall has impacts in urban safety, infrastructure and preventing disasters due to flooding and unavailability of water. Besides the economic impact, of course. Furthermore, reliable forecasts can also be used for enhancing energy efficiency in hydroelectric power plants. Nowadays, it has been done using short-term (Monteiro et al. 2013) and long-term forecasts. The latter has been done since the first dams were built, but, it used to be done by hand by the technicians and operators. With the increase of novel storage devices, researchers are also investigating the impact of these forecasts of pumped-hydro storage plants (Muche 2014).

The proposal that forecasts should be expressed in probabilistic terms, rather than deterministic ones, was argued from the common sense and theoretical perspectives for

nearly a century. Even though most of the hydrological forecasting operating systems produce deterministic predictions (Bennett et al. 2014, Nastos et al. 2013), most works in operational hydrology have been devoted to find the best estimation rather than quantifying the predictive uncertainty (Krzysztofowicz 1999).

Wind power forecast

Zhang et al. (2014) emphasized that probabilistic wind power forecasting is an efficient tool for dealing with randomness and intermittence of wind resources. The randomness and intermittency of wind resources is the biggest challenge for the integration of wind energy into the power system. The development of accurate forecasting tools for wind power generation is an efficient way for dealing with such problem. Conventional wind power generation forecasts produce a single future value for each point, depending on a value obtained from past data. However, in any prediction of future values, uncertainty is always involved. Deterministic forecasts define a single value forecast, while a probabilistic forecast defines a set of possible values. For decisions in uncertain environments, the probabilistic prediction is a better choice.

In the present state-of-the-art studies, wind power forecast has been performed by probabilistic methods. The latter, compared with other methods, obtains a greater range of values for a given forecasting horizon, more robustness, for the soft sensors, than those using deterministic measurements.

2.4 Conclusion

This chapter provided a brief overview related to Smart Grid and how a mesh of MG will compose it. Key points for making this new envisioned power system reality were pointed out. A literature review and some state-of-the-art works related to ESS were presented. In special, the motivation for handling microgrid forecasting problems was highlighted.

Chapter 3

Hybrid self-adaptive fuzzy model

"I have seen the future and it is very much like the present, only longer."
— Kehlog Albran, The Profit

This chapter discusses the proposed hybrid self-adaptive fuzzy forecasting model, comparing it to other models found in the literature. The flexibility of the proposed framework allows it to be applied to the different types of datasets, since it is calibrated using a metaheuristic based algorithm.

Some definitions regarding time series and forecasting problems are introduced in Section 3.1. Section 3.2 presents the proposed fuzzy model. Section 3.3 describes the heuristic model used to optimize the hybrid fuzzy model. Section 3.3.1 introduces how to represent the fuzzy rules into matrices, examples are given in Section 3.2.2. Section 3.3.2 describes how to evaluate a given model regarding its accuracy of forecasting a given historical time series, and Section 3.3.3 details the proposed algorithm for calibration of the fuzzy model rules and weights during the training phase. Computational experiments related to the application of the proposed model for load forecasting problems are presented in Section 3.4. Its application and extension for generating probabilistic forecasting quantiles is presented in Section 3.5. Conclusion and extensions for the proposed model are presented in Section 3.6.

3.1 Definitions

The class of forecasting problems sought to be solved by the HFM model described in this thesis may be formulated as follows:

- a set of time series $TS = \{y, z^1, ..., z^e\}$, composed of $e + 1$ different historical time series, including the variable of interest y and, optional, exogenous variables $z^i \quad \forall i \in [1, e]$

- The target time series $y = y_1, ..., y_t$ comprises a set of t observations; The optional set of e exogenous time series is represented by $z^i = \{z_1^i, ...z_t^i, ...z_{t+k_e}^i\}$, $\forall i \in [1, e]$. The index k_e means that the exogenous variables can also have previously forecasted values in its time series.

The goal is to estimate the forecasts of a finite sequence $\{\hat{y}_{t+1}, ..., \hat{y}_{t+k}\}$, with k indicating the number of steps to be predicted, namely forecasting horizon.

These steps ahead to be predicted are precisely following the sample time t, that is, the forecast are the k steps ahead starting from $t + 1$ to $t + k$. The vector of exogenous variables include information prior to time t and might also include predicted future points $t + h$. It is even possible to have $k_e > k$.

Finally, each predictable point p_t can be composed of combinations of lags from the target time series y_t and variables z_t^i.

In this current chapter, we tackle load forecasting, which is a type of time series. Forecasting models are required to estimate time series future evolution in terms of past samples and, occasionally, being assisted by the use of some exogenous variables that affect the future load (Lahouar & Slama 2015). As an example of a time-series, Figure 3.1 depicts an hourly load historical data.

3.2 Fuzzy model

Each input of the model $u_i, i = 1, \ldots, r$, with $u_i = y(t - x)$, $u_i = z(t - x)$ or $u_i = z(t + x)$, represents a choice for the composition of lags that will be used to obtain the forecast, the backshift operators. For simplicity of the didactic description of the model, only lags from the target time series y will be stated in the mathematical description of the fuzzy model. Thus, the model will only use lags provided by the

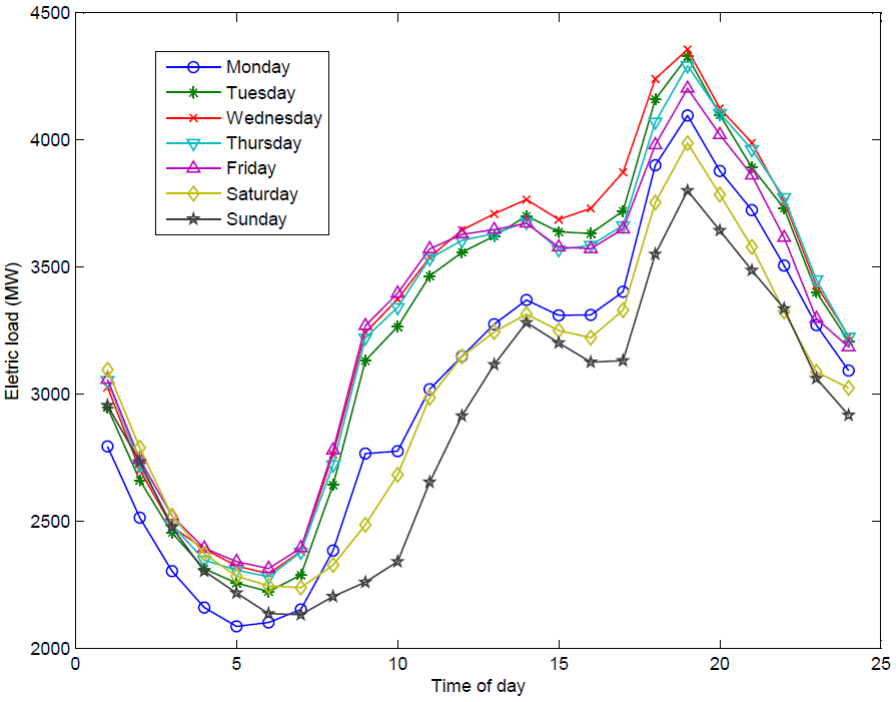

Figure 3.1: Average intraday cycle for each day of the week from EirGrid electricity load dataset from 02/01/2012 to 10/08/2014.

historical time series y, being $u_i = y(t-x) = y_{t-x} = B^x y(t)$, being B the lag operator or backshift for lags x prior to time t.

For instance, two different lags can be selected as inputs, $u_1 = y(t-24)$ and $u_2 = y(t-1)$, for forecasting a specific horizon from the previously described sequence $p(t)$, with $t-24$ and $t-1$, respectively.

Based on these inputs of the model (or even a combination of them) the fuzzy rules are generated and described as follows, for $i = 1, \ldots, r$:

$$\begin{cases} \text{if } \; u_i \tilde{>} a_i \; \text{ then } \; f(t) = v_i \\ \text{if } \; u_i \tilde{<} b_i \; \text{ then } \; f(t) = w_i \end{cases} \tag{3.1}$$

Each input u_i is associated with up to 2 inequalities. The rules are based on fuzzy inequality relations $\tilde{<}$ and $\tilde{>}$, which are described by fuzzy membership functions, and the parameters a_i and b_i. The forecast value suggested by each rule is given by the

parameters v_i and w_i. The main idea behind this model is to divide, in a fuzzy sense, each input into intervals. Whenever the input value is within a given interval, then the consequent of the rule contributes to the forecast value. New rules create new intervals and consequently more complex relationships between the inputs and the forecast output.

Figure 3.2 exemplifies the effects of the rules. The first one, Figure 3.2a, shows the effects of one rule for one input and Figure 3.2b introduces the notion of the fuzzy space when a new rule is added. These examples consider the use of a backshift operator $y_{t-x} = B^x y(t)$, for the input lag x prior to time t. Each fuzzy interval provides a different weight for forecasting a given point y_t, given by the combinations of the weights v_1, v_2, w_1 and w_2.

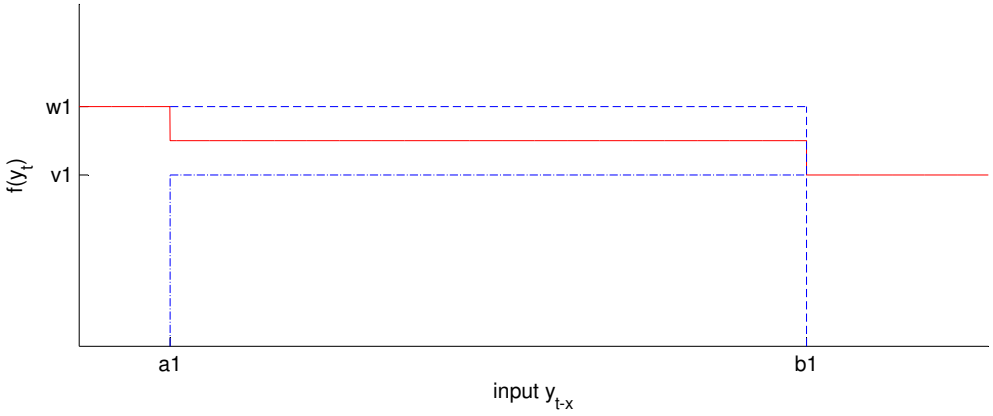

(a) Effects of one rule for one input

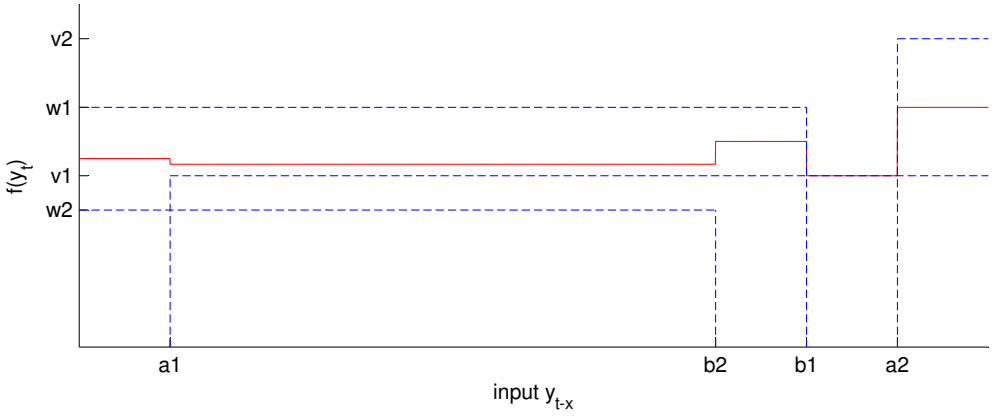

(b) Effects of adding a new rule

Figure 3.2: Rules effects

The fuzzy set $A_i = \{x, \mu_{A_i} > 0 \mid x \in X\}$ represents the set of values that satisfy the inequality $u_i \tilde{>} a_i$. The membership degree to this set is modeled by fuzzy membership functions, such as:

$$\mu_{A_i}(u_i; a_i, \epsilon_i) \begin{cases} 0, & \text{if } u_i \leq a_i - \epsilon_i \\ 1 + \frac{(u_i - a_i)}{\epsilon_i}, & \text{if } a_i - \epsilon_i < u_i \leq a_i \\ 1, & \text{if } u_i > a_i \end{cases} \tag{3.2}$$

with $\epsilon_i \geq 0$.

In a similar way, the fuzzy set $B_i = \{x, \mu_{B_i} > 0 \mid x \in X\}$ represents the set of values that satisfy the inequality $u_i \tilde{<} b_i$. The membership degree to this set is modeled by fuzzy membership functions, such as:

$$\mu_{B_i}(u_i; b_i, \epsilon_i) \begin{cases} 1, & \text{if } u_i \leq b_i \\ 1 + \frac{(b_i - u_i)}{\epsilon_i}, & \text{if } b_i < u_i \leq b_i + \epsilon_i \\ 0, & \text{if } u_i > b_i + \epsilon_i \end{cases} \tag{3.3}$$

with $\epsilon_i \geq 0$.

The weight of each rule in the final forecast value depends on the membership degree of the input u_i to the fuzzy set associated with that rule. The overall output of the proposal model is given by Eq. (3.4).

$$f(t) = \sum_{i=1}^{r} \hat{\mu}_{A_i}(u_i) v_i + \hat{\mu}_{B_i}(u_i) w_i \tag{3.4}$$

where the parameters a_i, b_i, ϵ_i were omitted in the membership functions just to simplify the notation. Additionally:

$$\hat{\mu}_{A_i}(u_i) = \frac{\mu_{A_i}(u_i)}{\sum_{i=1}^{r} \mu_{A_i}(u_i) + \mu_{B_i}(u_i)} \tag{3.5}$$

$$\hat{\mu}_{B_i}(u_i) = \frac{\mu_{B_i}(u_i)}{\sum_{i=1}^{r} \mu_{A_i}(u_i) + \mu_{B_i}(u_i)} \tag{3.6}$$

$\hat{\mu}_{A_i}(u_i)$ and $\hat{\mu}_{B_i}(u_i)$ represent the strength of the rules in the forecast.

Figure 3.3 exemplifies the effects of two pairs of rules with linear or sigmoid fuzzy rules. The same position depicted in Figure 3.2 was kept for this example. As can be noticed, when a non-linear membership function was used the regression became smoother.

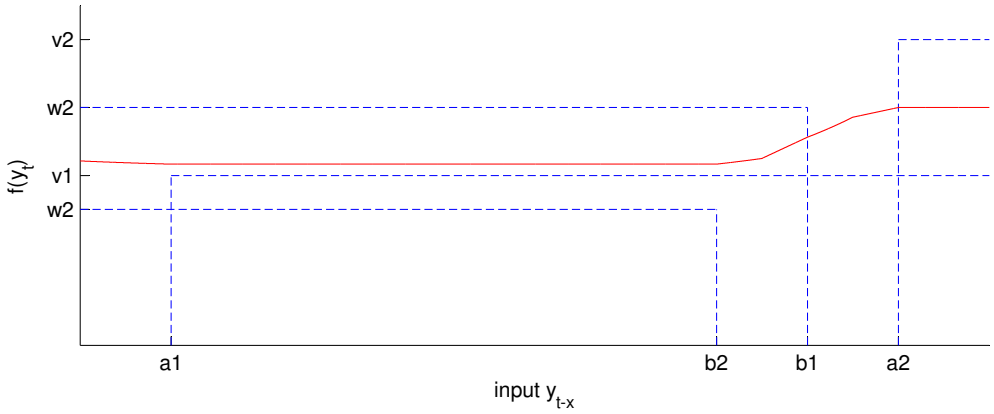

(a) Rules with linear membership function

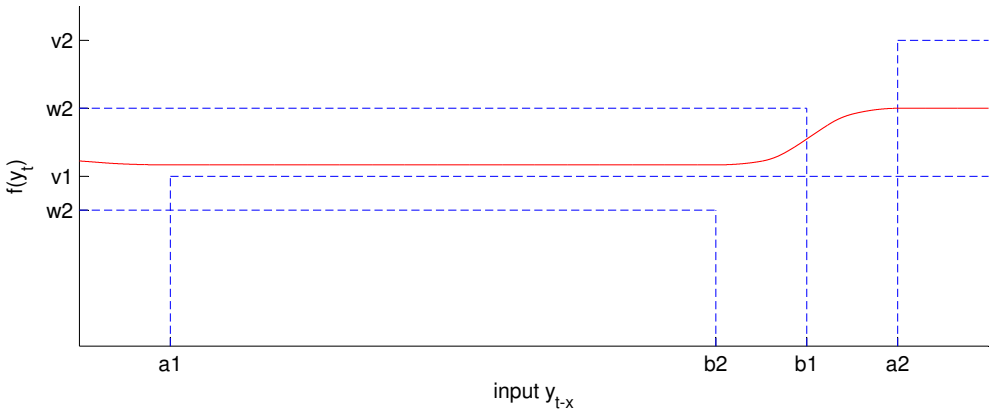

(b) Rules with sigmoid membership function

Figure 3.3: Rules effects with linear and non-linear membership functions

3.2.1 What's the rationale?

The correlation between past lags and current observations has been studied for decades. Several models and analyses try to extract characteristics from the old lags and correlate them in order to achieve efficient forecasting models. For instance, the trivial random-walk (Pearson 1905), proposed more than 100 years ago, tries to face time series that show irregular growth by calculating the first differences. Plotting efficient and well-designed ACF and Partial Autocorrelation Function (PACF) is still being researched. A brief introduction about the current state-of-the-art of the use of ACF can be checked in Hyndman (Hyndman 2014).

Figure 3.4 shows a mini/microgrid residence with maximum load of 273kW, composed by the historical load time series and forecasts provided by an Autoregressive Integrated Moving Average – ARIMA (Hyndman & Khandakar 2008) and Random Walk forecasting models.

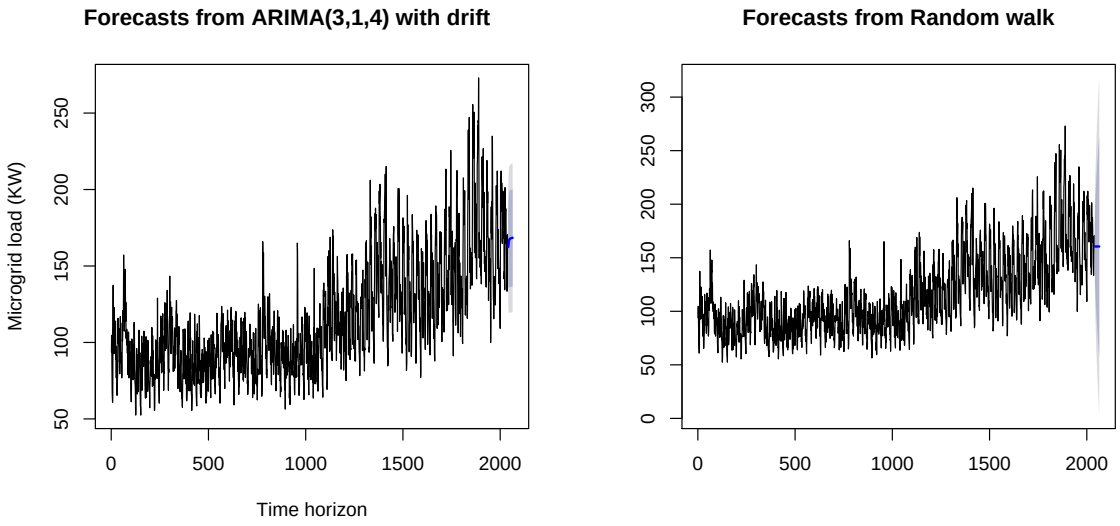

(a) ARIMA

(b) Random-walk-without-drift

Figure 3.4: MG with one-day ahead forecast

The relationship between the lags and the output can provide useful information for designing the inputs that will be used by the forecasting model. The Autocorrelation Function (ACF) describes the tendency for observations made at adjacent time points to be related to one another. However, these correlations can not be easily interpreted and adapted when time series with high fluctuations are dealt, such as loads from MG

(Amjady et al. 2010), wind power generation (Zhang et al. 2013), wind speed (D'Amico et al. 2014), among others. For a better understanding of the ACF and results discussed in this section, the autocorrelation functions of four microgrids (A, B, C and D), described in Section 3.4.2, are summarized in Figure 3.5.

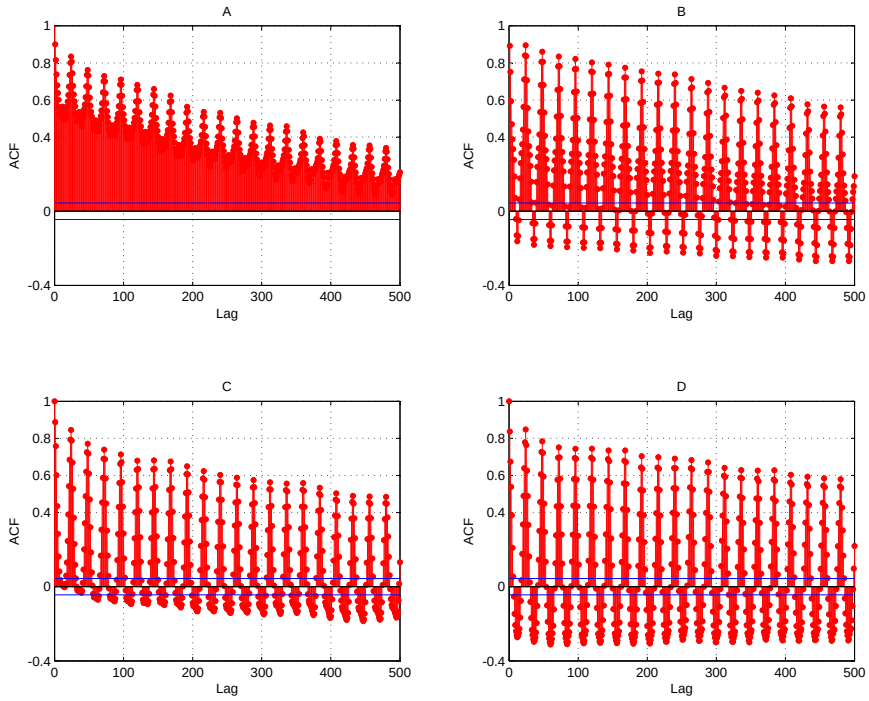

Figure 3.5: Autocorrelation functions for microgrids A, B, C and D with 500 lags

Compared to a typical, presented in Figure 3.6, ACF generated with energy demand from two European countries (obtained from the dataset provided Taylor & McSharry (Taylor & McSharry 2007)), mini/microgrid systems consumption are subject to much more higher fluctuations. As can be verified in Figure 3.5, the four microgrid profiles presented different autocorrelation values, as well as a residential area composed only with positive ACF values. The high fluctuations over the residential area A make its ACF values the lowest. Furthermore, the latter decreases quicker in relation to older lags.

3.2.2 Example

Suppose that after analyzing the most prominent inputs from an ACF, from a given time series (load, temperature, wind speed, etc.), the following inputs were selected to

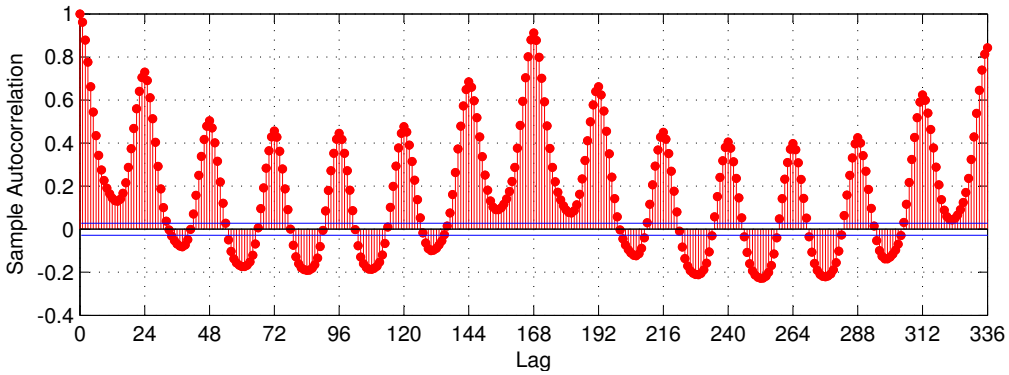

(a) Energy consumption in Spain

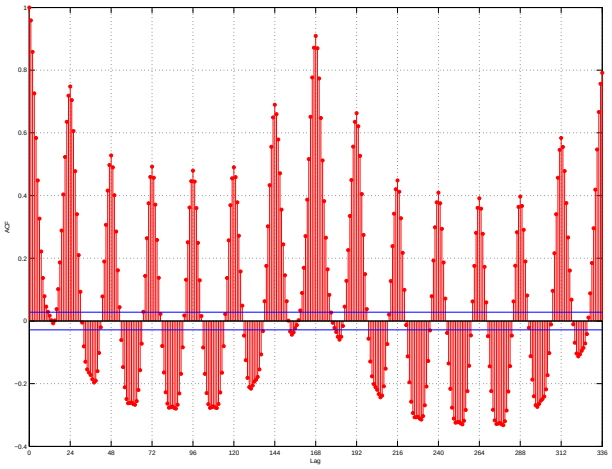

(b) Energy consumption in Italy

Figure 3.6: Autocorrelation functions of hourly samples of energy consumption in 2005

the model.

$$u = \begin{bmatrix} u_1 \\ u_2 \\ u_3 \\ u_4 \end{bmatrix} = \begin{bmatrix} y(t-1) \\ y(t-5) \\ y(t-40) \\ y(t-5) \end{bmatrix}$$

As should be noticed, the model can have repeated inputs, this is not a problem. In the representation chosen here, different columns can represent different weights and rules for the type of input.

Therefore, we have the following rules:

$$\begin{cases} \text{if } u_1 \tilde{>} a_1 \text{ then } f(t) = v_1 \\ \text{if } u_1 \tilde{<} b_1 \text{ then } f(t) = w_1 \end{cases} \tag{3.7}$$

$$\begin{cases} \text{if } u_2 \tilde{>} a_2 \text{ then } f(t) = v_2 \\ \text{if } u_2 \tilde{<} b_2 \text{ then } f(t) = w_2 \end{cases} \tag{3.8}$$

$$\begin{cases} \text{if } u_3 \tilde{>} a_3 \text{ then } f(t) = v_3 \\ \text{if } u_3 \tilde{<} b_3 \text{ then } f(t) = w_3 \end{cases} \tag{3.9}$$

$$\begin{cases} \text{if } u_4 \tilde{>} a_4 \text{ then } f(t) = v_4 \\ \text{if } u_4 \tilde{<} b_4 \text{ then } f(t) = w_4 \end{cases} \tag{3.10}$$

The forecast value is determined by the following equation:

$$\begin{aligned} f(t) \;=\; & \hat{\mu}_{A_1}(u_1)v_1 + \hat{\mu}_{B_1}(u_1)w_1 \\ & + \hat{\mu}_{A_2}(u_2)v_2 + \hat{\mu}_{B_2}(u_2)w_2 \\ & + \hat{\mu}_{A_3}(u_3)v_3 + \hat{\mu}_{B_3}(u_3)w_3 \\ & + \hat{\mu}_{A_4}(u_4)v_4 + \hat{\mu}_{B_4}(u_4)w_4 \end{aligned} \tag{3.11}$$

Rule positions (a_i and b_i) and corresponding weights (v_i and w_i) are calibrated during the optimization process. In this current study, the weights and positions of the rules are calibrated according to an evolutionary metaheuristic algorithm. Additionally, the strategy is able to insert, remove and adapt rules during the training process, as will be detailed in Section 3.3.3.

As a didactic example, Figure 3.7 depicts a defuzzification with 5 and 30 different pairs of fuzzy rules, using Heaviside step or sigmoid functions. Rules and weights were

generated in the same interval $[0, 1]$. Sigmoid membership function was defined with $\epsilon = 0.15$.

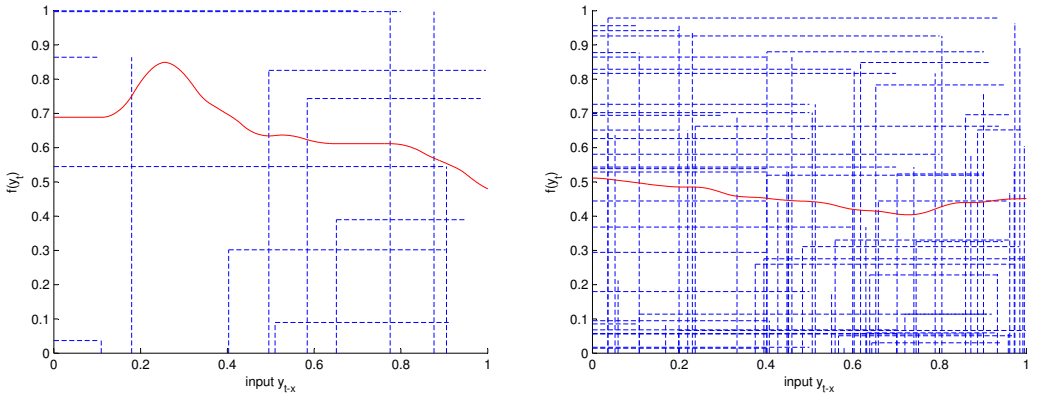

(a) Five rules with sigmoid membership functions

(b) Thirty rules with sigmoid membership functions

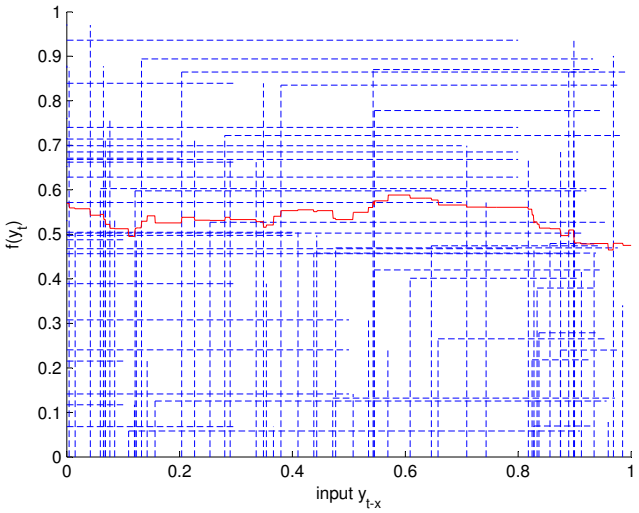

(c) Thirty rules with Heaviside step functions

Figure 3.7: Many rules effects with Heaviside and Sigmoid membership functions

3.3 Model optimizer

3.3.1 Solution representation of the forecasting model

The following generic parameters describe the proposed model into a single matrix:

$$S = \begin{bmatrix} A \\ V \\ B \\ W \\ E \end{bmatrix} = \begin{bmatrix} a_1 & \cdots & a_i & \cdots & a_r \\ v_1 & \cdots & v_i & \cdots & v_r \\ b_1 & \cdots & b_i & \cdots & b_r \\ w_1 & \cdots & w_i & \cdots & w_r \\ \epsilon_1 & \cdots & \epsilon_i & \cdots & \epsilon_r \end{bmatrix} \tag{3.12}$$

with $i = 1, \ldots, r$ being a specific model's rules.

Table 3.1 illustrates a possible solution that uses four inputs over its model. The first two columns are related to values of a didactic load time series and the other two are inputs obtained from an associated temperature time series. Thus, in order to estimate a given forecast at time t, the model receives historical data from two different time series:

- $y(t)$, which returns the values from a historical load time series;
- $z(t)$, exogenous variables which provide values from a temperature time series.

and different lags:

- $y(t-1)$ and $y(t-2)$ are the load consumption one and two hours before the forecasting (hour is used didactically to represent a given discrete interval of data acquisition), respectively.
- $z(t-1)$ and $z(t-24)$ are the temperatures of the residence one and 24 hours before the desired forecasting.

The first and the last inputs were modeled as triangular fuzzy rules, since both columns have $\epsilon > 0$;

Values used in this example stated by Table 3.1 were arbitrarily chosen. Temperature values are used only didactically to emphasize the flexibility of the model in handling inputs from different time series. Brief results related to this mechanism are described in Section 3.4.4.

$$s = \left[\begin{array}{c|cccc} & y(t-1) & y(t-2) & z(t-1) & z(t-24) \\ \hline A & 87 & 95 & 15 & 30 \\ V & 70 & 80 & 80 & 100 \\ B & 100 & 90 & 30 & 50 \\ W & 110 & 50 & 115 & 80 \\ E & 10 & 0 & 0 & 5 \end{array}\right]$$

Table 3.1: Solution example.

3.3.2 Objective function and solution evaluation

A solution s is evaluated by its ability of forecasting values of the training set T, comparing its forecasts with the historical measured ones.

Most models are trained to minimize the Mean Squared Error (MSE), since it is well-known that the mean of the forecast distribution is obtained by minimizing the squared error loss function $S(\hat{y}(t+h), y(t+h)) = (\hat{y}(t+h) - y(t+h))^2$, where $\hat{y}(t+h)$ is the point forecast and $y(t+h)$ is the current observation obtained in the horizon h. However, other loss functions are also able to lead to the forecast mean (Savage 1971). This topic is still being investigated with new diagrams and conditions (Hyndman & Koehler 2006) (Ehm et al. 2015).

Furthermore, the objective function can be any desired quality indicator or even more than one, in the case of multiobjective approaches. Different metrics for defining the accuracy of forecasting models have been discussed in the literature. In the 90's, Makridakis (Makridakis 1993) proposed a discussion of theoretical and practical application of some loss functions.

3.3.3 GES training algorithm

The proposed calibration algorithm, called *GES*, which tackles the rules optimization, consists on the combination of the metaheuristic procedures Greedy Randomized Adaptive Search Procedures – GRASP (Resende & Ribeiro 2010) and Evolution Strategy – ES (Beyer & Schwefel 2002a). The pseudocode is outlined in Algorithm 3.1.

From the GRASP procedure, the construction phase was used to generate initial forecasting models, as can be verified in the BMIR (Build Model Inputs and Rules)

Algorithm 3.1: GES

Input: Function $f(.)$, greedy feature extraction limit α, populations sizes μ and λ
Output: Population Pop

for $i \leftarrow 1$ ***to*** μ **do**
  $S \leftarrow$ BMIR(α) (see Algorithm 3.2)
  $M \leftarrow$ BuildStdVectors (see Eq. (3.13))
  $ind \leftarrow S + M$
  $Pop_i \leftarrow ind$
end
while *stop criterion not satisfied* **do**
  for $i \leftarrow 1$ ***to*** λ **do**
    Generate a random number $x \in [1, \mu]$
    $ind \leftarrow Pop_x$
    $ind \leftarrow$ UpdateParameters
    $ind \leftarrow$ ApplyMutation
    $ind \leftarrow$ MutateAddRemoveLags
    $Pop_i^{offspring} \leftarrow ind$
  end
  $Pop =$ Selection (f, Pop, $Pop^{offspring}$)
end
return Pop

procedure, detailed in Algorithm 3.2. The initial population of the algorithm (lines 1 to 6 of Algorithm 3.1) consists in generating μ individuals. Each individual is generated according to the BMIR procedure and is, usually, of a different forecasting model from each other.

Algorithm 3.2: BMIR

Input: historical data sets TS, number of different historical time series $nTimeSeries$, greedy feature extraction limit α, maximum lag $maxLag$, maximum initial number of rules $maxNRules$

Output: Initial solution s

```
1  for ts ← 1 to nTimeSeries do
2  |  mean_ts, σ_ts ← mean value and standard deviation of the time series TS_ts,
   |  respectively
3  |  RCL_ts ← featureExtractionTechnique(α_t s,maxLag,TS_t s)
4  end
5  r_nRules ← random number [1, maxNRules]
6  for i ← 1 to r_nRules do
7  |  select a random time series ts ∈ nTimeSeries
8  |  select a random input lag ∈ RCL_ts
9  |  S_i ← lag as the current input of its column i
10 |  S_i ← [A_i, V_i, B_i, W_i, E_i]' with random values according to a normal
   |  distribution N(mean_ts, σ_ts)
11 end
12 return s
```

Variable α regulates the size of the RCL, named Restricted Candidate Lags, an abstraction of the Restricted List of Candidates in GRASP. That is, input lags that have low correlation values, according to the desired feature extraction technique, will not be considered to be inserted in the model (line 3 of Algorithm 3.2). We denote variable α_{ts} with subscript ts to emphasize the possibility of limiting different lags according to the historical time series that the rule will use. The feature extraction technique receives the current greedy limit α, the maximum oldest lag able to be used by the model $maxLag$ and the historical data. Section 3.4.3 discusses the influence of the greedy limit using a didactic example with ACF. The historical time series data are stored in the dataset TS. The number of time series is given by the variable $nTimeSeries$. Variable r indicates the number of rules (basically, $2 \times r$) that will be initialized in the model of solution s. From lines 6 to 11 of Algorithm 3.2, each column of the initial solution s receives a random input from the RCL. A trivial solution generator would be a feature extraction technique that returns a vector with all possible lags from 1 to $maxLag$, then, the model would receive a random input lag for its rules. Position and weights of each fuzzy rule

are initialized in accordance with a normal distribution (line 10), centered at $mean_{ts}$ with standard deviation σ_{ts}. A special case for the weights v and w is that they are all initialized with $mean_1$ and σ_1, i. e. $ts = 1$. It was defined like this because, as standard, the first time series is the target that we need to forecast (in this current study, load time series). The other ones are auxiliary time series, such as temperatures, wind speed, presence of people at home, etc. Following this procedure, in average, all the solutions generated by this procedure can forecast the mean values of the target load time series.

Line 4 of Algorithm 3.1 merges the solution s and the standard deviations matrix M. The matrix M is generated in connection with the size of the model of s (as stated by Eq. 3.13).

$$M = \begin{bmatrix} \sigma_A \\ \sigma_V \\ \sigma_B \\ \sigma_W \\ \sigma_E \end{bmatrix} = \begin{bmatrix} \sigma a_1 & \cdots & \sigma a_i & \cdots & \sigma a_r \\ \sigma v_1 & \cdots & \sigma v_i & \cdots & \sigma v_r \\ \sigma b_1 & \cdots & \sigma b_i & \cdots & \sigma b_r \\ \sigma w_1 & \cdots & \sigma w_i & \cdots & \sigma w_r \\ \sigma \epsilon & \cdots & \sigma \epsilon_i & \cdots & \sigma \epsilon_r \end{bmatrix} \tag{3.13}$$

with $i = 1, \ldots, r$ being the standard deviation for adapting each pair of model rules.

From now on, the following nomenclature is used:

- ind^S is the solution s, the fuzzy model, codified in the individual ind;
- ind^M is the matrix with the standard deviation values, used to guide evolution of the population through the generations.

In line 11 of Algorithm 3.1 the mutation procedure is activated by a random individual of the current population. Eq. (3.14) describes how the mutation is done. Each cell of the matrix ind^M is updated with a normal distribution, centered at zero with standard deviation σ_{update},

$$M_{row,col} \leftarrow M_{row,col} + N(0, \sigma_{update}) \tag{3.14}$$

The procedure ApplyMutation (line 12 of the Algorithm 3.1) is illustrated in Eq. (3.15). Each rule, $ind^{S_{ij}}$, its position and weights, are updated according to a normal distribution centered at zero and with standard deviation obtained from the respective cell of the mutation matrix $ind^{M_{ij}}$.

$$ind = \begin{bmatrix} A + N(0, M_{\sigma_A}) \\ V + N(0, M_{\sigma_V}) \\ B + N(0, M_{\sigma_B}) \\ W + N(0, M_{\sigma_W}) \\ E + N(0, M_{\sigma_E}) \end{bmatrix} \tag{3.15}$$

Line 13 of the Algorithm 3.1 has the ability of mutating the model lag using the neighborhood structures described in Section 3.3.4. Each of the three NS have probabilities p^{NS_1}, p^{NS_2}, p^{NS_3} of being applied for mutating model's inputs.

Finally, the selection procedure (line 16 of the Algorithm 3.1) can be any desired selection strategy, as long as the strategy returns a population with μ individuals. The one used here is described as competition $(\mu + \lambda)$, following the same notation of Beyer & Schwefel (Beyer & Schwefel 2002a). In this selection process there is competition between parents and offspring. Thus, the μ best individuals are selected among parents and offspring.

3.3.4 Expert model input adjustment using Neighborhood Structures

Three different NS were designed in order to adapt model's input during the training phase. A brief view of the movements is described below:

Change lag – $\boldsymbol{NS^{CL}(s)}$: This move increases or decreases in one unit the lag of column x $[x \in [1, r]]$ of solution s.

Remove rule – $\boldsymbol{NS^{RR}(s)}$: This move deletes one column from solution s (if the solution has, at least, $r > 1$).

Add rule – $\boldsymbol{NS^{AR}(s)}$: This move consists in adding a new rule with $lag \in [1, maxLag]$ for the solution s, with the same procedure described for Algorithm 3.2.

The role of designing expert input selection mechanisms has been envisioned by different researches, a considerable part of them generates specific subsets of features to be evaluated. Several approaches, such as those based on ANN (Lahouar & Slama 2015), usually, define pairs composed of inputs and outputs, $T^t_{training} = (x^t_{training}, y^t_{training})$, being $y^t_{training}$ the historical measured values from the time series and $x^t_{training}$ a N-dimensional vector of exogenous variables for the t^{th} time instance of a given time series.

The feature sets are analyzed according to different feature selection methods (Koprinska et al. 2015), based on traditional statistical methods or artificial intelligence and machine learning strategies. Using prepocessing analysis, a specific set of inputs is chosen and, then, machine learning algorithms, based on different learning paradigms, are applied over the datasets. However, are these sets of feature the optimal values for those models? Some works in the literature have been claiming a strategy that finds the "best" set of inputs, but, it sounds to be a further discussion to achieve an optimal set of lags for a given forecasting model.

On the other hand, our proposal handles with time series as a sequence instead of defining sets of pairs of exogenous variables and desired outputs. Thus, the inputs required by a given solution s are only accessed when this solution is being evaluated regarding its performance in the training set. This strategy provides the tool of real-time inputs searching. The expert input selection strategy proposed allows the model to be updated in any stage of the learning process, that is done using a metaheuristic procedure.

3.4 Computational experiments with load forecasting problems

This section is divided into five subsections. Section 3.4.1 presents the computational resources, some considerations about the code and model parameters. Section 3.4.2 introduces the real datasets. Section 3.4.3 presents the results related to model inputs selection. Section 3.4.4 presents some results compared with the literature. Finally, Section 3.4.5 presents results of our hybrid fuzzy model, applied in real-time MG load forecasting scenario, compared with well-known forecasting models.

3.4.1 Basic configurations

The GES calibration algorithm was implemented in C++ with assistance from OptFrame (Available at http://sourceforge.net/projects/optframe/) (Coelho et al. 2011a).

In general, frameworks are based on the researchers experience with the implementation of multiple methods for different problems. This optimization framework has been successfully applied in guiding the implementation of neighborhood structures (see Coelho et al. (Coelho, Souza, Coelho, aes, Lust & Cruz 2012)). Souza et al. (Souza et al. 2010) and (Coelho et al. 2015) employed OptFrame to solve an open-pit-mining problem and a large-scale multi-trip vehicle routing problem. It is important to point out that all code used in this research is, from this moment, available as an example on OptFrame core, as an open-source tool under GNU LGPL 3.0.

The tests were carried out on a OPTIPLEX 9010 Intel Core i7-3770, 3.40 x 8 GHZ with 32GB of RAM, with operating system Ubuntu 12.04.3 precise, and compiled by g++ 4.6.3, using the Eclipse Kepler Release.

According to empirical calibration and parameters suggested by the literature (Beyer & Schwefel 2002a), the size of the population, μ, and number of offspring, λ, generated in each generation were fixed: $\mu = 10$ and $\lambda = 60$, respectively. Initial values for the standard deviation matrix M were chosen at random from $[1, 10]$ and σ_{update} was fixed to be 1. The fine tuning of these values is not presented here since the main focus of the batches of experiments is to discuss the load forecasting regarding different set of inputs. The objective function (Section 3.3.2) to be minimized during the fuzzy rules calibration process was chosen to be the Mean Absolute Percentage Error – MAPE quality indicator (Makridakis 1993).

3.4.2 Datasets

Large grids datasets were obtained by extracting parts of the dataset from Taylor & McSharry (Taylor & McSharry 2007). Microgrids datasets were kindly provided by Liu, Tang, Zhang & Liu (Liu et al. 2014). Another real MG residence dataset composed with load and temperature time series (measured in Fahrenheit) was obtained from the Global Energy Forecasting Competition 2014 – GEFCOM2014 (Hong 2014).

Taylor & McSharry (Taylor & McSharry 2007) dataset consists in intraday electricity demand measurements, from 10 European countries for the 30 week period from Sunday, 3 April 2005 to Saturday, 29 October 2005. It is made up with hour (5040 samples), and half-hour (10080 samples) load demand acquisitions.

Liu, Tang, Zhang & Liu (Liu et al. 2014) dataset is composed of four different microgrid users data (composed of users from small residential areas, commercial buildings or factories). Instances A and B are the load of residential areas, C and D are the load of

commercial buildings. The load time series from these four MG were divided into two different sets:

- $\frac{2}{3}$ of the data (1368 samples) is used for training the model;
- $\frac{1}{3}$ of the data (672 samples) is used as blind validation, in a way to evaluate the performance of the model after the GES rules calibration.

Several characteristic indices are extracted separately from the historical time series of loads from these different databases, in the same way as Liu, Tang, Zhang & Liu (Liu et al. 2014). Table 3.2 presents the calculation results of these indices, which are described below:

1. Load variations in several months V (Eq. (3.16)), normalized mean square, which indicates the load variation of the normalized ([0,1]) load power;

$$V = \sum_{i}^{N} (x'_i - u'_i) \tag{3.16}$$

   where $x'_i = \frac{\sum_i^N x'_i}{N}$ and $u'_i = \frac{x'_i}{max(x)}$. N is the total number of samples of the historical time series.

2. load variations between two adjacent days, D_{avg} (Eq. (3.17)) and D_{max} (Eq. (3.18)), which indicate the average and maximum variation between two adjacent days, respectively;

$$D_{avg} = \frac{1}{N_d - 1} \sum_{j=1}^{N_d - 1} \sqrt{\frac{\Delta X_j \Delta X_j^T}{L}} \tag{3.17}$$

$$D_{max} = max \sqrt{\frac{\Delta X_j \Delta X_j^T}{L}}, \forall j = 1, ..., N_d - 1 \tag{3.18}$$

   where X_j is the load curve of each day $j \in N_d$ and $\Delta X_j = X_{j+1} - X_j$.

3. load variations in a day, R (Eq. (3.19)) and R_{min} (Eq. (3.20)), which indicate the daily load rates compared to the average load and minimum values of each day of the historical time series, respectively;

$$R = \frac{1}{N_d} \sum_{j=1}^{N_d} \frac{\bar{x_j}}{x_j^{max}} \tag{3.19}$$

$$R_{min} = \frac{1}{N_d} \sum_{j=1}^{N_d} \frac{x_j^{min}}{x_j^{max}} \tag{3.20}$$

where $\bar{x_j}$, x_j^{min} and x_j^{max} are, respectively, the average, minimum and maximum load for a given day $j \in N_d$.

4. load variations in a hour, M_{avg} (Eq. (3.21)) and M_{max} (Eq. (3.22)), which represents the average and maximum slope, respectively.

$$M_{avg} = \frac{1}{N-1} \sum_{i=1}^{N-1} \left|\left| \frac{x'_{t+1} - x'_t}{t_{i+1} - t_i} \right|\right| \tag{3.21}$$

$$M_{max} = Max \left(\left|\left| \frac{x'_{t+1} - x'_t}{t_{i+1} - t_i} \right|\right| \right); i = 1, ..., N-1 \tag{3.22}$$

As can be verified in Table 3.2, fluctuations over the MG are higher than those in the Large Grid (LG). Average values of the load for each day are calculated and compared to the maximum load of that day (R measure). Large grids presented higher values, since the average is closer to the peak values. Following the same reasoning, the minimum daily load rate (R_{min}) is lower for the microgrids historical load data. The European load consumption presented similar behaviors for the analyzed characteristics. As can be seen in the last four lines of the Table 3.2, daily load variation over the temperature time series of the MC residence is similar to the load grid variation over large grids. On the other hand, difference between two adjacent days is much higher than in large grids and fluctuates like MG systems.

3.4.3 Expert input selection

As an example, we present a solution generator based on the ACF as a feature extraction technique for assisting the choice of the model inputs. Other feature extraction

Table 3.2: Analysis results of load characteristics for the micro and large grids

Objects	V ($\times 10^{-3}$)	Max. load	R (%)	R_{min}(%) (%)	M_{avg} ($\times 10^{-2}$)	M_{max} ($\times 10^{-2}$)	D_{avg} ($\times 10^{-2}$)	D_{max} ($\times 10^{-2}$)
Micro-grid instances (Liu et al. 2014)								
A	18,11	273	75,03	52,50	4,52	24,95	20,46	53,62
B	26,04	463	62,47	34,85	5,58	52,39	24,69	69,94
C	28,73	1853	63,23	30,37	5,44	44,52	36,81	131,76
D	33,45	2215	65,69	31,22	7,32	42,46	28,23	91,22
Average	26,58	1201	66,60	37,23	5,72	41,08	27,55	86,63
European large-grid dataset (Taylor & McSharry 2007)								
Italy	20,85	48970	83,66	62,48	3,04	15,18	14,94	70,77
Norway	9,53	17929	90,64	78,81	1,48	11,70	5,38	21,74
Spain	10,39	34756	88,11	74,58	2,18	11,12	8,11	31,11
Sweden	11,62	21433	89,02	74,62	1,80	11,33	6,91	26,72
Belgium	11,37	12255	87,58	71,56	1,41	14,12	8,73	32,34
Finland	19,12	12016	90,58	77,21	1,05	11,78	6,43	34,40
France	11,16	64761	88,03	71,85	1,33	8,36	7,63	29,95
GB	17,07	50622	84,46	62,09	1,57	9,80	9,24	30,21
Ireland	17,78	4158	82,99	58,85	1,73	10,20	8,78	37,23
Portugal	17,34	7367	83,10	62,29	1,79	10,64	10,43	38,38
Average	14,62	27427	86,82	69,43	1,74	11,42	8,66	35,28
GEFCOM2014 (Hong 2014)								
Load	25,58	315	78,27	57,84	2,64	15,18	13,55	66,90
T1	36,04	102	82,10	65,88	1,97	14,71	16,90	70,01
T2	32,98	103	84,35	70,53	1,67	13,59	15,10	67,33
T3	32,18	98	85,39	71,89	1,70	14,29	14,27	90,85

techniques (Saeys et al. 2007) could be adapted to our greedy randomized solution generation BMIR.

The goal is to compare the models generated using inputs with high ACF value and the ones generated at random (when $\alpha = -1$). Model's input should respect the maximum lag $maxLag$. This first experiment intends to present the influence of ACF values for building an initial fuzzy model. Figure 3.8 indicates the lower MAPE errors generated in "NSOLS" initializations.

These experiments provide an initial insight about how building several initial solutions could enhance the chance of obtaining better initial models, in terms of model's performance measured by a MAPE indicator. This ability is reality in our approach due to the use of the GRASP procedure as the initial step of our training algorithm.

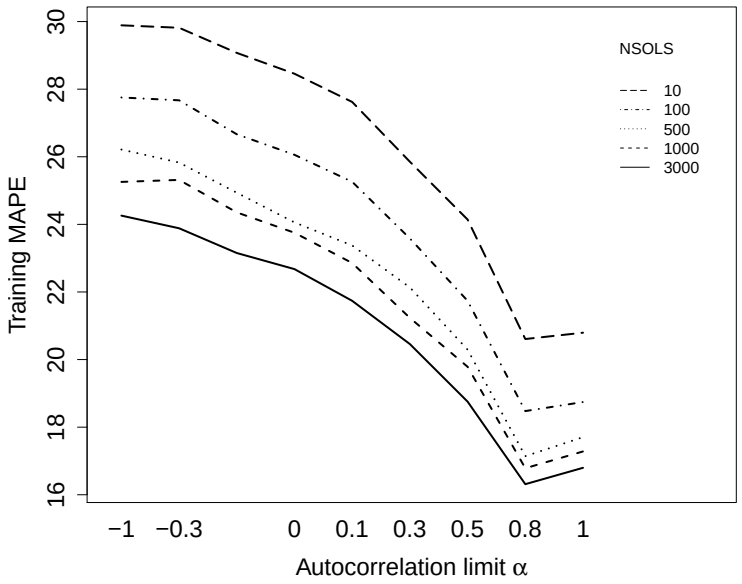

Figure 3.8: Two-way interaction plot of greedy ACF limit α and number of generated solutions

Model inputs are obtained from a given limit α which only consider lags with correlation higher than it, as introduced in Section 3.3.3. It should be noticed that we adapt the procedure for reducing the maximum lag until it reaches the input with maximum lag value. For instance, if the given MG had the maximum ACF value equal to 0.8, the results obtained with $\alpha = 1$ would be the same of those with $\alpha = 0.8$. However, as can be checked in ACF plots depicted in Figure 3.5, the maximum ACF values of each MG

have slightly different peak values.

A second batch of experiments sought to analyze the behavior of different ACF limits α guiding the first initial population of the whole procedure. Additionally, we wanted to check if the expert self-adaptive input selection, using the NS described in Section 3.3.4, might be able to mutate model's lag, add and remove rules (as pointed in line 13 of Algorithm 3.1), during the training phase. The batch of experiments was composed of 4000 executions with learning time equal to two minutes. All the normality, independence and variance assumptions were verified and accomplished. The design of experiment was an effect model with different $\alpha = [-1, -0.3, -0.1, 0.3, 0.5, 0.8, 1]$, maximum number of rules $maxNRules = [10, 100, 500, 1000]$, applied for learning the next step ahead of four different MG load time series (A,B,C,D). An Analysis of variance (ANOVA) test (Shapiro & Wilk 1964) was used for analyzing the differences between group means. The maximum lag ($maxLag$) was set to be 672. On the other hand, since the oldest lag used in the model of Liu, Tang, Zhang & Liu (Liu et al. 2014) was set to be 170 (set of inputs: ($z(t-1)$, $z(t-2)$, $z(t-22)$, $z(t-23)$, $z(t-24)$, $z(t-166)$, $z(t-167)$, $z(t-168)$, $z(t-169)$ and $z(t-170)$)), this same value will be fixed in the benchmark results of Section 3.4.4.

Figure 3.9 depicts an interaction plot considering different α limits and the use of the expert input selection mechanism. Dashed lines show the variances of the model with and without the expert input selection. Best obtained models are depicted with points in shape of triangles. It can be noticed that when the model's input was only determined by the BMIR, it improved the results when α values were around 0.3, indicating that the model responded well for using input lag with low autocorrelation values. On the other hand, when the expert inputs adjustment was being used during the evolutionary process, the use of inputs with high ACF values improved the training performance. The expert input selection strategy reduced the average MAPE errors from 13.9% to 12% for a two minutes training. By analyzing the dashed line it can be seen that the variance of the model was also dramatically reduced by activating the self-adaptive mechanism.

It was felt that the model might be able to reduce the training MAPE even when fed by inputs with low ACF value, if it has enough time for adjusting its parameters. Thus, in Figure 3.10 we present the effects of the training time, TIMEES (seconds), using the proposed self-adaptive inputs selection strategy. Obtained results indicate the ability of the model in adjusting its input lag during long-runs training phases, an useful feature for long-term forecasting.

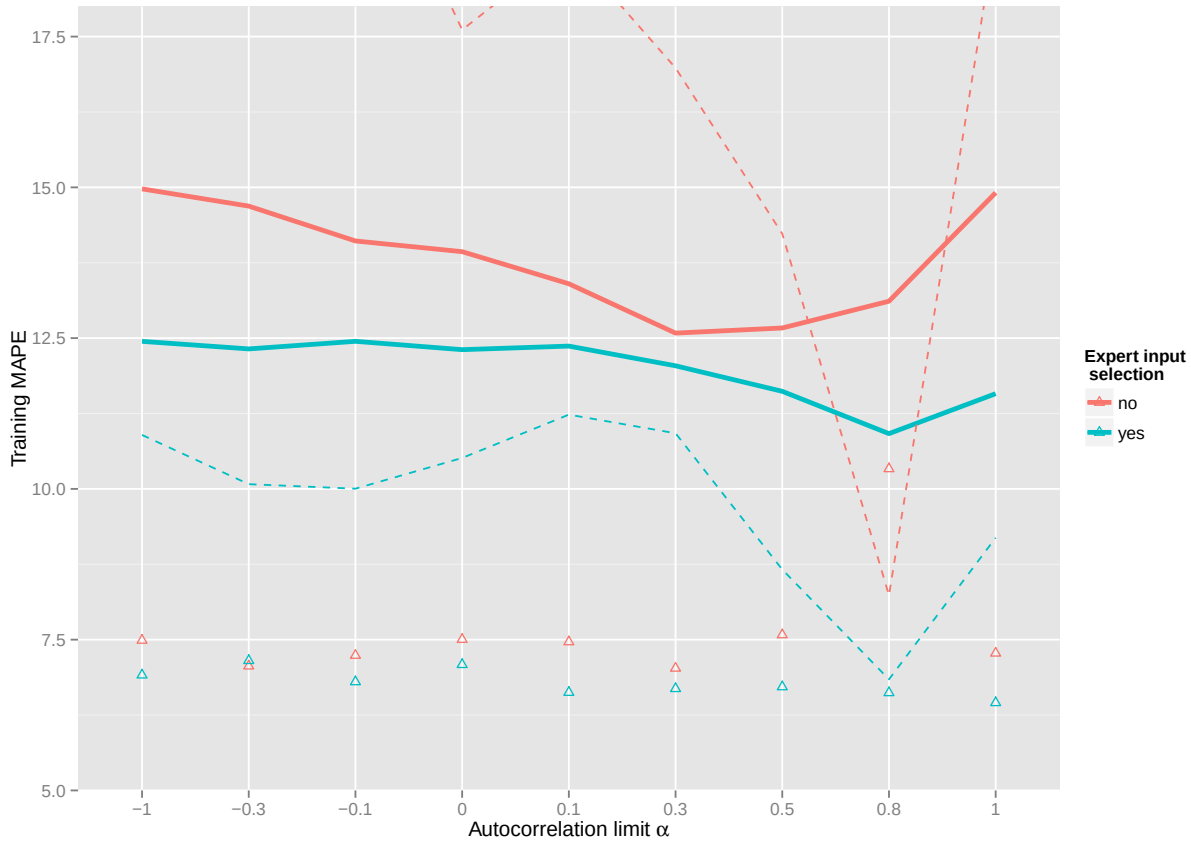

Figure 3.9: Autocorrelation limit α

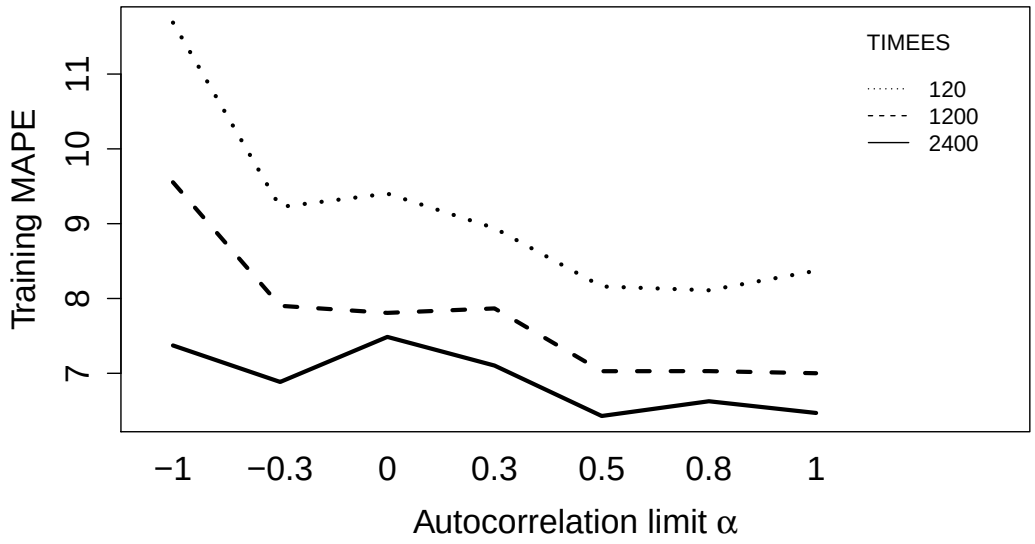

Figure 3.10: Two-way interaction between training time and model performance with different initial input lags

Regarding the number of rules, the model performed better forecasts when initialized with a maximum number of rules equal to $maxNRules = 100$ or $maxNRules = 500$, as can be verified in Figure 3.11. Thus, following some advices from the literature, we will keep the constructive phase generating simpler models with an upper limit of 100 rules. Further studies should analyze if higher number of rules can result in model over-fitting, as already verified for Fuzzy Time Series (FTS) (Enayatifar et al. 2013).

From now on, the constructive method will create initial models which have inputs with autocorrelation values greater than $\alpha = 0.5$ and $maxNRules = 100$ maximum rules.

3.4.4 Benchmark results

The benchmark results are divided into three parts: The first one presents the benchmark over the MG datasets; The second part 3.4.4 shows the performance of the model in a case of study involving the use load time series and temperature measurements, while the last Subsection 3.4.4 indicates the results over the large grids.

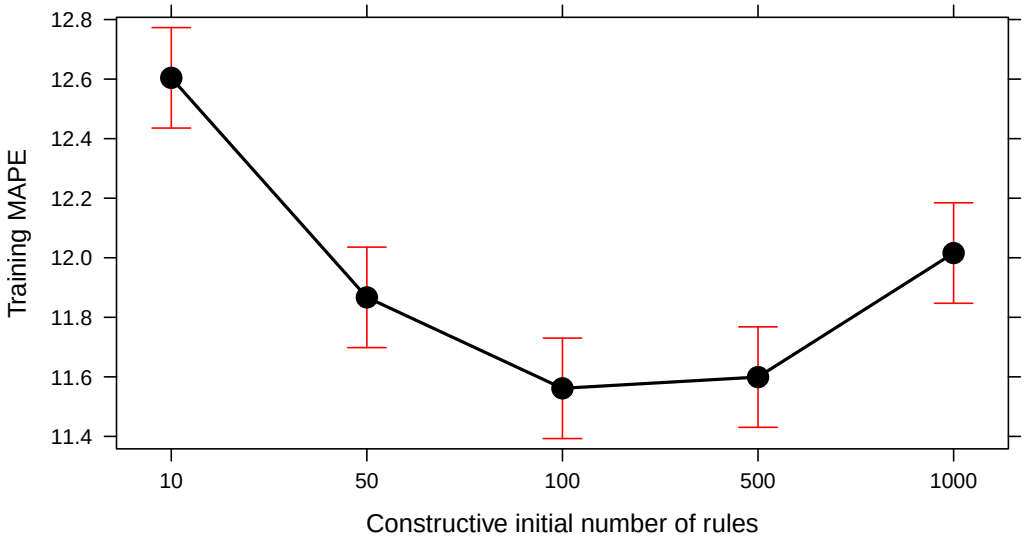

Figure 3.11: Effects of the initial number of rules and model's performance

Results over the MG dataset

The hybrid heuristic fuzzy model is compared with the EMD-EKF-KELM of Liu, Tang, Zhang & Liu (Liu et al. 2014). Their model combines Empirical Mode Decomposition – EMD, Extended Kalman Filter – EKF, Extreme Learning Machine with Kernel – KELM and Particle Swarm Optimization – PSO. The forecasting horizon is one step ahead, $k = 1$. MAPE and Root-Mean-Square Error – RMSE errors are presented for each week of the validation set. A batch of 30 executions was done. Tables 3.3 and 3.4 summarize the results of the new self-adaptive hybrid fuzzy model proposed in this work compared to the EMD-EKF-KELM. The values in bold indicate the best values which are better than the best values of the EMD-EKF-KELM hybrid model, average values are not compared since they only reported the best achieved forecasts.

As can be verified in Tables 3.3 and 3.4, the hybrid fuzzy model was able to obtain good mean results for both MAPE and RMSE quality indicators. Among the batch of 30 executions, at least one of the obtained model had better MAPE than the literature. For the RMSE, in four cases it was not able to achieve the best values reported by the literature.

Apart from the first week of the microgrid C, all other best results presented MAPE

Table 3.3: Hybrid fuzzy model × EMD-EKF-KELM – MAPE (%)

Microgrid	1st week	2nd week	3rd week	4th week
Best results of Liu, Tang, Zhang & Liu (Liu et al. 2014)				
A	8,363	9,003	10,376	7,866
B	10,672	8,369	8,010	7,201
C	13,522	13,788	9,917	7,836
D	6,630	6,888	5,531	**6,224**
Proposed hybrid load forecasting model – HFM				
Average values ± Standard deviations				
A	$9,033 \pm 0,232$	$8,395 \pm 0,133$	$10,224 \pm 0,199$	$8,320 \pm 0,416$
B	$9,145 \pm 0,404$	$9,794 \pm 0,852$	$7,285 \pm 0,188$	$7,625 \pm 0,263$
C	$14,211 \pm 2,923$	$9,536 \pm 1,024$	$9,298 \pm 1,291$	$7,689 \pm 0,765$
D	$5,697 \pm 0,169$	$5,999 \pm 0,123$	$6,117 \pm 0,197$	$7,455 \pm 0,173$
Best forecasts				
A	**8,303**	**7,726**	**9,555**	**7,495**
B	**8,054**	**8,231**	**6,555**	**6,840**
C	**11,448**	**8,090**	**7,661**	**6,374**
D	**5,039**	**5,469**	**5,341**	6,508

Table 3.4: Hybrid fuzzy model × EMD-EKF-KELM – RMSE (MW)

Microgrid	1st week	2nd week	3rd week	4th week
Best results of Liu, Tang, Zhang & Liu (Liu et al. 2014)				
A	16,081	15,164	**18,759**	18,335
B	37,659	**24,937**	23,066	21,079
C	177,674	132,779	122,219	90,831
D	107,715	97,320	**81,147**	**101,686**
HFM				
Average values ± Standard deviations				
A	$16,236 \pm 0,452$	$14,058 \pm 0,274$	$20,299 \pm 0,659$	$17,844 \pm 1,034$
B	$28,192 \pm 5,122$	$29,958 \pm 6,565$	$20,939 \pm 1,989$	$23,145 \pm 2,690$
C	$157,624 \pm 100,669$	$95,777 \pm 23,830$	$123,005 \pm 185,266$	$88,481 \pm 38,705$
D	$88,081 \pm 31,545$	$91,982 \pm 23,939$	$110,707 \pm 46,645$	$124,826 \pm 69,844$
Best forecasts				
A	**15,204**	**13,162**	18,932	**16,456**
B	**24,411**	25,954	**19,059**	**20,548**
C	**144,491**	**88,355**	**104,616**	**76,621**
D	**77,955**	**82,738**	95,751	107,210

error lower than 10,25%. As described in Liu, Tang, Zhang & Liu (Liu et al. 2014), it is known that when the MAPE is more than 10%, the operation cost of microgrids would increase sharply. If the obtained results were applied in real online situations, the archived forecasting errors would not lead to sharp increase of operation cost, indicating that implementing the presented method over microgrid systems could bring benefits. Furthermore, the model was able to give good results with low variability, being the high standard deviation equal to 2,92%.

Another advantage of our approach is that it was competitive using one single set of parameters during the whole learning process. Liu, Tang, Zhang & Liu (Liu et al. 2014) divided the learning process in 48 groups of optimal parameters in workdays and holidays, obtained with an off-line parameter optimization using a PSO based algorithm. Here, we could do the same and trained 48 different models for each of their groups. For simplicity, and as a way of showing our model's flexibility, we use only one single model with a single set of parameters for each MG load time series.

Figure 3.12 shows the forecast of our best execution for the first week of the testing set. Forecasting errors are depicted in black dashed lines in the bottom of the figure, representing the absolute error between each prediction and the real value from the historical time series.

Finally, Figures 3.13a and 3.13b depict forecasts for one day and one week ahead. Figure 3.13a indicates the forecasts for one day, over the first week of the validation set while Figure 3.13b presents the forecasts for the whole first week ahead ($k = 168$). Even for one week ahead, the model was able to predict different slopes and load fluctuations over the analyzed MG.

MG forecasting with temperature measurements

A MG load historical data along with three different historical temperature time series, located in the surroundings of the MG, is considered in this section. As mentioned before, this historical dataset was obtained from the GEFCOM2014. The goal of this batch of experiments is to analyze the fuzzy model's performance towards the inclusion of new information from temperature time series. Figure 3.14 exhibits the load autocorrelation function for this MG, with maximum load of 325 kW, together with the autocorrelation for one of the temperature time series.

A batch of 30 executions with each of the four different combination of exogenous variables as input of the model was performed.

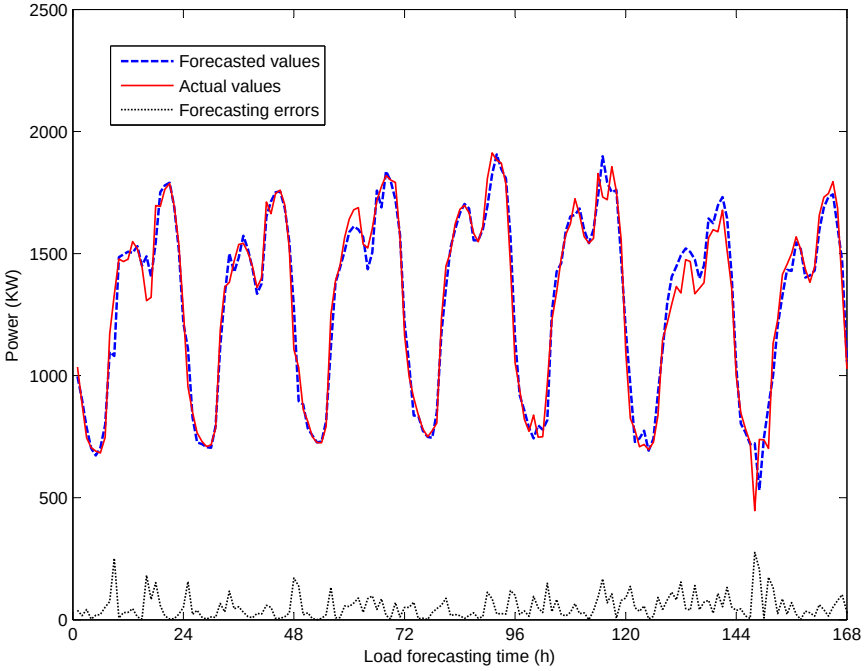

Figure 3.12: Forecasting results of D in 1st week.

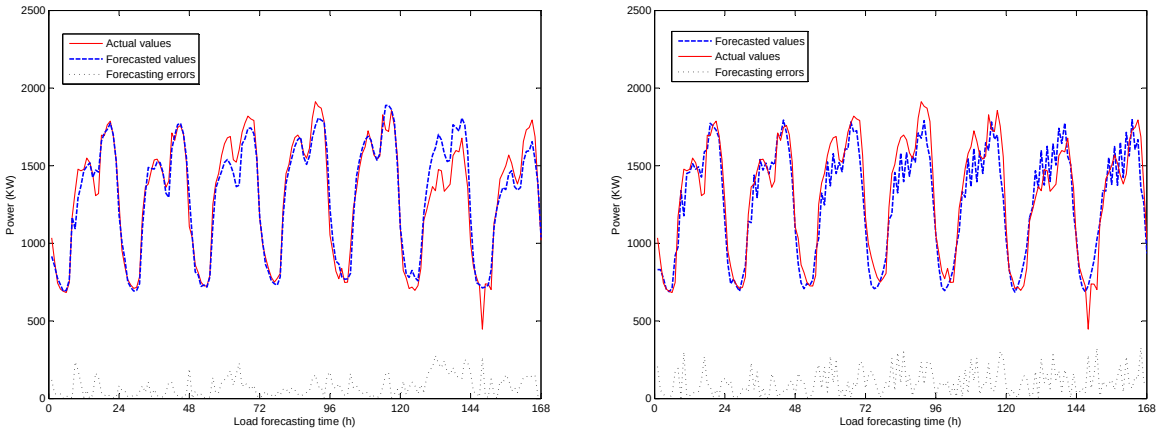

(a) One day ahead.

(b) One week ahead

Figure 3.13: Forecasting results for the 1st week of MG D

- Four different time series as input of the model:

  1. Only load historical data;
  2. load data + one temperature time series;

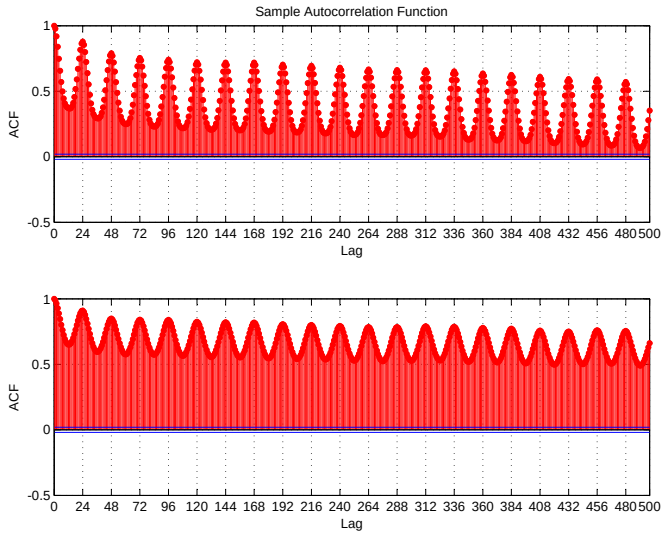

Figure 3.14: Autocorrelation function for load and temperature of a small MG residence

3. load data + two temperature time series;
4. load data + three temperature time series.

The effect of the new temperature time series as input of the model can be seen in Figures 3.15a and 3.15b. Labels "1.Temp", "2.Temp" and "3.Temp" refer to the use of the different historical temperature time series. As can be verified, the proposed fuzzy model is able to handle new information and can take profit from it in terms of optimizing model's precision and performance. Average MAPE and RMSE decrease from 14,02% and 23,24% to 11.55% and 19,78%, respectively, when the three temperature time series were considered as model's input.

Other time series could be included here and improvements could be expected. Tascikaraoglu & Sanandaji (Tascikaraoglu & Sanandaji 2016) recently detected an interesting trend between the data from a target house and the data from its surrounding houses. Following the same reasoning of the experiment conducted in this section, new load time series from the surrounding MG could be included to be handled and enhance model's forecasting performance.

Since the model is mainly based on metaheuristic it can be improved in order to use exogenous variables from different time series in some specific applications. The flexibility of the model and the use of NS makes the model suitable for real world

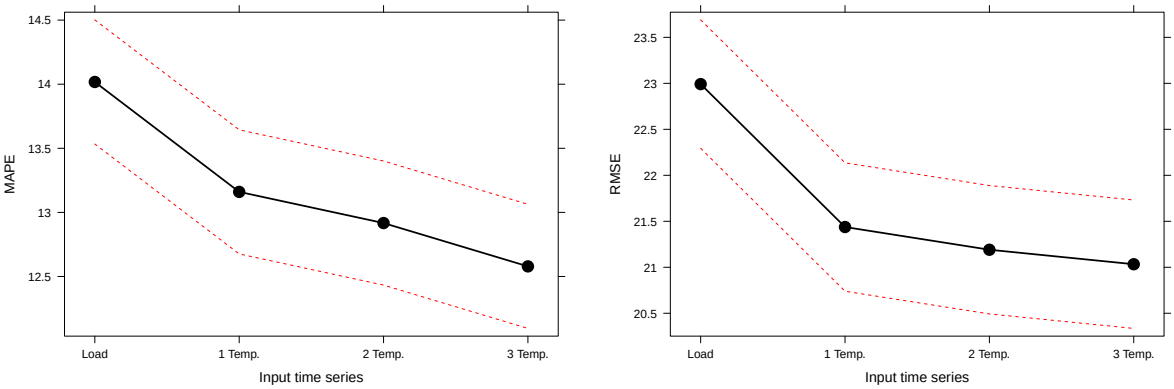

(a) Improvement on testing set MAPE

(b) Improvement on testing set RMSE

Figure 3.15: Additional exogenous variables as input of the fuzzy model

applications, since new structures can be designed in order to change and adapt specific parts of the current model.

Results over the large grid datasets

Using the same set of parameters used for the MG, the model was applied to forecast load from large grids. For the European dataset of Taylor & McSharry (Taylor & McSharry 2007), the first 20 weeks of each series were used to train the algorithm, the remaining ten weeks to evaluate post-sample accuracy of 1-24 hours ahead forecast.

A batch of 30 executions was done for each historical time series, average MAPE values are shown in Table 3.5. ELD_{hourly},ELD being the European Load Dataset, indicates the average MAPE for all the hourly historical time series (Italy, Norway, Spain and Sweden). $ELD_{halfhourly}$ indicates the average MAPE for all the half-hourly historical time series (Belgium, Finland, France, GB, Ireland and Portugal). All standard deviations were lower than 1.0% of MAPE.

Table 3.5: MAPE for the LG historical load time series

Large power grid	MAPE (%)
ELD_{hourly}	3.523 ± 0.972
$ELD_{halfhourly}$	2.983 ± 0.621

The results presented in Table 3.5 indicate that the model was also able to obtain

average MAPE errors from 3.52% to 1.22% over the large-grid datasets. Compared to analyses made by Taylor & McSharry (Taylor & McSharry 2007), the model also showed to be competitive.

3.4.5 Real-time online forecasting

In some applications, off-line learning is performed and, periodically, re-trained if it is detected that the model is increasing its errors. This strategy was explored and detailed in the work of Liu, Tang, Zhang & Liu (Liu et al. 2014), updating their model if the MAPE increased more than a desired limit.

Since our proposal was able to obtain competitive results with two minutes training using low computational resources, we will check the performance of the proposed model considering a real-time training strategy. This strategy is useful to overcome brutal changes in MG loads (Lahouar & Slama 2015).

Furthermore, in future microgrids scenarios, the owner of the microgrid would take profit of the accuracy of the forecasting, since an efficient power dispatch will require precise schedules (Rigo-Mariani et al. 2014). It is expected that it will be a reality not only for microgrid renewable energy generation, but also for MG users, which will do the best to train their models as the new data is available.

The concept of Number of Training Rounds (NTR), Eq. (3.23), generates an important traded-off for forecasting models. NTR defines the number of samples used during the training phase related to a given forecasting horizon k. In the last experiments we used the NTR available from the literature, without checking if the use of less data during the training phase could improve the model's performance. It is an important aspect for understanding the behavior of the model with the size of the training set in a specific training time. The NTR is most frequently associated with the testing set error because it is known that the error of the training set increases when the problem starts to learn big data problems. The Bias and Variance dilemma reinforces that increasing the training set size might provide more variability for the model for predicting information not seen before. On the other hand, the higher the NTR value is, the model requires more computational time to learn the historical load data.

$$NTR = \frac{\#nTrainingSamples}{k} \tag{3.23}$$

Since MG requires quick response from the autonomous forecasting agent (Dimeas & Hatziargyriou 2005), we run our experiment with ten seconds training for different sizes of the training set. Figure 3.16 shows an interactive plot of the NTR for the first week of the testing set of MG-A (red) and MG-C (blue). The points in shapes of triangles and crosses indicate respectively the minimum and maximum MAPE obtained in a batch of 10 executions. There are two types of lines representing each testing set, the dashed line indicates the standard deviation while the thicker line shows the average MAPE.

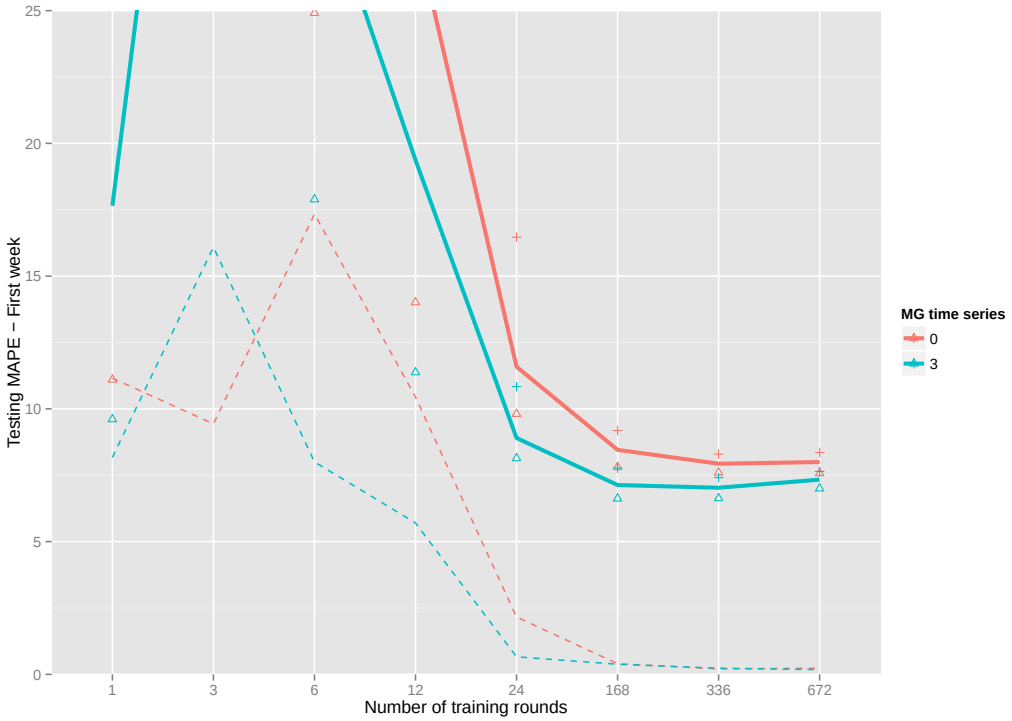

Figure 3.16: Number of training rounds with two minutes training

Finally, we compare our results with the methods ARFIMA (Hyndman & Khandakar 2008), AUTO.ARIMA (Hyndman & Khandakar 2008), Exponential Smoothing State Space model (ETS) (Hyndman et al. 2002), Naive Random Walk and trivial MEANF (historical mean of the training set). The AUTO.ARIMA uses a variation of the Hyndman and Khandakar (Hyndman & Khandakar 2008) algorithm which combines unit root tests, minimization of the AICc and MLE to obtain an ARIMA model. For the automatic ARFIMA, auto-arima combined with a Fractionally-Differenced ARIMA, we consider the parameters calibrated through Haslett-Raftery, so-called ARFIMA-LS, and full MLE, denominated ARFIMA-MLE.

Table 3.6 indicates average MAPE for some well-known forecasting models and the

proposed hybrid load forecasting model, abbreviated as HFM.

Table 3.6: MG results with real-time online forecasting

Microgrid	$k = 1$	$k = 24$	$k = 168$	$k = 672$
	672	336	168	24
First week of the testing set of MG-A				
ETS	9.926	9.705	9.701	9.792
AUTO.ARIMA	10.030	9.982	9.606	10.344
ARFIMA-LS	9.890	9.774	9.768	10.064
ARFIMA-MLE	9.862	9.775	9.822	10.145
RW	9.680	9.680	9.680	9.680
MEANF	22.614	18.597	18.646	18.574
HFM	7.996	7.933	8.456	11.588
First week of the testing set of MG-C				
ETS	13.796	14.032	13.948	15.012
AUTO.ARIMA	14.063	13.465	15.547	15.936
ARFIMA-LS	14.047	14.037	14.829	15.819
ARFIMA-MLE	13.873	14.287	14.861	15.913
RW	13.804	13.804	13.804	13.804
MEANF	34.589	34.844	37.361	32.920
HFM	7.334	7.029	7.131	8.903

As can be verified in Table 3.6, the proposed HFM model was competitive with the automatic ARFIMA-LS, ARFIMA-MLE, AUTO.ARIMA, ETS and, as expected, trivial models naive RW and MEANF, reporting lower average MAPEs.

Since this model is mainly based on a metaheuristic calibration algorithm, it can be useful in real world applications that requires quick training, like the 10 seconds training performed in this last experiment. Furthermore, an intrinsic relationship with expected improvements on the metaheuristics quality will also enhance the performance of our training strategy.

3.5 Probabilistic forecasts

This section aims at the generation of multiple quantiles covering the requested forecasting horizon. Here, the use of the HFM applied in two different forecasting problems, rainfall and wind power forecast, is reported.

As mentioned in Section 2.3.1, rainfall forecast is of paramount importance for various

applications for water resources management. However, the variability of rainfall in space and time makes this prediction very difficult. This is due to the fact that the amount of rainfall as well as its distribution depend on many variables such as speed and wind direction, pressure, and temperature. With the phenomenon of El Niño (Sathicq et al. 2015, Islam & Gan 2015), slight variations will be expected over the course of the next year. Thus, the use of flexible and smarter forecasting models, able to generalize data from our given historical data, will be important for understanding these new unseen informations. On the other hand, the wind power forecast is, currently, a challenging and very useful problem to be dealt by the Energy Industry. An effective management of the forthcoming RER, such as the wind power turbines, can be useful for coordinating and planning energy storage (Mohammadi et al. 2014), as well as enhancing self-generated energy use (Wang et al. 2015).

In particular, historical rainfall dataset from the city of Vitoria, located in the state of Espírito Santo, Brazil is considered. Meanwhile we handle with a real data from a wind farm, provided by the Irish EirGrid institute (Center 2015), for analyzing our proposed probabilistic forecasting framework. The main contribution of this section is to adapt a novel HFM for performing probabilistic forecast in two different time series scenarios with high fluctuations.

The remainder results and informations involving probabilistic forecasts are organized as follows. Section 3.5.1 presents the adaptation of the HFM for generating probabilistic quantiles from the hybrid evolutionary forecasting model, while Section 3.5.2 presents the computational experiments.

3.5.1 Methodology for generating probabilistic forecasting

Since the heuristic model is based on a fuzzy model calibrated using a bio-inspired metaheuristic algorithm, the proposal here is to take advantage of the stochasticity of the proposed framework. By running the model several times, it is naturally able to provide different forecasting models that optimize different characteristics from a given time series.

Thus, the core of our idea is to train the hybrid fuzzy model fm times. As mentioned, given the stochasticity of this class of training models which uses metaheuristic procedures, we can achieve different forecasting models by simply initializing the training phase with different random seeds. Thus, the core of the idea is to check if different executions of the HFM can be used together in order to generate probabilistic quantiles.

From the set of different forecast models, predicted values are sorted from the lowest to the highest values and, then, quantiles are determined. In our didactic example, we combine the different forecasting models by putting them in order and extracting normal quantiles. As mentioned by Adhikari (Adhikari 2015), it is an effective and easy way of obtaining a probabilistic distribution of the forecasts. Basically, a quantile function is defined, which provides a given probability in the probability distribution of a random variable (in our examples, expected rainfall and wind power generation).

In terms of the distribution function F, the quantile function Q returns the value x such that it gives the probability that the values can be above x, as described in Eq. (3.24). Thus, it provides the value at which the probability of the random variable being less than or equal to this value is equal to the given probability p, provided by the quantiles Q_p. It is also known as the percent point function or inverse cumulative distribution function.

$$F_X(x) := Pr(X \leq x) = p \tag{3.24}$$

Here, we define quantiles $Q = \{1, ..., 99\}$. Theoretically, the quantile Q_0 is equal to $-\infty$ and $Q_{100} = \infty$, respectively, the lower and upper bounds of any historical time series. In our cases of study, the minimum expected values would be 0 for the lower quantiles Q_0, given that we know, surely, that we have 0% of chance of having a rainfall or wind power generation lower than 0mm or 0W, respectively. Following the same reasoning, we could define better upper limits for the quantile Q_{100}, looking at the literature and following historical values of the time series. However, this thesis will only focus on the ability of our proposal in obtaining, automatically, the quantiles Q_1 to Q_{99}.

3.5.2 Initial probabilistic forecasts computational experiments

Historical datasets

The dataset used as didactic example for the wind power turbine was obtained from the EirGrid Database (Center 2015). It consists in intraday wind power generation (MW) for the 50 week period from November, 18th of 2013 to February, 18th of 2014 (2160 samples). All experiments used hourly data. The obtained wind power generation time series can be seen depicted in Figure 3.17, as well as its ACF plot 3.18. As can be noticed, the ACF values decay quickly and show weak autocorrelation.

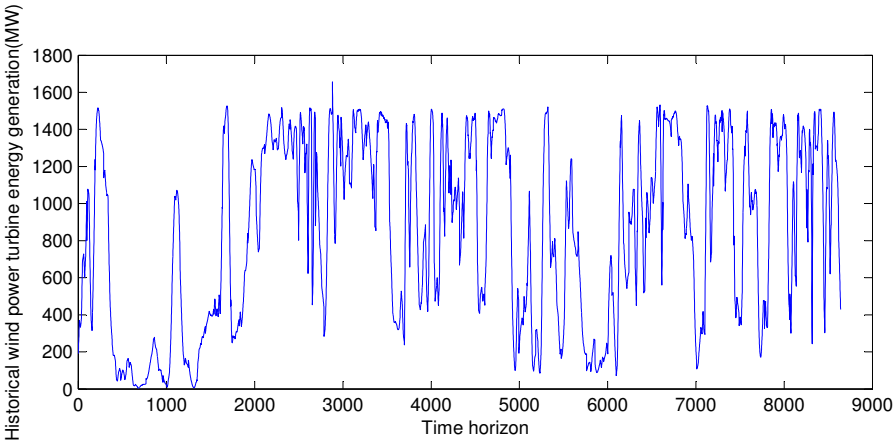

Figure 3.17: Historical power generation from a wind turbine

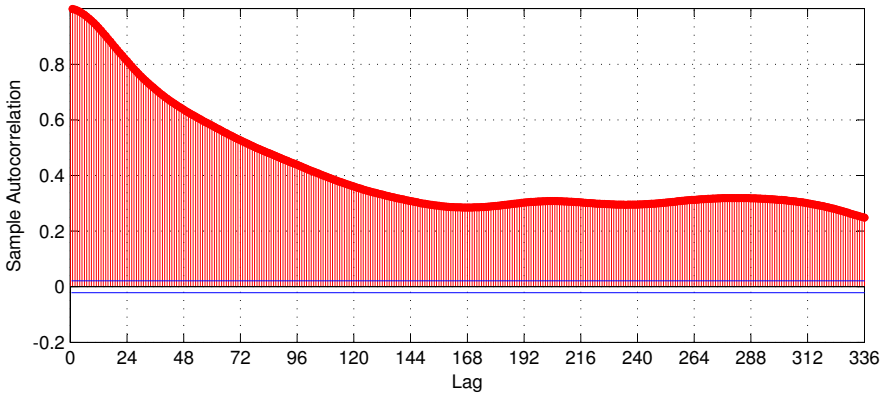

Figure 3.18: Autocorrelation function of the power generated from the historical data from the wind turbine

Real data from the city of Vitoria was extracted from the Brazilian "Agência Nacional de Águas", comprising different years from 1926 to 2013. The maximum monthly rainfall precipitation can be seen depicted in Figure 3.19, as well as its ACF plot (Figure 3.20). As can be verified, there is almost no correlation between the maximum monthly rainfall, reinforcing the difficulty of establishing useful inputs/lags for the forecasting model.

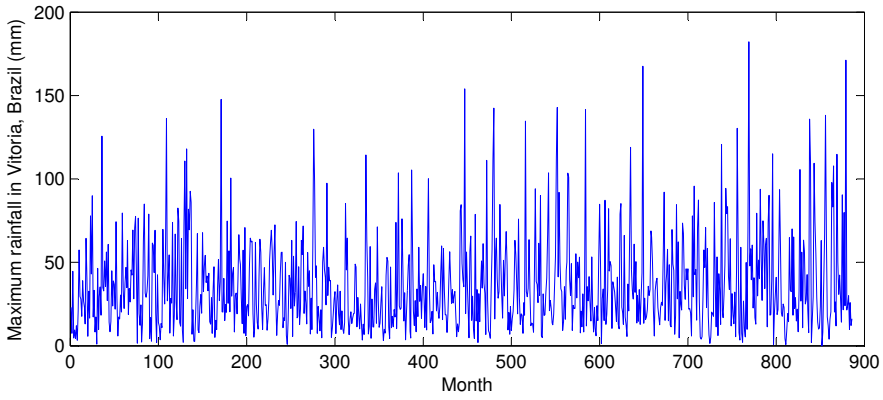

Figure 3.19: Maximum rainfall in Vitoria (maximum month per mm)

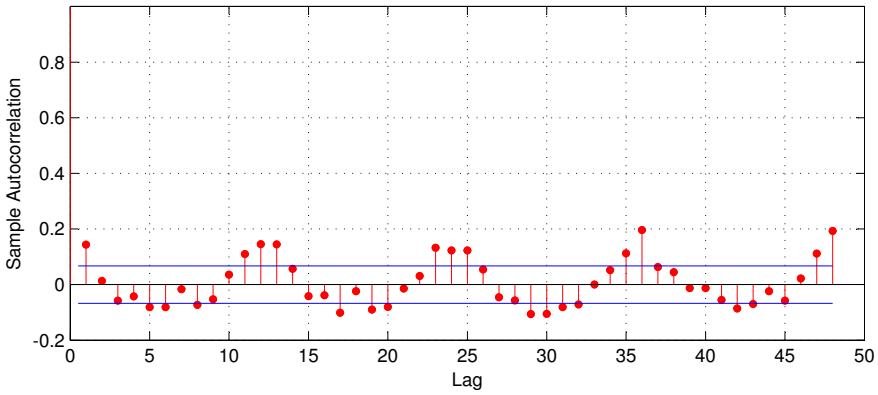

Figure 3.20: Autocorrelation function of the monthly maximum rainfall in Vitoria

Obtained probabilistic forecasts

The batch of experiments for generating the probabilistic forecasting model was composed of 500 executions of 240 seconds of training. The size of the validation set was set to be 5 times the forecast horizon, thus, for a forecasting horizon of 168 steps ahead

(one-week ahead) of wind power generation, 840 samples were used during the training set and the consecutive 168 samples used for comparing the obtained probabilistic forecasts.

The same parameters adopted in Section 3.4 were kept here. Thus, as introduced in Section 3.5.1, the model was run $tm = 500$ times with different seeds, obtaining different forecasting models.

Figure 3.21 shows a whole set of forecasts obtained for one week ahead of wind power generation. On the other hand, Figure 3.22 shows an example of probabilistic quantiles for a forecasting horizon of one-week ahead, the thicker line shows the real measured data.

A reasonable probabilistic approximation can be seen comprised in the quantiles of Figure 3.22, fitting a reasonable forecasting for one week ahead planning. Quantiles are able to fit the maximum and minimum amount of energy generated, as can be checked analyzing the upper (Q_{99}) and lower bound quantiles (Q_1). A denser concentration of quantile can be found in the middle section of the probabilistic forecast, from the range of 650MW to 900MW.

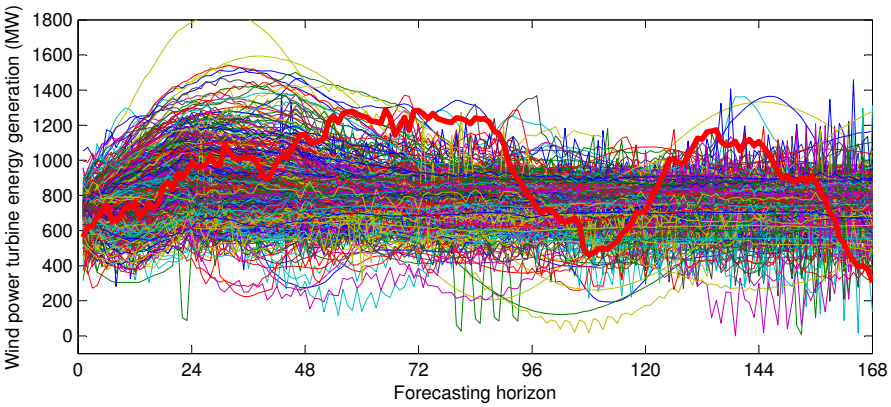

Figure 3.21: Obtained hourly forecasts for one week ahead of wind power generation

For the rainfall forecasts, a first experiment focused on obtaining one step ahead deterministic forecast. This was initially done in order to check if the hybrid model could, at least, generate visually viable forecasts. As can be verified in Figure 3.23, the model was able to generate one-step ahead forecast with a maximum error, of rainfall precipitation, around 75 mm, considering a blind testing set of 24 months. This fact

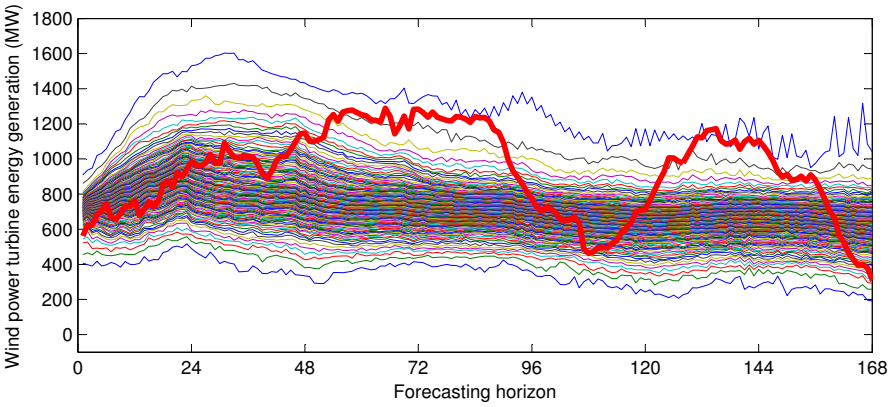

Figure 3.22: Probabilistic hourly forecasts for one week ahead of wind power generation

motivated a new batch of experiments to check larger forecasting horizons considering probabilistic, which, implicitly, provide mean and variance forecast.

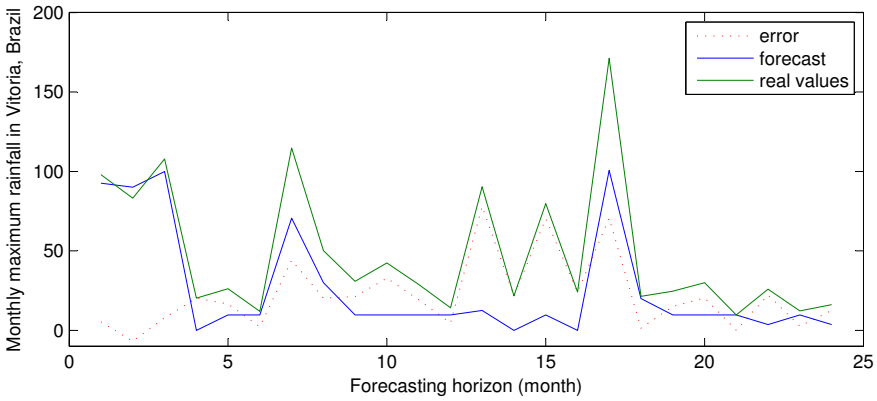

Figure 3.23: One step ahead forecast for maximum monthly rainfall

Figures 3.24 and 3.25 show two different probabilistic forecasts for one and two years ahead forecasts, respectively, 12 and 24 steps ahead of maximum monthly rainfall. This kind of forecast are handful and useful for decision making for investments in infrastructure and understanding the risk for the next years.

Figure 3.24 depicts specific quantiles, facilitating the visualization and interpretation of the results, namely Q_1, Q_{25}, Q_{50}, Q_{75}, Q_{99}. As expected, the lower bound were forecasted as 0mm for each month, a fact that occurs in the absence of precipitation.

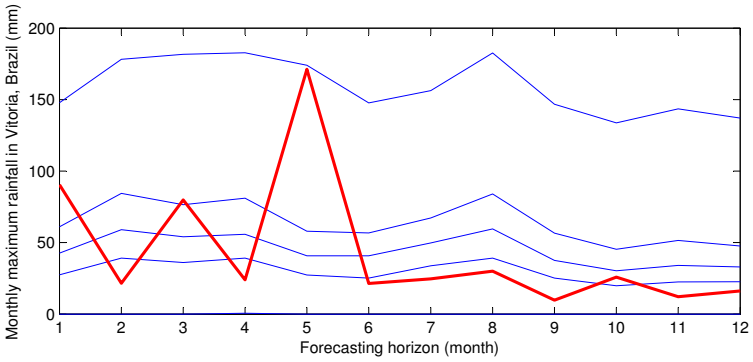

Figure 3.24: One year ahead of maximum monthly rainfall for the city of Vitoria in the year of 2013

The upper bound limited the maximum raining below an approximated value of 150mm. The probabilistic distribution indicates that for the next year (in the example, 2013), the maximum monthly precipitation had an approximated probability of 75% to 70mm, considering the average of the 12 months. On the hand, it has forecasted with 50% of chance that the rainfall would be close to 50mm.

Finally, analyzing Figures 3.25 and 3.26, it can be seen that, even for 24 and 120 steps ahead, the proposed model was able to produce consistent forecasting quantiles. In special, for two year ahead forecasting of maximum monthly rainfall, the forecasts were able to cover covered the real measured rainfall.

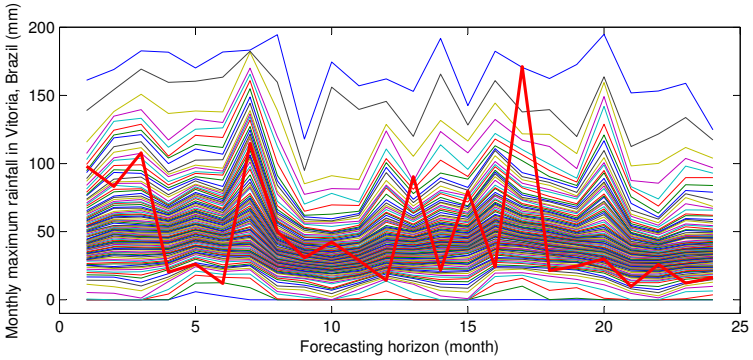

Figure 3.25: Two years ahead (24 steps ahead) of maximum monthly rainfall for the city of Vitoria in the years of 2012 and 2013

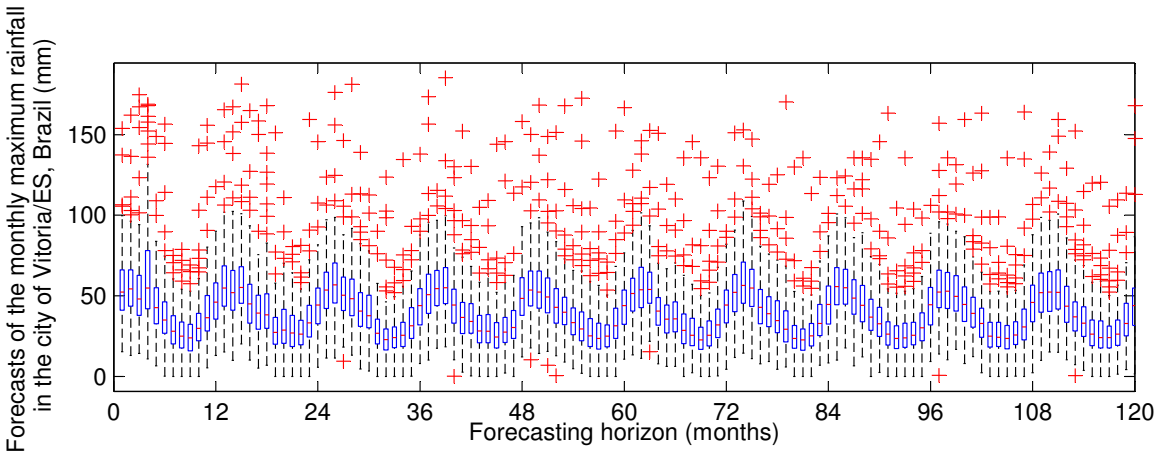

Figure 3.26: Boxplot with ten years ahead (120 steps ahead) of maximum monthly rainfall for the city of Vitoria in the years of 2012 and 2013

3.6 Considerations and conclusions

In this chapter, a class of forecasting problem with realistic assumptions in Smart Grid scenarios was discussed. Despite its practical relevance, these variants of forecasting had received little attention of hybrid models based on metaheuristic. Because of its difficulty and large number of different forecasting scenarios in a future Smart Grid (SG) environment, a new flexible framework for forecasting was proposed.

This new approach consisted on a novel self-adaptive fuzzy model bio-inspired by Evolution Strategies to calibrate its parameters and model's input. Thus, forecasting models are generated based on the constructive procedure GRASP, which can consider an open range of feature extraction techniques. The calibration process, done by the GES algorithm was able to go through a large search space of solutions with several different fuzzy rules and weights. The expert input selection and adaptation using NS allows more compact forecasting model, smaller training sets and easier training. Consequently, our new proposed model represents a step forward in determining a general procedure for input variable selection.

Real databases provided by Liu, Tang, Zhang & Liu (Liu et al. 2014), the Global Energy Forecasting Competition 2014 – GEFCOM2014 (Hong 2014) and Taylor & McSharry (Taylor & McSharry 2007) were used in order to verify the efficiency of the proposed model. It was shown to be able to find good quality forecasting models for

microgrids and large-grids.

The methodology was able to obtain better results than the hybrid model of Liu, Tang, Zhang & Liu (Liu et al. 2014). Particularly in view of the method's flexibility, as it is mainly based on metaheuristics, it can be used in various everyday situations with minor adjustments.

A real-time microgrid forecasting scenario was also described and the model was compared with well-known forecasting models from the literature, presenting competitive results and lower MAPE for the analyzed historical MG time series.

3.6.1 Considerations regarding probabilistic forecasts generation

The HFM was adapted in order to obtain different forecasting models, which have different abilities for generating specific forecasting. Thus, these various models are used in order to obtain probabilistic quantiles. Since the model is calibrated through the use of metaheuristic procedures, the training phase of the proposed methodology was executed several times in order to achieve different forecasting models.

Two different forecasting problems, one for rainfall and another for wind power generation forecast, both with high fluctuation and slopes, were used as didactic examples. The obtained forecasts from the different models were sorted and quantiles were determined. By analyzing the obtained graphs, evidences pointed out that the model could provide useful forecasts and assist decision making of the new generation of soft/smart sensors.

Chapter 4

Hybrid self-adaptive evolution strategies

"Quando fecha-se uma porta, abre-se o caminho da rua/mundo, uma nova jornada repleta de incertezas e tropeços, mas com uma bela trajetória para ser percorrida."

— Vitor Nazário Coelho

This chapter presents an Evolution Strategy (ES) based algorithm, designed to self-adapt its mutation operators, guiding the search into the solution space using a Self-Adaptive Reduced Variable Neighborhood Search procedure. The proposed variant uses the Greedy Randomized Adaptive Search Procedure (GRASP) with different greedy parameters for generating its initial population, providing an interesting exploration-exploitation balance. To validate the proposal, this framework is applied to solve different $\mathcal{NP}$-Hard combinatorial optimization problems, such as the Open-Pit-Mining Operational Planning Problem (OPMOP) with dynamic allocation of trucks, Unrelated Parallel Machine Scheduling Problem with Setup Times (UPMSP-ST), a large-scale Heterogeneous Fleet Vehicle Routing Problem with Multiple Trips, Targeted Offer Problem in Direct Marketing Campaigns and also the calibration of a hybrid fuzzy model for Short-Term Load Forecasting.

4.1 Introduction

In this chapter, the class of Evolutionary Algorithms (EA) known as Evolution Strategies (ES) (Beyer & Schwefel 2002b) is investigated and a new ES variant is proposed,

being able to solve challenging combinatorial optimization problems. In special, it is applied in order to calibrate the HFM introduced in Chapter 3. The idea is to combine the diversity of the population-based algorithms with the power of Reduced Variable Neighborhood Search (RVNS) (Hansen & Mladenović 2001), a well known trajectory search algorithm. Moreover, the strategy supplies RVNS with adaptive rules, producing a new variant so called Adaptive RVNS (ARVNS). EA are search and optimization methods inspired by well-known evolutionary principles, such as random mutations and selective pressure for evolution and adaptation of its population. On the other hand, VNS and other trajectory based approaches such as Tabu Search (TS) (Glover 1996a) and Iterated Local Search (ILS) (Lourenço et al. 2003) take advantage of the flexibility in designing and exploring different Neighborhood Structures (NS) of the problem, using the simple fact that the local minimum with respect to one neighborhood structure is not necessarily so with respect to another.

Biological evolution in nature is an inspiration for the ES, which is mainly guided by operators: mutation and selection. This class of methods have often been applied for solving continuous optimization problems (Kashan et al. 2015, Chaquet & Carmona 2012, Andersen & Santos 2012, Aler et al. 2012, Costa & Oliveira 2001). While EA have already been applied to solve several combinatorial optimization problems (Prado et al. 2014, Qaurooni & Akbarzadeh-T 2013, Freitas & Guimaraes 2011), only few articles in the literature address combinatorial optimization problems using ES (Cai & Thierauf 1996, Rajasekaran 2006, Kashan et al. 2015). The current focuses os the proposal is on a mechanism for guiding the search in the solutions space, mainly based on a weighting system for applying move operations from k_{max} distinct neighborhoods. The motivation to develop an ES for combinatorial optimization, combined with use of different NS, come from the successful applications in both fields, numerical and combinatorial optimization.

Adaptive local search techniques have been exploited by researchers (Dong et al. 2015, Li et al. 2015, Schneider et al. 2014, Hosny & Mumford 2010). This family of methods have the ability of exploring attraction basins with iterative moves, combining it with smart strategies that, in general, check the success of previous steps done by the methods. In this context, an ILS with self-adaptive shaking procedure was applied for tackling a flow shop problem (Dong et al. 2015) and multi-depot Vehicle Routing Problem (VRP) (Li et al. 2015). Following the same idea, Schneider et al. (2014) proposed an adaptive mechanism for guiding the shaking step of a VNS applied on a VRP. Their approach select and favored route and vertex according to their success within the search.

By Reduced VNS method a random point from the k-th neighborhood $N_k(s)$ ($k =$

$1, ..., k_{max}$) of the current incumbent solution x is taken, and no descent from there is made. RVNS has been showing to be useful in solving large instances, for which local search is costly (Xiao et al. 2011, Hansen et al. 2009).

The adaptive variant of the RVNS designed in this thesis, the ARVNS, explores specific parts of each N_k, playing with probabilities evolved through the ES evolutionary process. Our proposal implicitly considers the problem specific characteristics and the success of a given N_k within the search. There is no need of mechanisms for analyzing previous success of the N_k, since it is inherited through the genes, ES mutation operators, from the parents to the offspring. The later are generated after mutations over the ARVNS application probabilities and are expected to survive if interesting changes had occurred.

Here, an evolution strategy based algorithm is introduced, abbreviated as GES, which generates its initial population through a diversified and greedy procedure. Thus, we suggest the use of the Greedy Randomized Adaptive Search Procedures (GRASP) (Resende & Ribeiro 2010). GRASP construction phase is responsible to fill the initial population with individuals generated with different random greedy parameters. Other versions with simpler solution generation procedures could be also used, such as generating solutions at random or initializing a homogeneous initial population. ES mutation operator vectors are kept as the main search operator in the solution space, however, being guided by new data structures incorporated with each individual representation. The proposed adaptive operators regulate the rate of moves application of different NS, in a special case of a RVNS search. An optional intensification phase is also suggested for some problems, in order to accelerate the convergence of the algorithm.

Problems already tackled by the author of this thesis were used as cases of study. Thus, I took profit from the optimization framework OptFrame, see (Coelho et al. 2011b), a computational framework for the development of efficient metaheuristic algorithms for combinatorial optimization problems. Three different (and very challenging) combinatorial optimization problems are considered in this work as cases of study:

1. Open-Pit-Mining Operational Planning (OPMOP) problem (Souza et al. 2010);
2. Unrelated Parallel Machine Scheduling Problem with Setup Times (UPMSP-ST) (Al-Salem 2004), implemented in a Java platform with OptFrame ideas;
3. Calibration of a hybrid fuzzy model calibration for the Short-Term Load Forecasting Problem (STLFP) described in Chapter 3.

Since we are dealing with many $\mathcal{NP}$-Hard problems, exact solution methods have restricted applicability. This fact motivates us to search for solutions by means of metaheuristic procedures.

The abstraction of the concepts involving the proposed discrete ES and its application over the aforementioned problems was not found in the literature and shows up as a novel evolutionary framework for combinatorial optimization problems.

The remainder of this chapter is organized as follows. Section 4.2 details the proposed self-adaptive ES. Section 4.3 describes an application for the OPMOP. Analogously, Sections 4.4 and 4.5, describe mutation operators behavior of the proposed algorithm over the STLFP and UPMSP-ST, respectively. Section 4.6 draws the final considerations and future works.

4.2 Self-adaptive evolution strategy

Evolution Strategies (ES) were developed in the 60's and 70's by P. Bienert, I. Rechenberg and H.-P Schwefell in the Technical University of Berlin. The initial version operated with single individuals, subjected to mutation and selection among its descendants. Beyer & Schwefel (2002b) provide a detailed description about ES in their comprehensive introduction.

ES use natural problem-dependent representations according to each problem that is being tackled. One advantage is its searching ability over the evolution process that is guided, primarily, by mutation and selection. Here, the strategy takes advantage of the basic principle, introducing the ARVNS, a RVNS guided by probabilities. A widely range of genetic operators can be used in order to generate the offspring population. Novel mechanisms are still being explored and developed in the literature (Chuang et al. 2015). Mutation operators from ES usually can change all components of a parent vector at the same time, but with minor changes since it is assumed that in the real biological evolution small mutations occur frequently but large ones only rarely.

In the 90's, Cai & Thierauf (1996) proposed a general ES for solving discrete optimization problems, suggesting that not all components of a parent vector should be mutated, but only a few should be randomly changed every time. This strategy was quite smart, since, in discrete sets, differences between any two adjacent values are usually not small. This approach have been used/followed in different applications (Hasancebi 2007, Chen & Chen 2009, Yao et al. 2011). Li et al. (2013) introduced an Mixed Integer ES able of handling parameter consisted of discrete and integer variables.

Motivated by successful applications in the literature, it was felt that the ES could deal with combinatorial optimization problems in partnership with a self-adaptive strategy based on moves generated from simple NSs where neighborhood structures guide the individuals through the solution space. Thus, a special care in the design of the algorithm was given, exploring the RVNS ability of handling random moves in N_k, $k = 1, ..., k_{max}$. The details will be discussed along this chapter. The use of NS is well-know in the literature and has been widely applied for solving $\mathcal{NP}$-Hard problems (Johnson et al. 1988, Kirkpatrick 1984, Glover 1989, Mladenovic & Hansen 1997, Lourenço et al. 2003, Lust & Teghem 2010, Pisinger & Ropke 2010).

In this sense, a compact and efficient encoding is designed for adapting NS use and strength in connection with individual mutation operators, described in the next section.

4.2.1 Mutation operators

According to the problem that is being solved, a desired data structure, or *representation*, is selected and a solution to the problem is defined as s. Here, each individual *ind* is comprised of two additional mutation vectors, defined as P and A, presented in Equations (4.1) and (4.2) respectively, embedded within the solution representation s.

Following this strategy, each individual of the population is defined as described in Equation (4.3) as a triple formed by s, P and A.

$$P = [p_1, p_2, ..., p_k, ..., p_{NSmax}] \tag{4.1}$$

$$A = [a_1, a_2, ..., a_k, ..., a_{NSmax}] \tag{4.2}$$

$$ind = (s, P, A) \tag{4.3}$$

The first mutation vector P represents the likelihood associated with the choice of each NS in a set composed of $NSmax$ neighborhood structures. This vector guides the probability of applying each NS used to walk on the search space. Each position stores

the probability $p_k \in [0,1], p_k \in \mathbb{R}$ of the application of a given move $m \in N_k$.

The second mutation vector A stores integer values for controlling the strength of the disturbance, once a NS is selected to be applied and shake the solution s. Each position $a_k \in [0, nap_k], a_k \in \mathbb{N}$ of this vector indicates the number of random moves $m \in N_k$ to be applied from neighborhood k, with nap_k representing the maximum *number of applications* of different moves in each mutation event.

Both vectors are adapted across the generations of the evolutionary process, according to well-know probability distribution functions. The evolution of these two mutation vectors will be discussed for each application described in this current study. Other set of parameters could also be included for adapting the distributions along the generations.

4.2.2 Generic evolution strategy pseudocode guideline

The proposed self-adaptive evolution strategy algorithm pseudocode is outlined in Algorithm 4.1. As emphasized by Lust & Teghem (2010), generating an initial population diversified and with good potential is a very important feature for the convergence of population based algorithms. Thus, use the GRASP procedure in partnership with the proposed algorithm is suggested.

The initial population (lines 1 to 7 of Algorithm 4.1) consists in generating a set μ individuals. Line 3 calls the GRASP procedure and generates each solution of the initial population with different random greedy parameter γ. Achieving a diversified initial population is an important stage for the algorithm convergence, as can be verified in Lust et al. (2011), therefore, different γ parameters are used, in order to control the size of the candidates list. Thus, a random GRASP is designed here. In the second step (line 4 of the Algorithm 4.1), the self-adaptive mutation vectors P and A are built for each individual. The procedure BuildMutationVectors (outlined in Algorithm 4.2) describes a generic and simple idea for generating initial values for the mutation vectors. Line 5 merges the triple formed by a GRASP solution s and the mutation operators P and A. In this sense, the following nomenclature is defined: let ind^S be the solution s of the individual ind; ind^P be the probability parameter vector; ind^A be the application

parameter vector.

Algorithm 4.1: GES

Input: greedy parameter γ, Function $f(.)$, population size μ, offspring size λ, random individuals selected for local searching κ

Input: N neighborhoods

Output: Population Pop

for $i \leftarrow 1$ ***to*** μ **do**
  Generate a random number $\gamma \in [0, 1]$
  $s \leftarrow$ GRASP(γ)
  $(P, A) \leftarrow$ BuildMutationVectors($|N|$)
  $ind \leftarrow (s,\ P,\ A)$
  $Pop_i \leftarrow ind$
end
while *stop criterion not satisfied* **do**
  for $i \leftarrow 1$ ***to*** λ **do**
    $ind \leftarrow$ Random individual Pop_x with $x \in [1, \mu]$
    $ind' \leftarrow$ UpdateParameters(ind, σ_{real}, $\sigma^{p}_{binomial}$,$\sigma^{n}_{binomial}$, $|N|$)
    $ind'' \leftarrow$ ARVNS(ind', N)
    $Pop_i^{offsprings} \leftarrow ind''$
  end
  for $i \leftarrow 1$ ***to*** κ **do**
    Generate a random number $x \in [1, \lambda]$
    localSearchProcedure($Pop_x^{offsprings}$) – (optional)
  end
  $Pop =$ Selection (f, Pop, $Pop^{offsprings}$)
end
return Pop

Algorithm 4.2 fills the probabilities vector, P, random numbers generated between the interval $[0, 1]$ and the same idea is applied for the vector of applications, A, respecting

the range $[1, nap_k]$.

Algorithm 4.2: BuildMutationVectors

Input: number of neighborhoods max

Output: Mutation parameters vector P and A

```
1 P ← Initialize Vector of Probabilities P for r neighborhoods
2 A ← Initialize Vector of Applications A for r neighborhoods
3 for k ← 1 to max do
4 |   P_k ← Generate a random number ∈ [0, 1]
5 |   A_k ← Generate a random number ∈ [1, nap_k]
6 end
7 return P,A
```

In line 11 of Algorithm 4.1, individual parameters are updated, the pseudocode of the procedure "UpdateParameters" is described in Algorithm 4.3. Vectors of mutation parameters A and P, are updated and adapted according to a Normal or Binomial Distribution, both centered at mean zero and standard deviation σ_{real} and $\sigma^p_{binomial}$, respectively. For the binomial distribution, an additional parameter $\sigma^n_{binomial}$ indicating the number of trials is required. Parameter $\sigma^p_{binomial}$ regulates the probability of successes in a sequence of $\sigma^n_{binomial}$ independent yes/no experiments. Updates of the vectors ind^P and ind^A can be viewed in lines 2 and 3, respectively, in the Algorithm 4.3. Line 5 checks if the limits of both mutation operators are respected after the mutation. As expected, the maximum value assigned for the application probability, of each cell from vector ind^P, should be between 0% to 100%. Following a similar reasoning, the maximum number of application, for each cell k from vector ind^A, should be nap_k and no less than

1.

Algorithm 4.3: UpdateParameters

Input: Individual ind, Standard Deviation σ_{real} e $\sigma_{binomial}$, number of neighborhoods max

Output: Individual ind updated

```
1 for k ← 1 to max do
2 |   ind_k^P ← ind_k^P + N(0.0, σ_real)
3 |   ind_k^A ← ind_k^A + B(0.0, σ_binomial^p, σ_binomial^n)
4 end
5 Check the limits of the operators ind^P and ind^A
6 return ind
```

Line 12 of the Algorithm 4.1 calls the mutation procedure, a special case of the classical RVNS, called ARVNS, illustrated in Algorithm 4.4, In line 2 of the Algorithm 4.4, a random number $z \in [0, 1]$ is generated and then, line 3 checks if this number satisfies the probability ind_k^P. In the positive case, the neighborhood structure N_k allocated in the current index k is applied ind_k^A times. The neighborhood order of this parameter vector is chosen at random. An optional mutation rate parameter can be added in each individual representation in order to regulate the sequence that the NS are applied.

Algorithm 4.4: ARVNS

Input: Individual ind

Input: N neighborhoods

Output: Individual ind

```
1  for k ← 1 to max do
2  |   Generate a random number z ∈ [0, 1]
3  |   if z < ind_k^P then
4  |   |   for a ← 1 to ind_k^A do
5  |   |   |   s' ← MOVE_k(ind^S)
6  |   |   |   ind^S ← s'
7  |   |   end
8  |   end
9  end
10 return s
```

Line 17 of the Algorithm 4.1 opens the possibility of calling an optional intensification phase, usually done by local search techniques, such as Variable Neighborhood Descent (VND). When triggered, an intensification phase refines κ random solutions in the offspring population. It should be emphasized that this phase is optional, since several variations could be implemented here according to the combinatorial optimization problem that is being tackled.

Finally, the selection procedure, line 19 of the Algorithm 4.1, can be any desired selection strategy, as long as it returns a population with cardinality μ. Two basic forms of competition, both with the same notation of Beyer & Schwefel (2002b), are used. In the first one, denoted by $(\mu + \lambda)$, there is competition between parents and offspring. In this strategy, μ best individuals are selected among the union of parents and offspring. In the second selection strategy, denoted by (μ, λ), only the offspring compete for survival. It is clear that using the strategy $(\mu + \lambda)$ as a way of selection, the population of the next generation suffers a considerable higher selective pressure than using the strategy (μ, λ).

4.3 Open-pit-mining operational planing problem

The OPMOP involves the allocation of mining equipment to the pits, which may be of ore or waste rocks, as well as determining the number of trips for each truck so that both the production goals and the desired mineral composition of the ore are fulfilled. The goal is to find a mining rate on every pit that minimizes deviations from production goals, quality, and also the number of trucks required for the process. Dynamic truck allocation is considered, which is the possibility to allocate the trips from a certain truck to a different pit. This allocation system contributes to an increased fleet productivity and, therefore, to reduce the number of trucks needed for the production process. Figure 4.1 shows a graphical example of the OPMOP, composed of pits with different mineral compositions, two shovels and different trucks.

A briefly literature review is described below.

Costa (2005) developed a heuristic algorithm based on GRASP and VNS using six different types of movements to explore the solution space. A comparison was made between the results obtained by this heuristic algorithm and those found by the solver LINGO, version 7, applied to a mathematical programming model developed in Costa et al. (2004). Results showed that the heuristic algorithm was able to find better solutions faster. Guimarães et al. (2007) presented a computer simulation model to validate results

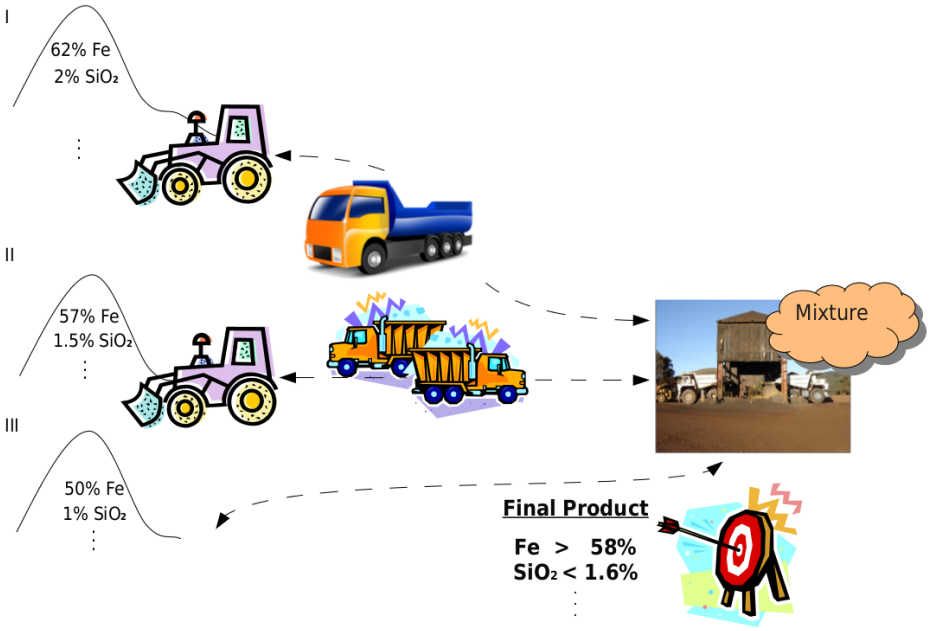

Figure 4.1: OPMOP example

obtained by applying a mathematical programming model to determine the mining rate in open-pit mines (e.g. occurrence of queues).

Souza et al. (2010) proposed an algorithm, called GGVNS, which combines the metaheuristics General Variable Neighborhood Search (GVNS) (Hansen et al. 2008) and GRASP procedure. The GVNS was chosen due to its simplicity, efficiency and capacity of its natural local search to deal with different neighborhoods. The authors compared the results generated by GGVNS with those achieved by CPLEX optimizer 11.0.1, using eight test problems. Computational experiments showed that the algorithm was competitive and, in most instances, capable of finding new optimal solutions - with a gap $< 1\%$ - requiring a short computational time.

Coelho, Souza, Coelho, Guimaraes, Lust & Cruz (2012) developed the first multi-objective application to the OPMOP. Three multi-objective heuristic algorithms were validated based on Two-phase Pareto Local Search with VNS (2PPLS-VNS), proposed by Lust & Teghem (2010), Multi-objective Variable Neighborhood Search (MOVNS), presented by Geiger (2004), and Non-dominated Sorting Genetic Algorithm II (NSGA-II) developed by Deb et al. (2002). Approximations of Pareto sets generated by the developed algorithms were compared considering the hypervolume and spacing metrics. Computational experiments have shown the superiority of the algorithms based on VNS

methods, which were able to find better sets of non-dominated solutions, more diversified and with an improved convergence.

4.3.1 Representation and evaluation of a solution

Given a set of mining pits F, a set of trucks T and a set of shovels K, a solution for OPMOP is represented by a matrix $R = [Y|N]$, where Y is a matrix $|F| \times 1$ and N a matrix $|F| \times |T|$. Each cell y_i of the matrix $Y_{|F| \times 1}$ represents shovel $k \in K$ allocated to the pit $i \in F$. If there aren't trips made to the pit i, the shovel k associated with this pit is considered inactive and it is not penalized for a production below the minimum limit.

In the matrix $N_{|F| \times |T|}$, each cell n_{il} represents the number of trips performed by the truck $l \in T$ to the pit $i \in F$. The value 0 (zero) means no trip to that truck. The value X means that the truck is incompatible with the shovel allocated to the pit.

Table 4.1: Representation of a Solution

	$Shovel$	$Truck_1$	$Truck_2$	...	$Truck_T$
F_1	$(Shovel_1, 1)$	8	X	...	X
F_2	$(Available, 0)$	0	0	...	0
F_3	$(Shovel_8, 0)$	0	0	...	0
...	...	...	...	...	...
F_F	$(Shovel_5, 1)$	0	9	...	3

In Table 4.1, there is an example of a possible solution to the OPMOP. At the column $Shovel$, line F_1, the pair $(Shovel_1, 1)$, indicates that the loading equipment $Shovel_1$ is allocated to the pit F_1 and the number one means that it is operating. At the column $Shovel$, line F_3, the pair $(Shovel_8, 0)$ indicates that the loading equipment $Shovel_8$ is allocated to the pit F_3, but it is not operative. Finally, in line F_2, the value $(Available, 0)$ means that there is no loading equipment allocated to the pit F_2 and, therefore, this pit is available. The other columns represent the number of trips from the truck to the corresponding pit, considering the compatibility between the truck and loading equipment allocated to the front. Cells with values X indicate incompatibility between a truck and its loading equipment.

4.3.2 Mathematical model and solution evaluation

In the considered formulation of the OPMOP, extracted from Souza et al. (2010), the mono-objective function is given by Eq. (4.4):

$$\min f^{PM}(s) = \sum_{j \in T} \lambda_j^- d_j^- + \sum_{j \in T} \lambda_j^+ d_j^+ + \alpha^- D_O^- + \alpha^+ D_O^+ + \beta^- D_W^- + \beta^+ D_W^+ + \sum_{l \in T} \omega_l U_l \tag{4.4}$$

Eq. (4.4) seeks to minimize the positive and negative deviations from the goals of each control parameter j of the mixture, d_j^+ and d_j^- respectively, as well as the positive and negative deviations from the production goals of ore and waste rocks, represented, in this order, by decision variables D_O^+, D_O^-, D_W^+ and D_W^-. This function also considers the minimization of the number of used trucks, represented by the binary variable U_l, which is 1 if the truck l is used and 0, otherwise.

The constants λ_j^-, λ_j^+, α^-, α^+, β^-, β^+ and ω_l are weights that reflect the importance of each component of the objective function.

Since the movements generated by the used neighborhood structures can lead to infeasible results, a solution is evaluated by a function f to be minimized, composed of two parts. The first one is the actual objective function, f^{PM}, given by Eq. (4.4), and the second one consists of functions that penalize the occurrence of infeasibility in the solution. Thus, the function f, given by Eq. (4.5), measures the deviation of the goals and penalizes any violation of the constraints in the problem.

$$f(s) = f^{PM}(s) + f^p(s) + \sum_{j \in T} f_j^q(s) + \sum_{l \in V} f_l^u(s) + \sum_{k \in C} f_k^c(s) \tag{4.5}$$

where:

$f^{PM}(s)$ is a function that evaluates s with regard to the production goals and the quality of the final mixture.

$f^p(s)$ penalizes s if the limits for the production of ore and waste rocks are not respected;

$f_j^q(s)$ penalizes s if the limits for the j-th control parameter of the mixture are not respected;

$f_l^u(s)$ penalizes s if the maximum utilization rate for the l-th truck is exceeded;

$f_k^c(s)$, penalizes s if the productivity limits for the shovel k are not respected.

4.3.3 Neighborhood structures

In order to explore the solution space, as described in Section 4.2, eight neighborhood structures, introduced by Souza et al. (2010), are used to analyze the convergence of the proposed GES. As detailed in Algorithm 3.14, the NS are polarized during the GES algorithm execution and may, by chance, "generate/create" new structures. With this new proposed mechanism it is possible to create new ways to shake a given solution, since a solution s', generated from s, is a combination of $[0, nap_k]$ random moves from all $N_k(s)$, as described in Algorithm 3.15.

A short description of the movements that will guide the GES walk trough the solutions space are described below:

Movement number of trips – $\boldsymbol{NS^{NT}(s)}$: This move increases or decreases in one unit the number of trips a truck l performs to a pit i, in which there is a compatible load equipment. Thus, in this movement a cell n_{il} of matrix N has its value increased or decreased by one.

Movement load – $\boldsymbol{NS^{LD}(s)}$: It consists of swapping two distinct cells y_i and y_j of matrix Y, that is, swapping the load equipments allocated to pits i and j, if both pits have an allocated loading equipment. When there is an allocated load equipment on only one of the pits, this movement will relocate the load equipment to the available pit. To maintain compatibility between shovels and trucks, the trips made to the pits are relocated along with the load equipments.

Movement relocate trip from a truck – $\boldsymbol{NS^{TT}(s)}$: In this movement, two cells n_{il} and n_{kl} of matrix N are selected and one unit of n_{il} is transferred to n_{kl}. Thus, the truck l does one trip less to the pit i and it does one trip more to the pit k. Compatibility between equipments are observed, with relocation of the trip only if there is a match between them.

Movement relocate trip from a pit – $\boldsymbol{NS^{TP}(s)}$: Two cells n_{il} and n_{ik} of matrix N are selected and one unit of n_{il} is relocated to n_{ik}. This move relocates one trip

that the truck l performs to the pit i for the truck k. Compatibility between equipment restrictions are respected and there is relocation only when there is match between them.

Movement pit operation – $NS^{PO}(s)$: This operation consists on removing the load equipment that is operating in pit i. The procedure removes all trips made to the pit i, leaving the shovel equipment allocated to it inactive. The equipment only returns to operation once a new route is associated to the pit.

Movement truck operation – $NS^{TO}(s)$: Consists on removing from operation one truck l that is related to a pit i. Thus, the cell n_{il} of matrix N has its value set to zero.

Movement swap trips – $NS^{ST}(s)$: Two cells of the matrix N are selected and one unit of a cell is transferred to another one, which means the journey of a truck made to a pit is forwarded to another truck on another pit.

Movement swap shovels – $NS^{SS}(s)$: Two distinct cells y_i and y_k matrix Y have their values exchanged, that is, the load equipments operating on pits i and k are exchanged. Similarly to the neighborhood structure NS^{LD}, the load equipments are exchanged, but the trips made to the pits are not. To maintain compatibility between shovels and trucks, the incompatible trips made to the pit are removed.

4.3.4 Computational experiments and analysis

Computational experiments were carried on a Pentium Core 2 Quad (Q6600) with 8GB of RAM, operating system Ubuntu 14.04.

A first batch of experiments, discussed in Section 4.3.4, seeks to find good parameters of population size and selection strategy rates for the OPMOP. Time-to-Target plots (TTTplots) were used in order to find a set of parameters able to find good targeted solutions. This approach was used since the main idea was to demonstrate the convergence of the GES and, if possible, achieve comparable solution with the GGVNS algorithm of Souza et al. (2010). Thus, the main focus of the experiments section is to demonstrate the ability of the proposed algorithm in self-adapt its parameters during the evolution process. This feature is discussed in Section 4.3.4. In addition, the proposed hybrid self-adaptive GES is tested on a set of standard benchmark problem instances from the literature[1]. These test problems were the same used in Souza et al. (2010) to validate the GGVNS algorithm.

[1]Available at `http://www.decom.ufop.br/prof/marcone/projects/mining.html`.

GES calibration using Time-to-Target plots

Six variants with different set of parameters are analyzed here, Table 4.2 shows the parameters of these GES variants. The variants GES1-VND and GES2-VND include VND as local search procedure for refining some solutions. In these two variants, a portion of $\kappa = 3$ individuals from the offspring population are chosen for the local search procedure (as suggested in Line 17 of Algorithm 3.1). Only a small group of those NS described in Section 4.3.3 is used, namely: NS^{LD}, NS^{NT}, NS^{TT} and NS^{TP}. The expensive computational cost of the local search justifies this restriction. The maximum number of application was set as $nap_k = 15$ for each $k = 1, ..., 8$.

Table 4.2: GES proposed variants for the OPMOP

Acronym	μ	λ	Selection	VND
GES1	30	160	(μ, λ)	
GES2	30	160	$(\mu + \lambda)$	
GES3	100	600	(μ, λ)	
GES4	100	600	$(\mu + \lambda)$	
GES1-VND	30	160	(μ, λ)	$\surd$
GES2-VND	30	160	$(\mu + \lambda)$	$\surd$

Two TTTplots experiments were performed for checking the efficiency of the proposed variants in achieving targeted solutions. Run time distributions or TTTplots display, on the ordinate axis, the probability that an algorithm will find a solution at least as good as a given target value within a given running time, shown on the abscissa axis. These plots were first used in Feo et al. (1994). Run time distributions have been advocated also in Ribeiro & Resende (2011) as a way to characterize the running times of stochastic algorithms for combinatorial optimization.

Aiex et al. (2007) described a Perl program to create TTTplots for measuring times that are assumed to fit a shifted exponential distribution, closely following Aiex et al. (2002). Such plots are very useful to compare different algorithms or strategies for solving a given problem and have been widely used as a tool for algorithm design and comparison.

For a better comparison among the variants, their empirical probability curves were superimposed. On the first experiment, the algorithms were applied to the test problem

opm1, the target was set at 230.00 (2% of optimal value), Figure 4.2a. In the second one, the algorithms were applied to the instance opm8, the target was set at 164,024.00 (0.0033% of optimal value), Figure 4.2b. A battery of 100 executions was made and the performance ended only when the algorithm had found the target value. These times were then sorted in ascending order, and for each algorithm, were associated with the i-th largest running time t_i, a probability $p_i^{TTTplots} = (i - 1/2)/N$ and plot the points $z_i = (t_i, p_i^{TTTplots})$, for each $i = 1, ..., N$. The results of the experiments are shown in Figs. 4.2a and 4.2b.

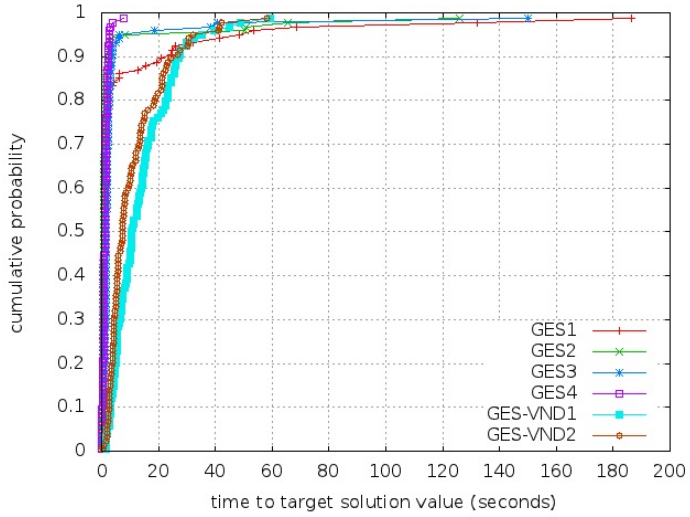

(a) opm1 Instance

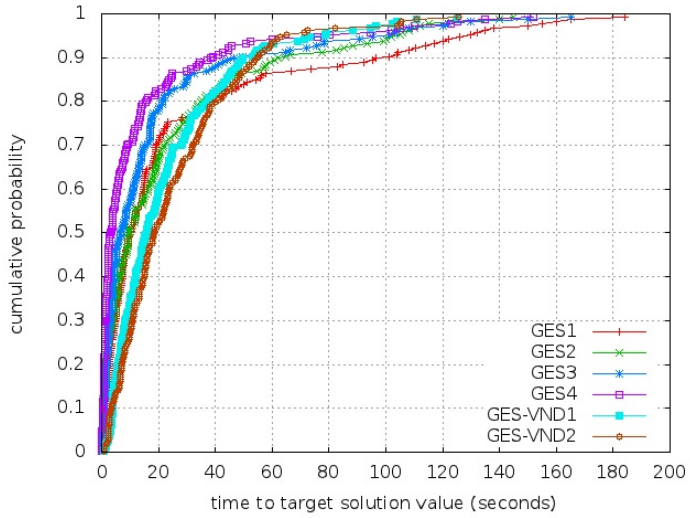

(b) opm8 Instance

Figure 4.2: Superimposed empirical distribution

Table 4.3: Convergence of the estimation of $Pr(X_i \leq X_j)$

	GES1	GES2	GES3	GES4	GES1-VND	GES2-VND
GES1		48.23%	42.74%	32.17%	66.34%	63.13%
GES2	50.16%		43.77%	34.19%	65.58%	62.65%
GES3	56.05%	53.94%		**37.68%**	72.52%	69.91%
GES4	**65.68%**	**61.72%**	**59.25%**		**80.28%**	**78.68%**
GES1-VND	33.52%	34.15%	27.28%	19.36%		45.85%
GES2-VND	36.83%	37.27%	30.02%	21.20%	54.15%	

Analyzing the empirical probability curves, it is possible to see that the variants that used the selection strategy $(\mu + \lambda)$ prevailed over the versions that used the selection (μ, λ). This fact shows that the competition between parents and offspring made those individuals with a good optimality potential persist for more generations. This result is consistent with the report of Herdy (1992), recommending the use of the $(\mu+\lambda)$ selection in discrete finite size search spaces.

In Figure 4.2a there is a total supremacy of the GES4, achieved by its selection strategy $(\mu + \lambda)$ combined with population size $\mu = 100$ and $\lambda = 600$. Since the initial instants of the search, the variant GES4 was able to generate better solutions than the other algorithms proposed. However, analyzing the curves of Figure 4.2b, one can notice that from 60 seconds and on, GES4 lost its performance being surpassed by the variant GES2-VND, which continues to progress systematically, being the first to reach the desired target with a probability of approximately 100%.

In order to deal with the situation shown in Figure 4.2b, a probability experiment according to Ribeiro & Rosseti (2009) is presented. Let A1 and A2 be two stochastic search algorithms applied to the same problem and let X1 and X2, be the continuous random variable represeting the time required for algorithm A1 and A2, respectively, to find a solution as good as the given target. Ribeiro & Rosseti (2009) developed a numerical tool to calculate the probability of the runtime of the algorithm A1 being less than or equal to the runtime of the algorithm A2, that is, $Pr(X_1 \leq X_2)$. This tool approximates the absolute error in the integration, by selecting appropriate value of ϵ. The latter optimizes the resulting approximation errors, called $\Delta(\epsilon)$, in order to make it sufficiently small. Using this tool to validate the analysis of the empirical experiment in Figure 4.2b, the Table 4.3 was generated.

Analyzing Table 4.3, it appears that even though the variant GES2-VND has a greater probability of finding the target starting from 60 seconds of execution, the variant GES4 has a probability of 78.68% to have the runtime less than or equal to the variant GES2-VND. In addition, it's clear that the variant GES4 outperforms all other variants.

This first set of experiment allows us to define, at least, a first set of parameters for the hybrid self-adaptive GES able to converge in a similar computational time than the one used by the literature. From now on, the variant GES4 will simply be named GES.

Evolution strategy self-adaptive mechanism

In order to verify the effect of the maximum number of application for each NS of the OPMOP, a first batch of experiments composed of 1800 executions, 225 for each of the eight instances, was performed with different limits nap_k (as presented in Section 4.2.1). Objective functions were normalized for each instance and an Analysis of Variance (ANOVA) test (Shapiro & Wilk 1964) was done for analyzing the differences between the limits nap_k. Figure 4.3 shows an effect plot with limits $nap_k = 1$, $nap_k = 15$, $nap_k = 100$, $nap_k = 1000$, for $k = 1, ..., 8$. As can be noticed, the only significant difference detected, with 95% confidence level, was the worse performance of the GES with strict limits $nap_k = 1$. Even though I believe that the model could be free to adapt the NS application naturally, thus, we might had left it with a large number $nap_k = 1000$. However, in order to keep the disturbances slighter, the maximum number of application for each nap_k as 15 was kept.

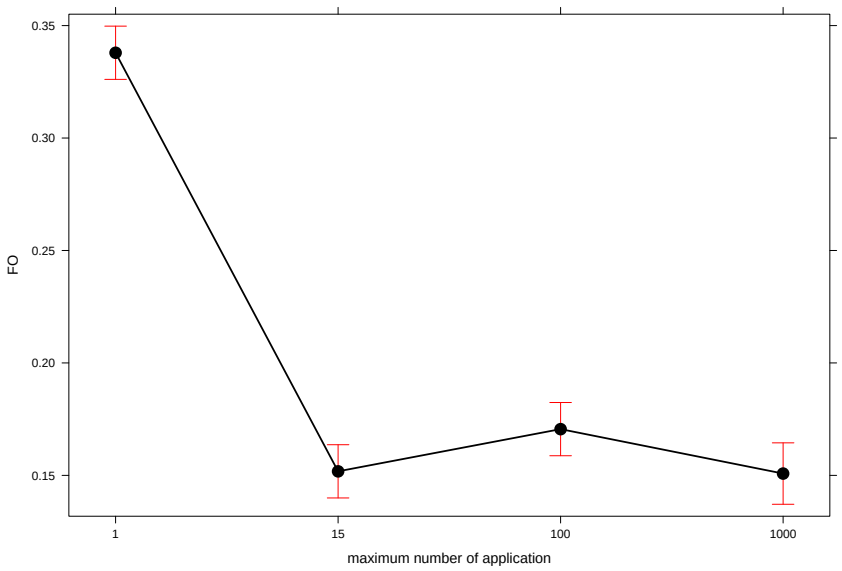

Figure 4.3: Effect of the maximum number of application nap_k for each NS

Instance opm1 was now solved and the mean values of the mutation vectors of typical 120 seconds execution are reported. The mutation operators were able to adapt its application probability during the evolutionary process, as can be seen in the Figure 4.4.

A special relationship was detected between some NS, thus, two other plots (Figures 4.5a and 4.5b), were generated focusing only in the specific ability of combining NS. As described in Section 4.3.3, the neighborhood $NS^{LD}(s)$ is able to swap shovels from different active pits. Due to the different ore composition between pits, it is interesting to reallocate trips for improving the final quality of the mixture after a swap done by $NS^{LD}(s)$. The GES was able to increase the number of moves from the neighborhood $NS^{TP}(s)$ at the same time that the probability of applying swaps from $NS^{LD}(s)$ increased. This was an interesting fact, since it was verified that improvements on the trip allocation had to be performed and $NS^{TP}(s)$ was able to attend these changes respecting the other pits, shovels and trucks.

Another interesting behavior of the mutation operators was detected between the neighborhood $NS^{PO}(s)$, able to remove a pit from operation, and the neighborhoods that deal with trucks trips $NS^{TP}(s)$ and $NS^{TT}(s)$. Again, GES was able to take profit of free trips from the trucks now free due to the higher probability of using $NS^{PO}(s)$ moves.

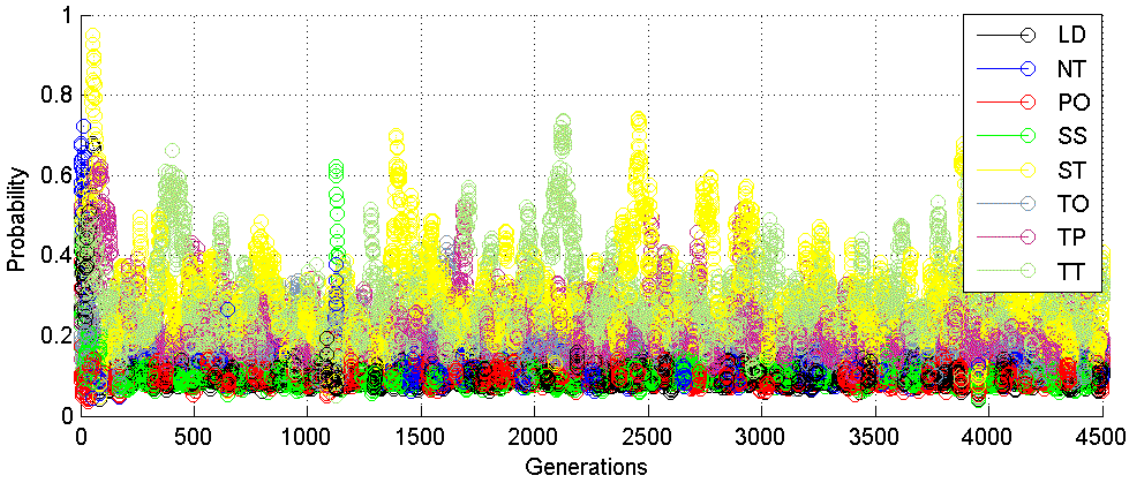

Figure 4.4: Mutation operators evolution – OPMOP

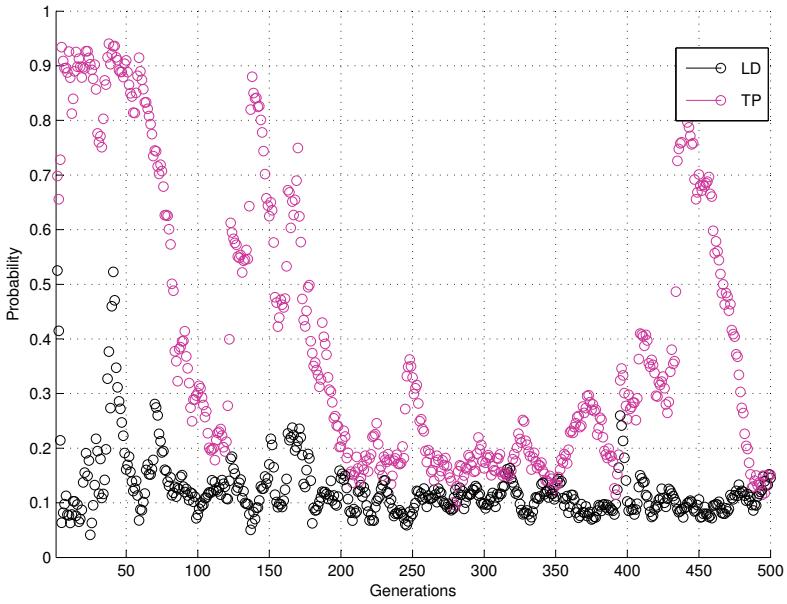

(a) Operators NS^{LD} and NS^{TP}

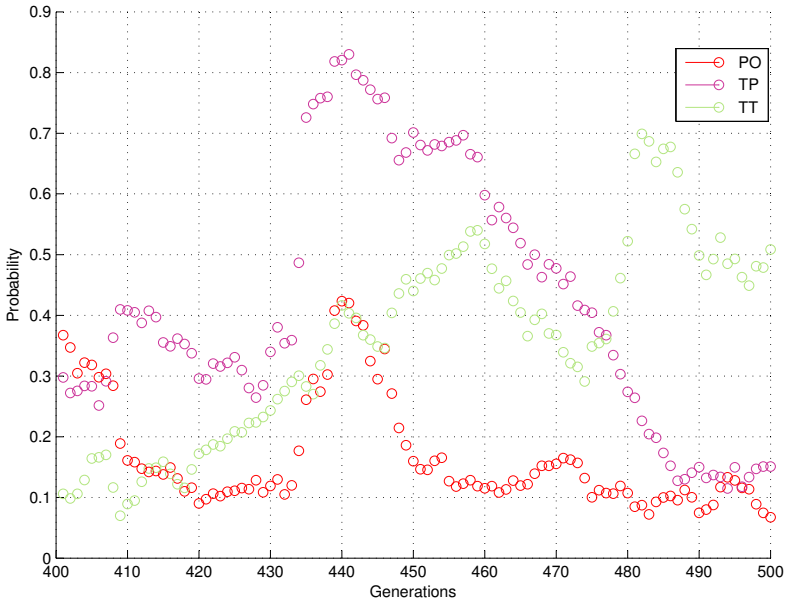

(b) Operators NS^{PO}, NS^{TP} and NS^{TT}

Figure 4.5: Mutation operators evolution

4.4 Short Term Load Forecasting Problem

The importance of load forecasting has been increasing lately and improving the use of energy resources remains a great challenge to the emerging Smart Grid (SG) systems.

Energy consumption forecasting in the context of economic development of a country was highlighted by Lee & Tong (2011). SG are considered as the future of power grids, able to manage production, transmission and electricity distribution. The task of optimizing the SGs has been mainly done by using Artificial Intelligence (AI) technique (Raza & Khosravi 2015, Olivares et al. 2014b, Rigo-Mariani et al. 2014).

In this sense, improving the calibration of a forecasting model trough the aid of an evolutionary algorithm seems reasonable. Here, the ability of the GES in calibrating the Hybrid Forecasting Model (HFM) introduced in Chapter 3 is verified. In its initial version, model's fuzzy rules were being calibrated by a trajectory search based algorithm and a classic evolution strategy using a mutation matrix fulfilled with standard deviations.

This problem will be used as a didactic case of study that combines the use of nine different NS. An acceptable convergence of the model is checked and verified in Section 4.4.3.

4.4.1 Representation and evaluation of a solution

A solution to the HFM is represented as a matrix of continuous values indicating fuzzy rules intervals and, respective, weights. An example of a solution representation s with three columns can be seen in Figure 4.6. For the batch of experiments analyzing the mutation operators, a solution with several different inputs, and approximately 1000 columns to be calibrated, will be used.

$$s = \left[\begin{array}{c|ccc} & z(K-1) & z(K-2) & \frac{z(K-1)+z(K-2)}{2} \\ A & 87 & 95 & 103 \\ V & 70 & 80 & 95 \\ B & 100 & 90 & 110 \\ W & 110 & 50 & 80 \end{array}\right]$$

Figure 4.6: Metaheuristic fuzzy model solution

The evaluating process is simple, the solution depicted in Figure 4.6 is evaluated by its ability in forecasting a given validation historical load time series. The rules of the matrix are applied considering previous measured data. Results of the combination of all rules and its weights give the next point forecast. These are very similar to artificial neural network based models (Drezga & Rahman 1999) and fuzzy time series (Song &

Chissom 1993). Errors between each forecast and the real measured point from the validation set are calculated using quality indicators (Goodwin & Lawton 1999).

4.4.2 Neighborhood structures

New didactic NS able to change each cell of the fuzzy matrix s with a disturbance X are designed. The NS will be called $NS^{add_X}(s)$ and is described below:

Movement add X – $NS^{add_X}(s)$: This move increase or decrease the value of a random cell of the rules and weights matrix of a solution s.

From this proposed NS, nine different structures with different disturbances parameters X are genered: $NS^{add_{0.1}}(s)$, $NS^{add_1}(s)$, $NS^{add_{\frac{M}{15}}}(s)$, $NS^{add_{\frac{M}{6}}}(s)$, $NS^{add_{\frac{M}{2}}}(s)$, $NS^{add_M}(s)$, $NS^{add_{2M}}(s)$, $NS^{add_{5M}}(s)$ and $NS^{add_{BM}}(s)$. Some of them use the average values of the historical load time series, namely M, as disturbance value. The special character B in $NS^{add_{BM}}(s)$ indicates a big value multiplied by the average M.

4.4.3 Computational experiments and analysis

Computational experiments were carried on a Intel Core i7-3537U CPU (2.00GHz), with 4GB of RAM, operating system Ubuntu 14.04. For simplicity, the configuration achieved after the OPMOP TTTplots calibration (Section 4.3.4) and confirmed in literature instances is used here.

The dataset used to check the mutation operators was kindly provided by Liu et al. (2014). It is composed of a microgrid user data from small residential area with maximum load of 273 KW. The dataset is composed of 1368 hourly samples for training and 672 samples used as blind validation. Section 4.4.3 reports obtained Mean Absolute Percentage Error – MAPE for the validation set, as a way of certifying the success of the GES in calibrating the metaheuristic fuzzy model.

Evolution strategy self-adaptive mechanism

A first batch of two minutes training, typical for online microgrids load forecasting, was performed and the behavior of the mutation operators are discussed in Figures 4.7, 4.8a and 4.8b.

Figure 4.7 plots the vector of probability multiplied by the current number of application of each NS, average values for the population are presented for each generation. The ability of the GES mutation mechanism in regulate the probability of the NS regarding to its power of disturbance is highlighted. Moves that slightly change the solution

matrix s are the most likely to be applied, as the case of $NS^{add_{0.1}}(s)$, $NS^{add_1}(s)$ and $NS^{add_{\frac{M}{15}}}(s)$. On the other hand, $NS^{add_{BM}}(s)$ was adapted and adjusted, through the generations, to be rarely applied.

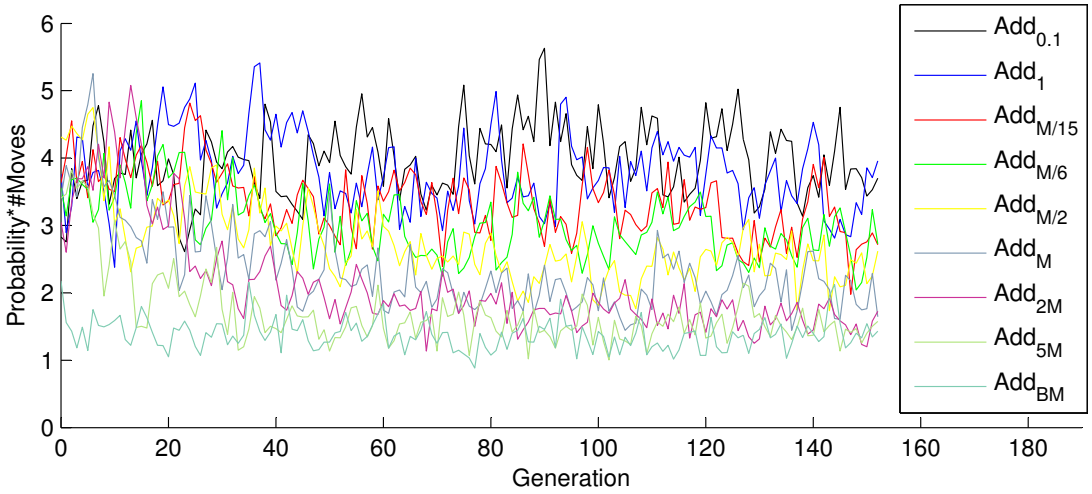

Figure 4.7: Mutation operators evolution $P \times A$ – STLFP

Figures 4.8b and 4.8a show groups of NS aggregated regarding to the impact they have in mutating the solutions.

The stem plot (Figure 4.8b) shows the higher number of moves that are applied for some NS and differences between application probabilities.

Another batch with two hour training was performed. Figure 4.9a shows the average values with $nap_k = 15 \quad \forall \quad k = 1, ..., 8$ and Figure 4.9b presents the results for a larger nap limit of 1000. We highlight that the operators seldom present slopes with higher probabilities and more moves applications. Specially, for the neighborhood $NS^{add_{BM}}(s)$ it happened in both cases, but few generations later it converged to a steady state, returning the average values of the population to low values of application probability. Even after the 3000 generation, Figure 4.9b, we believe that the number of applications would follow the same decrease after some generations.

GES convergence

A batch of 30 executions for the aforementioned dataset was executed and average MAPE errors of 9.5%, 8.5%, 9.8% and 8.2% were obtained for the 1st, 2nd, 3rd and 4th week, respectively. Thus, as described by Liu et al. (2014), it is known that when the MAPE is less than 10%, the applicability of the forecast model over microgrids becomes interesting and does not increase its cost sharply. The obtained results indicate, again,

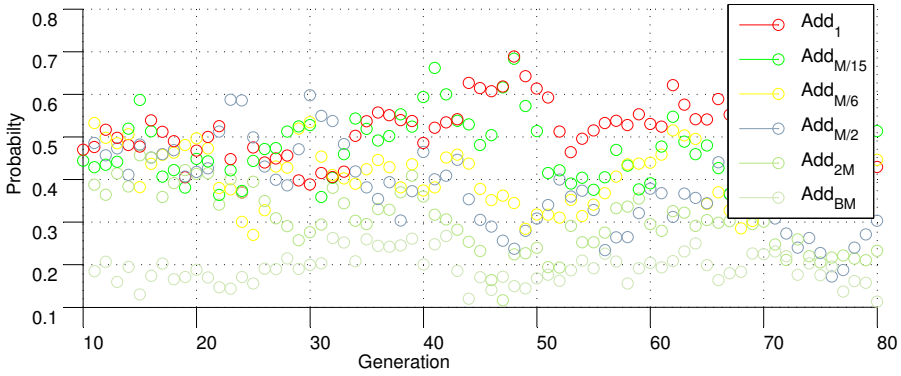

(a) Application probability of specific NS

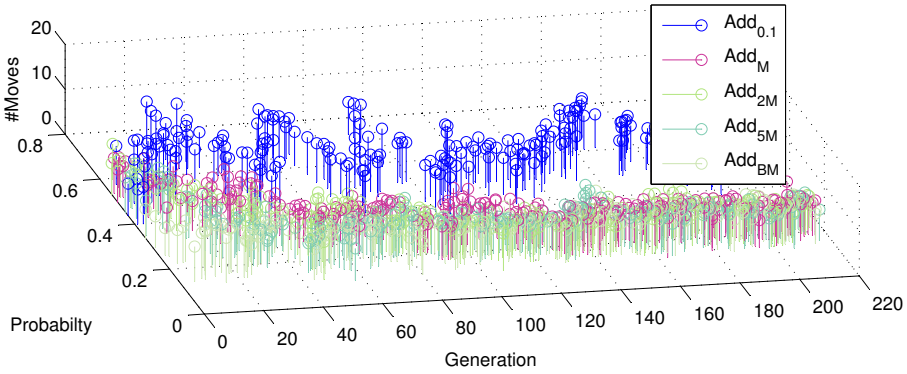

(b) Stem plot showing NS groups

Figure 4.8: Analysis of NS in STLFP

the ability of the GES in calibrating the matrix of weights and rules and achieve useful forecasting models.

4.5 Unrelated Parallel Machine Scheduling Problem with Setup Times

The UPMSP-ST tackled here has as the main goal the makespan minimization. This problem has great practical and theoretical importance. It belongs to the $\mathcal{NP}$-hard class, since it can be seen as a generalization of Parallel Machine Scheduling Problem with Identical Machines and without Setup Times (Garey & Johnson 1979). The UPMSP-ST is found in different industry sectors, such as: textile, chemicals, painting, semiconductors and paper production (Rabadi et al. 2006).

In the UPMSP-ST there is a set of N jobs and a set of M machines, with the

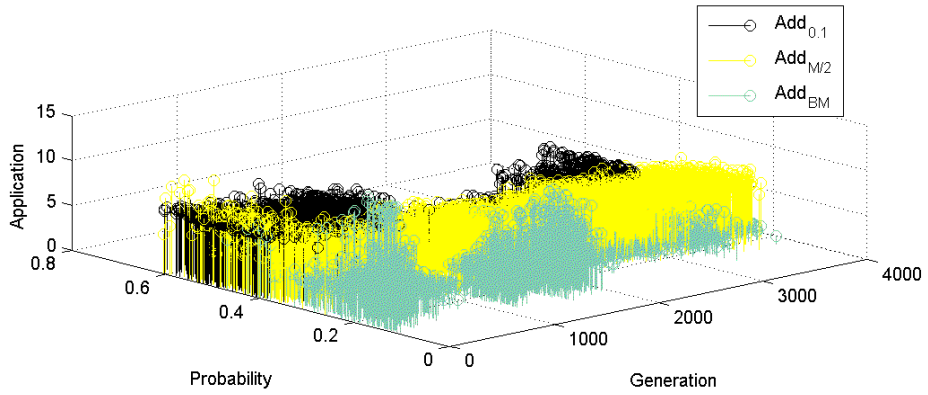

(a) Training with lower limits for nap_k

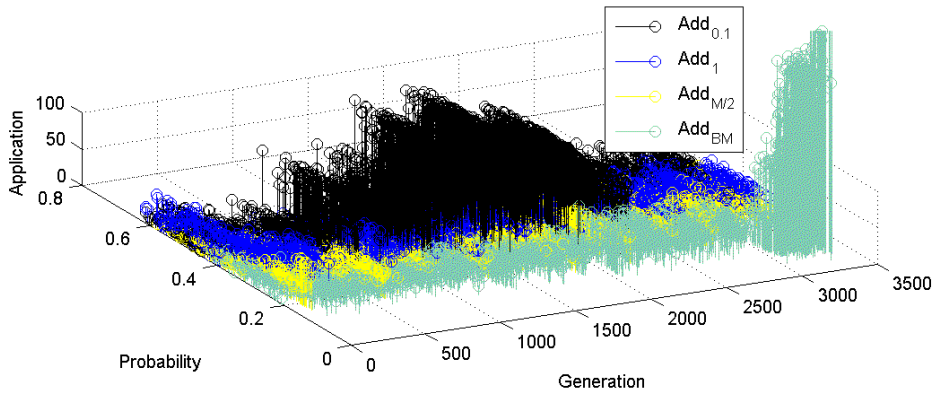

(b) Training with large limits for nap_k

Figure 4.9: Two hour training results

following features: *i*) each job must be allocated to only one machine; *ii*) each job j has a different processing time p_{ij} for each machine $i \in M$; *iii*) there is also a setup time S_{ijk} for calibrating the machine i after processing job j and before processing job k; *iv*) there is a calibration time S_{i0j} for processing the first job of a given machine $i \in M$.

Different approaches were used for solving the UPMSP-ST, initially, in (Al-Salem 2004), the authors developed a heuristic procedure called Partitioning Heuristic and introduced the UPMSP-ST. (Rabadi et al. 2006) proposed a metaheuristic for random prioritized search and described a mathematical formulation for the problem. In Ying et al. (2012), a Simulated Annealing algorithm was implemented with a smart strategy for eliminating unpromising jobs. Vallada & Ruiz (2011) analyzed two genetic algorithms

and published a benchmark set of instances at SOA website: http://soa.iti.es/problem-instances. In the works of Haddad et al. (2014), Cota, Haddad, Souza & Coelho (2014), Cota, Haddad, Souza & Martins (2014), Haddad et al. (2015), the authors proposed several trajectory search based algorithms, named: AIV, AIRP, AIA and HIVP, respectively. These methods were designed based on the ILS and VND, which obtained better results than Vallada & Ruiz (2011), and among them, AIRP had the best performance. The AIRP combines a greedy constructive procedure with the ILS and RIV (described in Section 4.5.2) metaheuristics. Also, periodically, the search is intensified and diversified by a Path Relinking (Glover 1996b) procedure. In this sense, comparing the proposed evolutionary framework against the AIRP, Section 4.5.3, is reasonable.

4.5.1 Representation and evaluation of a solution

A solution s for the UPMSP-ST is represented as a vector of integers with m positions, where each position represents one machine. Each active machine is associated with a list containing all jobs allocated to it.

Figure 4.10a shows an example of a possible scheduling for a instance with two machines and six jobs. In this example, machine M_1 will process jobs $3, 5$ and 1, in this order; and machine M_2, in turn, will process $4, 2$ and 6, following this order. The conclusion time of machine M_1 is calculated by the expression $C_{M_1} = 1+28+3+38+8+1 = 79$, while machine M_2 conclusion time is given by $C_{M_2} = 2+17+7+21+2+48 = 97$.

Figure 4.10b illustrates the solution representation of the example given in Figure 4.10a. Jobs $3, 5$ and 1 are scheduled to machine M_1 while the rest are scheduled to M_2.

In this single objective optimization, solution s is evaluated by the makespan, in other words, by the processing time of the last machine to finishes its jobs.

4.5.2 Neighborhood structures

Three well-know NS are tested in this application and they are described below:

Movement Swap In The Same Machine – $\boldsymbol{NS^{SSM}(s)}$: The movement of swapping jobs in the same machine originates a $N^{SSM}(s)$ neighborhood. It consists in changing the positions of two jobs that belong to the same machine.

Figure 4.11a illustrates the swap of jobs 5 and 6 in machine M_2.

Movement Swap Between Different Machines – $\boldsymbol{NS^{SMD}(.)}$: Similar to the $NS^{SSM}(s)$, but swapping one job from one machine with another job that belongs to a

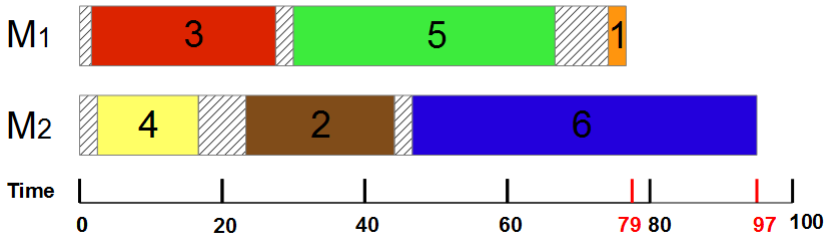

(a) Example of a possible scheduling

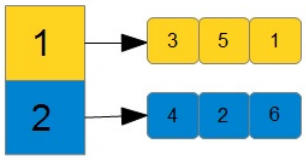

(b) Solution representation

Figure 4.10: Example of solution representation

different machine.

Multiple Insertion – $N^{MI}(.)$: It consists on relocating one job from one machine to any position of all machines.

Figure 4.11b shows how $N^{MI}(.)$ works, job 4 from machine M_2 is transferred to machine M_1, just before job 1.

RIV as an optional local search intensification phase

The optional local search phase of the GES, Line 17 of the Algorithm 4.1, activates the proposal of Cota, Haddad, Souza & Coelho (2014), namely RIV. The latter is inspired by the ILS with a Random VND.

The RIV uses the neighborhoods $N^{MI}(.)$ and $NS^{SSM}(s)$ with first and best improvements strategies, respectively, and explores, sporadically, the $NS^{SMD}(.)$ neighborhood for perturbing the solutions.

4.5.3 Computational experiments and analysis

The proposed algorithm for the UPMSP-ST was implemented in JAVA using the Netbeans 8.0.2 IDE. Computational experiments were carried on a Core i7 (1.9 GHz) with 6GB of RAM and Windows 7.

The method was re-implemented, following OptFrame first version in C++, and the

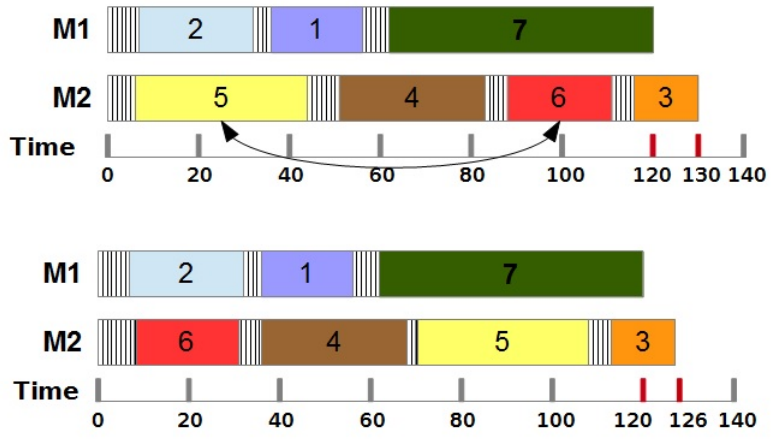

(a) Swap in same machine

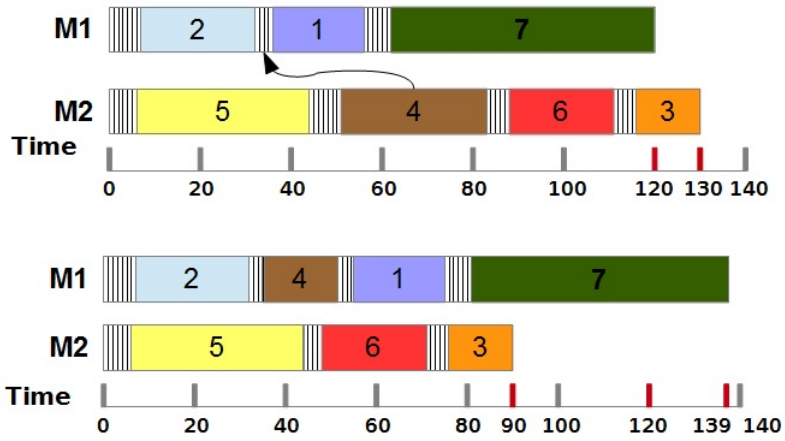

(b) Multiple Insertion

Figure 4.11: Example of operators

ideas introduced in Section 4.2. This seems to be a good opportunity for analyzing and ensuring the convergence of the proposal in a different environment, considering new codes programmed in a similar language.

Benchmark results

Eight different configurations of the GES algorithm were designed, as described in Table 4.4. Six, among these variants, were allowed to activate RIV local search in $\kappa = 3$ individuals from the offspring population, picked at random (See Section 4.3.4). The other two variants, with the same population size as the ones used for the previous cases of study, were analyzed without the RIV intensification phase.

Table 4.4: GES proposed variants for the UPMSP-ST

Acronym	μ	λ	Selection	RVI
GES_1	50	150	$(\mu + \lambda)$	$\surd$
GES_2	20	60	$(\mu + \lambda)$	$\surd$
GES_3	50	150	(μ, λ)	$\surd$
GES_4	20	60	(μ, λ)	$\surd$
GES_5	100	600	$(\mu + \lambda)$	$\surd$
GES_6	100	600	(μ, λ)	$\surd$
GES_7	100	600	$(\mu + \lambda)$	
GES_8	100	600	(μ, λ)	

The stopping criterion adopted was the processing time, given by: $executionTime = n \times (m/2) \times t$ milliseconds, being n the total number of jobs, m the total number of machines and three different values for t (10, 30 and 50). These values adopted for t were the same ones by Cota, Haddad, Souza & Coelho (2014).

A batch of 30 executions was performed using 36 SOA instances. These instances involve combinations of 50, 100 and 150 jobs with 10, 15 and 20 machines. The average values of each instance were calculated and the deviations between the best results for each instance were measured. Due to the stochastic character of the search, the different GES configurations were executed 30 times for each instance and for each t value, as already has been done for the AIRP.

Figure 4.12 shows a box plot graph with average objective function values.

It is noteworthy that the selection strategy $(\mu + \lambda)$ was again able to direct the evolutionary process to better performance. Even though the were able to obtain better solutions (10% better) than the ones found by the AIRP. This fact shows the potential of the proposal to combine NS and to find new solutions in the search space.

It should be noticed that the two variants with the intensification procedure RIV achieved better average objective function values. This fact induces that the RIV procedure was well designed by Cota, Haddad, Souza & Coelho (2014), being able to collaborate within the search as an intensification phase. Furthermore, it gives a brief motivation for using other smart strategies, based on metaheuristic procedures, in partnership with the proposed GES.

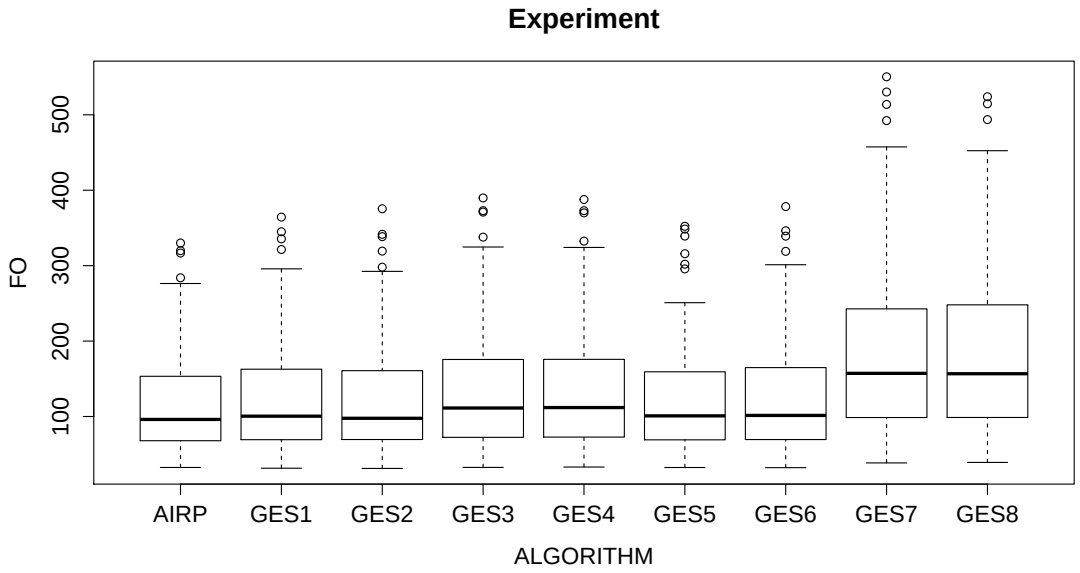

Figure 4.12: Box plot of the algorithms AIRP, GES_1, GES_2, GES_3, GES_4, GES_5, GES_6, GES_7 and GES_8.

Evolution strategy self-adaptive mechanism

Three different sizes of instances (large, medium and small size) were used for analyzing the mutation operators. Parameters $\mu = 100$ and $\lambda = 600$ were kept for this analysis. We aim now at two variants, verifying the convergence with and without the RIV intensification phase. For the sake of clarity, the best results among the two independent runs (using different seeds) are depicted in Figures 4.13, 4.14 and 4.15.

In these Figures, the lower bounds (some are optimum values) were plotted for enhancing bounds comprehension of the mutation operators behavior. The evaluation of the best known solution can be followed across the generations, exhibited with blue lines. Values were normalized for each of the three instances by dividing them by the maximum makespan found in the first generation.

The convergence of the variant using RVI was close to the lower bound in all executions. Figure 4.13 shows how operators keep trying to escape from local optimum, considerably improving the best known solution until the generation 150.

Figure 4.14 depicts an execution applied for solving a medium size instance, in which the population was guided only by the ARVNS. Analyzing Figure 4.14b, it can be verified that the mutation operators suffered an intensive change after the generation 50. This

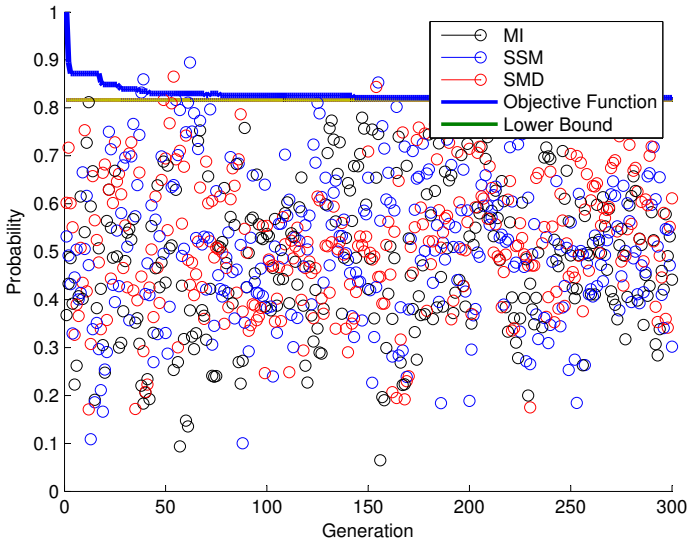

Figure 4.13: Average mutation operators values evolution in a Large instance of the UPMSP-ST using $\kappa = 3$

fact might had happened because of a local trap, which the population was able to escape near the generation 600 (Figure 4.14a). Four other improvements were also achieved from generation 600 until 1000.

Beyond shadow of doubt, it can be noted that the mutation operators become more randomized after finding local traps. For the cases showed in Figures 4.15a and 4.15b, both variants were able to reach the global optimum after generations 30 and 20, respectively.

4.6 Conclusions and extensions

A new hybrid self-adaptive algorithm based on the concepts of evolution strategies was introduced in this chapter. Three different combinatorial optimization problems were used as cases of study. For each of them, algorithm convergence and mutation operators behavior were analyzed.

The results have shown that the proposed evolutionary method is able to achieve competitive solutions. Even though the average performance of the GES, applied to the UPMSP-ST, was not considerably better than the literature, it was able to enhance the quality of the solutions in 10% of the analyzed problems.

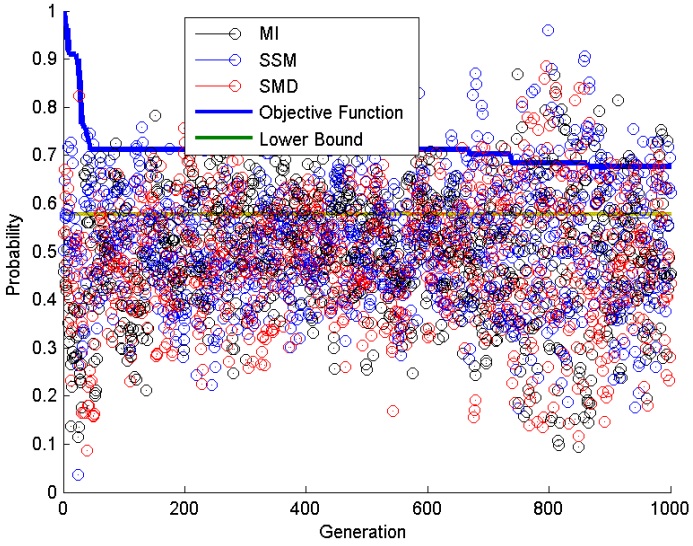

(a) From generations 1 to 1000

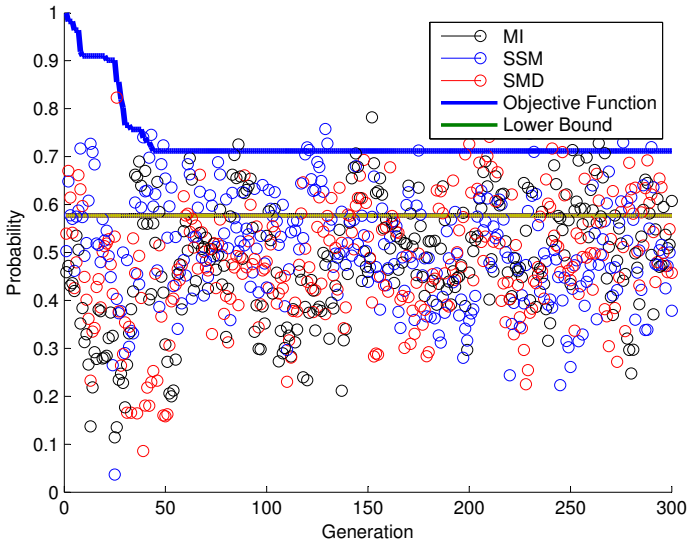

(b) From generations 1 to 300

Figure 4.14: Average mutation operators values evolution on a Medium instance of the UPMSP-ST without using RVI

The ability of adapting the probabilities of application was also verified in each of the three analyzed problems. The operators handled different NS and its application across different phases of the evolution process. The flexibility of the proposal makes it suitable for a wide area of practical applications, such as, in mining, scheduling and

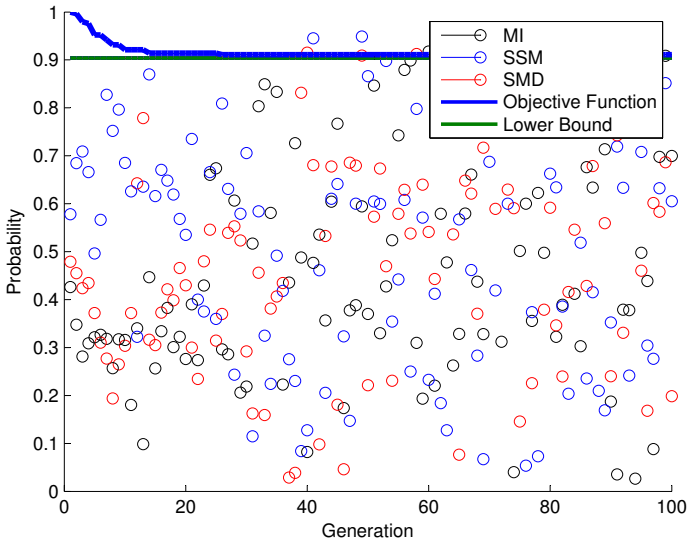

(a) Without RVI

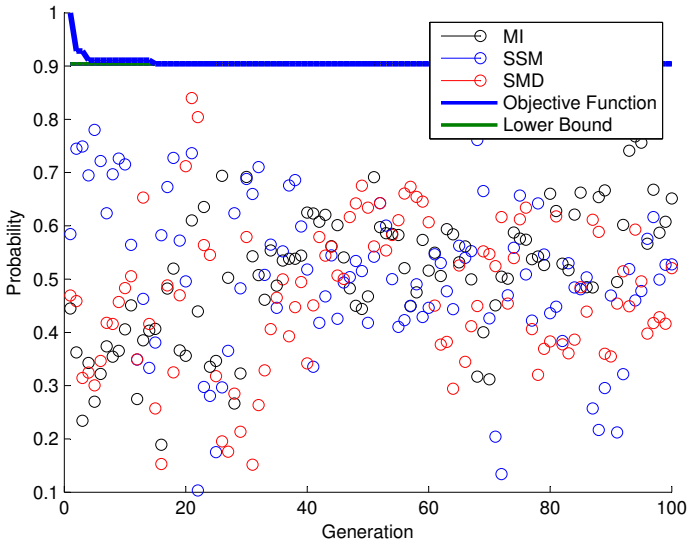

(b) With RVI

Figure 4.15: Average mutation operators values evolution on a small instance of the UPMSP-ST

electric load forecasting.

As could be verified, the self-adaptive ES was able to adapt the mutation operators in such a way that there is a balance between exploration and exploitation throughout the generations of the evolutionary process, being able to escape from local optima attraction

basins. This ability is related to the issue of performing small changes in the solution for finding local optima, and, on the other hand, enhancing the probability and strength of the mutation operators reflects in increasing the shaking and hence escaping from local traps. This fact promoted a self-adaptive balance between exploiting an attraction basin and jumping out of it.

Further experiments should focus on how close are the solutions from local optima. Thus, future works might investigate the fitness landscape of the problems discussed here. Improving and designing novel self-adaptive mechanisms is other possible extension, as well as parameter calibration. Finally, we suggest to implement a parallel version of the GES algorithm in order to take advantage of multi-core technology available in current devices.

Chapter 5

Multi-objective microgrid storage planning problem

"A natureza pode suprir todas as necessidades do homem, menos a sua ganância e busca pelo conhecimento divino.
Truth is god."
— Mahatma Gandhi

This chapter describes the proposed framework developed and used to solve the multi-objective energy storage planning problem. Section 5.1 presents the mathematical formulation developed in this thesis, as well as a description of the three main objective functions to be minimized. Section 5.2 introduces three other objective functions, criteria, used to evaluate energy storage schedule behavior in extreme and different scenarios. Section 5.3 introduces the proposed matheuristic pool search algorithm. Finally, Section 5.4 draws some final considerations and conclusions regarding the proposed problem, its mathematical formulation and the matheuristic.

5.1 Mathematical programming model

A MILP model was developed for optimizing an objective function based on the linear combination of three different energy storage planning objectives.

The following parameters were considered for the model:

$\boldsymbol{I}$**:** Set of discrete intervals from 1 to furthest desired storage time horizon k;

$\boldsymbol{q_i^d}$**:** demand of all customers at the interval $i \in I$;

$\boldsymbol{q_i^{rG}}$**:** indicates the energy production of all renewable energy resources at the interval $i \in I$;

$\boldsymbol{q_i^{sell}}$**:** energy selling price at the interval $i \in I$;

$\boldsymbol{q_i^{buy}}$**:** energy buying price at the interval $i \in I$;

$\boldsymbol{PEV}$**:** set of plug-in electric vehicles;

$\boldsymbol{pev_v^{SOC_{min}}}$**:** indicates the minimum Depth of Discharge (DoD) of the vehicle v;

$\boldsymbol{pev_v^{Power}}$**:** indicates PEV battery maximum capacity;

$\boldsymbol{pev_{vi}^{a}}$**:** indicates if the vehicle v is available at the SmartPark at the interval $i \in I$;

$\boldsymbol{pev_{vi}^{arr}}$**:** indicates if the vehicle v is arriving at the SmartPark at the interval $i \in I$;

$\boldsymbol{pev_{vi}^{SOC_{arr}}}$**:** indicates the battery percentage of the vehicle v at its arrival at the interval $i \in I$, obviously, only if $pev_{vi}^{arr} = 1$, otherwise it does not need to be attended;

$\boldsymbol{pev_{vi}^{dep}}$**:** indicates if the vehicle v is departing from the SmartPark at the interval $i \in I$;

$\boldsymbol{pev_{vi}^{SOC_{dep}}}$**:** indicates the battery percentage demanded by the vehicle v at its departure at the interval $i \in I$, only if $pev_{vi}^{dep} = 1$, otherwise it does not need to be attended;

$\boldsymbol{C}$**:** set of different battery cycles;

$\boldsymbol{pev_{vc}^{dRate}}$: battery discharge rate of the plug-in vehicle v with power cycle c.

$\boldsymbol{pev_{vc}^{dPrice}}$: price for discharging the battery of the plug-in vehicle v at a rate pev_{vc}^{dRate};

$\boldsymbol{pev_{vc}^{cRate}}$**:** indicates the charge rate of the vehicle v;

$\boldsymbol{pev_{vc}^{cPrice}}$: price for charging the battery of the plug-in vehicle v at a rate of charge cycle pev_{vc}^{cRate}.

The following decision variables were defined:

$\boldsymbol{y_{vci}^{c}}$: binary variable which indicates if the vehicle v is charging with power cycle c at the interval $i \in I$;

$\boldsymbol{y^{d}_{vci}}$: binary variable which indicates if the vehicle v is discharging with power cycle c at the interval $i \in I$;

Finally, some auxiliary decision variables are used for checking the constraints:

$\boldsymbol{y^{bR}_{vi}}$: variable with real values indicating the battery rate of the PEV v at the interval $i \in I$;

$\boldsymbol{e^{sell}_{i}}$: variable with real values indicating the amount of energy being sold at the interval $i \in I$;

$\boldsymbol{e^{buy}_{i}}$: variable with real values indicating the amount of energy being bought at the interval $i \in I$;

$\boldsymbol{e^{sellActive}_{i}}$: binary variable which indicates if any energy is being sold at the interval $i \in I$;

$\boldsymbol{e^{buyActive}_{i}}$: binary variable which indicates if any energy is being bought at the interval $i \in I$;

$\boldsymbol{tCD}$**:** real variable indicating the total charging and discharging expenses;

$\boldsymbol{f_{objTotalCost}}$**:** real variable indicating objective function that measures the MG total costs;

$\boldsymbol{f_{objBatteriesUse}}$**:** real variable indicating objective function that measures batteries use;

$\boldsymbol{f_{objMaxPeakLoad}}$**:** real variable indicating objective function that measures maximum peak load during the whole set of intervals $i \in I$.

The mathematical model proposed in this thesis can be seen from Eqs. (5.1) to (5.17). The global objective function to be minimized (Eq. (5.1)) is composed of the linear combination of three different objective functions, described in Eqs. (5.2), (5.3) and (5.4). Total MG cost (Eq. (5.2)) is measured by the total amount of energy that is being bought or sold at each interval $i \in I$ plus the cost associated with each vehicle charge or discharge, these two latter are paid to the PEVs owners (its calculation is described in Eq. (5.8)). Batteries use (Eq. (5.3)) is calculated as the sum of charges and discharges scheduled during the whole energy storage planning. Eq. (5.4) assigns the maximum peak load of the MG system to the value of the third objective function.

Eqs. (5.5), (5.6) and (5.7) force the system to either only buy or sell energy at each interval. Eq. (5.9) forces the PEVs to only either charge or discharge while Eqs. (5.10) and (5.11) make them charge or discharge only when PEVs are available at the SmartPark. Battery SOC limits, $pev_v^{SOC_{min}} \leq y_{vi}^{bR} \leq 100$, are defined in Eqs. (5.12) and (5.13). Eq. (5.14) ensures that PEVs' batteries will attend a minimum SOC wished at its departure. PEV's battery rate is updated according to Eqs. (5.15) and (5.16). Eq. (5.15) attends the special case of the first interval while Eq. (5.16) takes the rate of the last battery, if the vehicle is not arriving, and add or subtract energy from charges or discharges. Finally, in Eq. (5.17), the amount of energy that is being sold or bought, at each interval $i \in I$, is determined.

Finally, the set of M_i values, for each interval i, is calculated according to the maximum possible grid rates. The maximum rate of charge/discharge is considered and summed to the expected grid rate.

$$\text{minimize } \lambda_1 f_{objTotalCost} + \lambda_2 f_{objBatteriesUse} + \lambda_3 f_{objMaxPeakLoad} \tag{5.1}$$

S. T.:

$$f_{objTotalCost} = \sum_{i \in I} \left(e_i^{buy} q_i^{buy} - e_i^{sell} q_i^{sell} \right) + tCD \tag{5.2}$$

$$f_{objBatteriesUse} = \sum_{i \in I} \sum_{v \in PEV} \sum_{c \in C} \left(y_{vci}^{d} pev_{vc}^{dRate} + y_{vci}^{c} pev_{vc}^{cRate} \right) \tag{5.3}$$

$$f_{objMaxPeakLoad} \geq e^{buy} + e^{sell} \qquad \forall i \in I \tag{5.4}$$

$$e_i^{sellActive} * M_i \geq e^{sell} \qquad \forall i \in I \tag{5.5}$$

$$e_i^{buyActive} * M_i \geq e^{buy} \qquad \forall i \in I \tag{5.6}$$

$$e^{sellActive} + e^{buyActive} \leq 1 \qquad \forall i \in I \tag{5.7}$$

$$tCD = \sum_{i \in I} \sum_{v \in PEV} \sum_{c \in C} \left((y_{vci}^{d} pev_{vc}^{dPrice} + y_{vci}^{c} pev_{vc}^{cPrice}) pev_{v}^{Power} \right) \tag{5.8}$$

$$\sum_{c \in C} \left(y_{vci}^{d} + y_{vi}^{c} \right) \leq 1 \qquad \forall v \in PEV, i \in I \tag{5.9}$$

$$\sum_{c \in C} y_{vci}^{d} \leq pev_{vi}^{a} \qquad \forall v \in PEV, i \in I \tag{5.10}$$

$$\sum_{c \in C} y_{vci}^{c} \leq pev_{vi}^{a} \qquad \forall v \in PEV, i \in I \tag{5.11}$$

$$y_{vi}^{bR} \leq 100 \qquad \forall v \in PEV, i \in I \tag{5.12}$$

$$y_{vi}^{bR} \geq pev_{v}^{SOC_{min}} pev_{vi}^{a} \qquad \forall v \in PEV, i \in I \tag{5.13}$$

$$y_{vi}^{bR} \geq pev_{vi}^{SOC_{dep}} pev_{vi}^{dep} \qquad \forall v \in PEV, i \in I \tag{5.14}$$

$$\sum_{c \in C} y_{v1}^{bR} \leq pev_{v1}^{SOC_{arr}} pev_{v1}^{arr} + \sum_{c \in C} \left(y_{vci}^{d} pev_{vc}^{dRate} - y_{vci}^{c} pev_{vc}^{cRate} \right) \qquad \forall v \in PEV \tag{5.15}$$

$$\begin{aligned} \sum_{c \in C} y_{vi}^{bR} \leq{}& (1 - pev_{vi}^{arr}) y_{v(i-1)}^{bR} + pev_{vi}^{arr} pev_{vi}^{SOC_{arr}} \\ &+ \sum_{c \in C} \left(y_{vci}^{d} pev_{vc}^{dRate} - y_{vci}^{c} pev_{vc}^{cRate} \right) \\ &\forall v \in PEV, i \geq 2 \in I \end{aligned} \tag{5.16}$$

$$\begin{aligned} \sum_{v \in PEV} \sum_{c \in C} \left((y_{vci}^{d} pev_{vc}^{dRate} - y_{vci}^{c} pev_{vc}^{cRate}) pev_{v}^{Power} \right) + q_i^{rG} - q_i^{d} - \sum_{v \in PEV} \left(y_{vi}^{c} pev_{v}^{cRate} \right) \\ = e_i^{sell} - e_i^{buy} \qquad \forall i \in I \end{aligned} \tag{5.17}$$

5.2 Extreme energy storage scenarios

The energy storage schedule obtained by solving the mathematical model described in Section 5.1 is further evaluated regarding six criteria. The first three criteria are the three objectives used in the optimization problem, while three additional criteria are introduced in this section.

The fourth criterion, so-called $f_{objExtremeScenario}$, evaluates the schedule compared to the opposite case of it. In other words, a comparison of the total cost of the worst and the best case is made and the discrepancy is returned. It seeks to find solutions which are flexible to be applied even in extreme scenarios, that is, this criterion measures the robustness of the schedule. Thus, batteries charge and discharge schedule are kept and analyzed through the most different expected scenario.

Table 5.1 indicates some possible MG scenarios based on energy consumption, renewable energy production and main grid energy price. As can be seen, the worst possible case, regarding the total cost paid by the MG user, is the one when the consumption is the maximum possible (q_{99}) with the highest expected prices (q_{99}) and almost no renewable energy generation (q_1).

Section 6.3 explores the results when an energy storage schedule is performed considering the worst case scenario and the best case scenario happens and vice versa.

Table 5.1: MG scenarios based on probabilistic quartiles

	Current MG energy scenario		
scenario	consumption	production	price
worst case	q_{99}	q_1	q_{99}
best case	q_1	q_{99}	q_1
neutral	q_{50}	q_{50}	q_{50}

The fifth and sixth criteria, namely $f_{objSharpeRatioTotalCost}$, $f_{objSharpeRatioMaxLoad}$, evaluate the schedules over a wide range of possible scenarios and use the Sharpe Ratio to verify the total cost and maximum load volatility. Eqs. (5.18) and (5.19) measure Sharpe Ratio, known in the literature as reward-to-variability index, but, here, adapted and used as a cost-to-variability indicator.

The schedule with the highest expected cost and maximum peak loads is considered to be a constant risk-free return throughout the analyzed period. The optimum value

for objective function $f^*_{objBatteriesUse}$ provides this information, since it represents the solution where energy storage is performed only seeking to attend PEVs' constraints and save batteries use. This solution indicates an energy storage planning where all extra needed energy is bought from the main grid and the PEVs charge is scheduled to be done when the energy price is cheaper. In view that energy price can not guaranteed to be the cheapest, a small variability is also considered over $f^*_{objBatteriesUse}$. Thus, an adapted Sharpe Ratio (Ledoit & M. 2008) is designed, where the term $V_{f^*_{objBatteriesUse}}$ indicates volatility over the energy price (measured from probabilistic forecast variations from the time series depicted in Figure 6.4). Finally, volatility $V(f_{objTotalCost}(s))$ and $V(f_{objMaxPeakLoad}(s))$ are obtained from the standard deviation of objective functions $f_{objTotalCost}(s)$ and $f_{objMaxPeakLoad}(s)$, respectively, over a set of random scenarios. Random scenarios are generated from the combination of different quartiles of energy consumption, renewable energy production and energy prices. The behavior of the PEVs' scheduled charges and discharges of solution s are analyzed for each of those scenarios.

$$f_{SRTotalCost}(s) = \frac{f^*_{objBatteriesUse} - f_{objTotalCost}(s)}{V(f_{objTotalCost}(s)) - V_{f^*_{objBatteriesUse}}} \tag{5.18}$$

$$f_{SRMaxPeakLoad}(s) = \frac{f^*_{objBatteriesUse} - f_{objMaxPeakLoad}(s)}{V(f_{objMaxPeakLoad}(s)) - V_{f^*_{objBatteriesUse}}} \tag{5.19}$$

5.3 Smart Solution Pool Matheuristic

In order to find near efficient Pareto solutions for the MOMSPP in short computational time, we present the Smart Pool Search Matheuristic (SPSMH). The idea of SPSMH is to solve the mathematical model by using a commercial Black-Box solver for MILP problems with different weights for the three objective functions. This strategy is capable of providing a good balance between each of the objectives, by ensuring that a large number of weighted problems are solved. In particular, the current MILP model is searched in the branches of a Branch-and-Bound tree explored with CPLEX 12.5.1 Dynamic Search procedure.

Algorithm 5.1 presents the procedure used to generate weighted sum MILP problems, solve them, and filter the obtained solutions in order to create a Pareto front. MIP

starting solutions (line 5) are considered to be included in the beginning of the search done by the Black-Box solver. Several different MILP problems are generated by the linear combination of the weights λ_1, λ_2 and λ_3 (for each objective function). Since the handled MILP is convex, any Pareto-optimal solution regarding the objectives can be achieved by a specific combination of weights.

Algorithm 5.1: Smart Pool Search Matheuristic

Input: Number of linear combination intervals $nIntervals$, metaheuristic search time limit $timeLim$

Output: Set of non-dominated solutions Xe

1 $\Lambda = [0, \frac{1}{nIntervals}, ..., \frac{nIntervals-1}{nIntervals}, 1]$
2 $mipPop \leftarrow \emptyset$
3 **foreach** $(\lambda_1, \lambda_2, \lambda_3) \in \Lambda^3$ **do**
4 $\quad model \leftarrow$ MILP model with weights $\lambda_1, \lambda_2, \lambda_3$
5 $\quad mipSol^* \leftarrow$ best solution $\in mipPop$ regarding current $model$ weights
6 $\quad poolSol, poolEval_{[1...3]} \leftarrow$ Black-Box Solver($model$,$mipSol^*$,$timeLim$)
7 $\quad mipPop \leftarrow mipPop +$ new solutions from the current $poolSol$
8 $\quad poolAval \leftarrow$ evaluations of each solution $s \in poolSol$ regarding to $f_{objSharpeRatio}(s)$ and $f_{objExtremeScenario}(s)$ (optional)
9 $\quad$ **for** $nS \leftarrow 0$ ***to*** $|poolSol|$ **do**
10 $\quad\quad addSolution(Xe, poolSol_{nS}, poolEval_{nS})$
11 $\quad$ **end**
12 **end**
13 **return** Xe

Parameter $nIntervals$ guides the precision of the linear combination between the weights λ_1, λ_2 and λ_3 and the number of solutions generated. A set of possible values for these weights, namely Λ, is created in Line 1 of Algorithm 5.1. Basically, variable $nIntervals$ regulates a discrete number of real values, from the interval $[0, 1]$, that can be assigned to these weights.

Line 4 generates the MILP model described in Section 5.1 with weights λ_1, λ_2 and λ_3 for the objectives $objTotalCost$, $objBatteriesUse$, $objMaxPeakLoad$, respectively. The Black-Box solver solves the generated model by exploring a BB tree formed by linear programming relaxation nodes. In this process, different feasible (integer) solutions are usually achieved during the searching procedure. Those solutions are returned at the end of the search, which can be finished when optimal values have been reached or due to other stopping criteria, such as computational time. It is worth mentioning that the optimal values correspond to the best solution that minimizes a *specific weighted-sum single objective function*. So, it is necessary to solve multiple problems with different

weights, in order to satisfy the multi-objective nature of the problem. The matheuristic returns the obtained feasible solutions and its evaluations (regarding the first three objective functions). The obtained set of solutions is hereafter called Pool of Solutions (line 6). Optionally, each solution from the pool is now evaluated according to the three additional criteria described in Section 5.2.

The procedure addSolution (described in Algorithm 5.2), extracted from Lust & Tehrem (Lust & Teghem 2010), filters the dominated solutions in the obtained population. This latter mechanism (line 10) efficiently tries to add each obtained solution $s \in poolSol$ in the set of non-dominated solutions Xe. It is considered that a vector $z(x) = (z(x)_1, z(x)_2, z(x)_3)$, composed with the values of the three objective functions considered by the MILP model, *dominates* a vector $z(s) = (z(s)_1, z(s)_2, z(s)_3)$ if, and only if, $z(x)_k \leq z(s)_k \quad \forall k \in \{1,2,3\}$ and $\exists k \in \{1,2,3\} : z(x)_k < z(s)_k$. Thus, this relation is denoted by $z(x) \prec z(s)$. On the other hand, the relation $z(x) \preceq z(s)$ does not requires the last condition.

Algorithm 5.2: addSolution

Input: Population Xe potentially efficient; Solution s, and its evaluations $z(s)$
Output: Xe; Added (optional)

```
1  Added ← true
2  forall x ∈ Xe do
3  |  if z(x) ⪯ z(s) then
4  |  |  Added ← false; Break
5  |  end
6  |  if z(s) ≺ z(x) then
7  |  |  Xe ← Xe \ x
8  |  end
9  end
10 if Added = true then
11 |  Xe ← D ∪ s
12 end
13 return Xe
```

5.4 Conclusion

In this chapter, a new multi-objective power dispatching problem is introduced by planing energy storage into PEVs. The proposed framework optimizes three different

microgrid objectives functions. While the most common approaches try to minimize the total costs, related to the best time for buying and selling energy, the proposal also considers aspects for enhancing communitarian energy quality, such as grid maximum peak load. The idea of thinking and introduce a communitarian scenario can benefit mini/microgrid users. Undoubtedly, other environmental indicators could be inserted in the proposed MILP model. Finally, the use of PEVs battery was also analyzed as an objective function, which tries to minimize batteries wear and tear. Three additional criteria were also introduced in order to evaluate the robustness of a energy storage schedule.

In order to solve the MOMSPP, a smart matheuristic black-box was introduced. The proposed metaheuristic uses a pool of feasible solutions found over the branches of a BB tree. Another smart strategy tries to feed the MILP problems with the best known feasible solutions for that specific set of objective function weights.

Chapter 6

Computational experiments of the MOMSPP

"This is my simple religion. There is no need for temples; no need for complicated philosophy. Our own brain, our own heart is our temple; the philosophy is kindness."
— Dalai Lama

This chapter is divided into three Sections. Section 6.1 introduces how the MG scenarios were generated. Subsection 6.1.1 describes the model used for generating probabilistic forecast for the MG components. Section 6.2 describes the behavior of MILP model in solving the three objective functions. Thus, the latter considers deterministic energy storage management considering historical data. Section 6.3 analyzes the obtained Pareto Fronts regarding the three additional criteria. Non-dominated solutions visualization is assisted with Aggregation Trees (AT) (de Freitas et al. 2015), parallel coordinates and polar graphs.

The discussions about the obtained results of this Chapter are remarked in Chapter 7.

6.1 Microgrid scenario

In the microgrid considered in this study, all components are connected through a DC bus without power flow constraints. The scenario is composed of:

- **Consumption:** A building with a maximum contractual power of 243 kW.
- **Production:**
  1. Wind Power Turbine (WPT) with a total capacity of 160 kW;
  2. Solar PV array with a total capacity of 80 kW.
- **SmartPark storage unit:**
  - PEV car composed with a typical Lithium-ion battery 60kW/60kWh storage.
  - PEV car composed with three high speed flywheel 10kW/10kWh storage.
  - PEV car composed with a CAES 60kW/60kWh storage.

The problem of energy management described here consists in planning, with a time step of 1h, energy storage for each hour of a desired planning horizon. Two different storage planning time horizons are handled in this current work, 24 and 168 hours ahead.

Figures 6.1 and 6.2 show day and week month historical data of the analyzed periods. WPT data were adapted from EirGrid (Center 2015), Solar PV adapted from Hong, Wilson & Xie (Hong et al. 2014) and residential house (adapted from Liu, Tang, Zhang & Liu (Liu et al. 2014)). As can be verified in these figures, three different PEVs are shown. PEVs availability are stated between each pair of red and blue points (maybe a last red arrival point can be without a pair, since vehicle will only depart later than the last time stamp). When vehicle arrives there is a red symbol marking its arrival state of charge (SOC). Analogously, in each departure, the blue point marks the desired battery SOC. During the arrival until the last time stamp before departure, PEV is available as an extra energy demand/source for the MG. Both words (demand/source) are used here since each PEV may represent an extra demand, taking into account that its owner might require charging during its stay at the SmartPark, what would represent an extra demand. On the other hand, if available to be used, as will be shown along the chapter, it can represent a very useful and beneficial MG component.

The three PEVs depicted in Figures 6.1 and 6.2 were generated according to the procedure described in Algorithm 6.1.

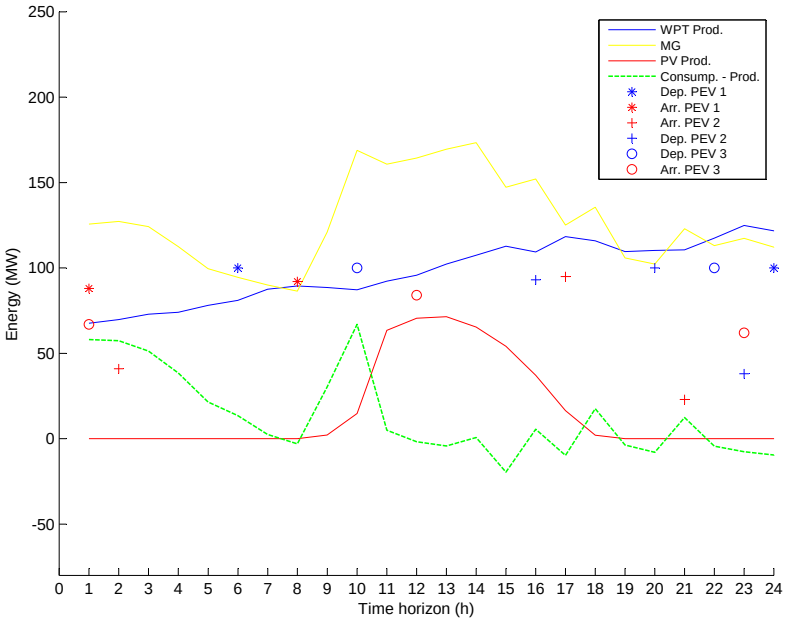

Figure 6.1: One day forecasts, 24 samples

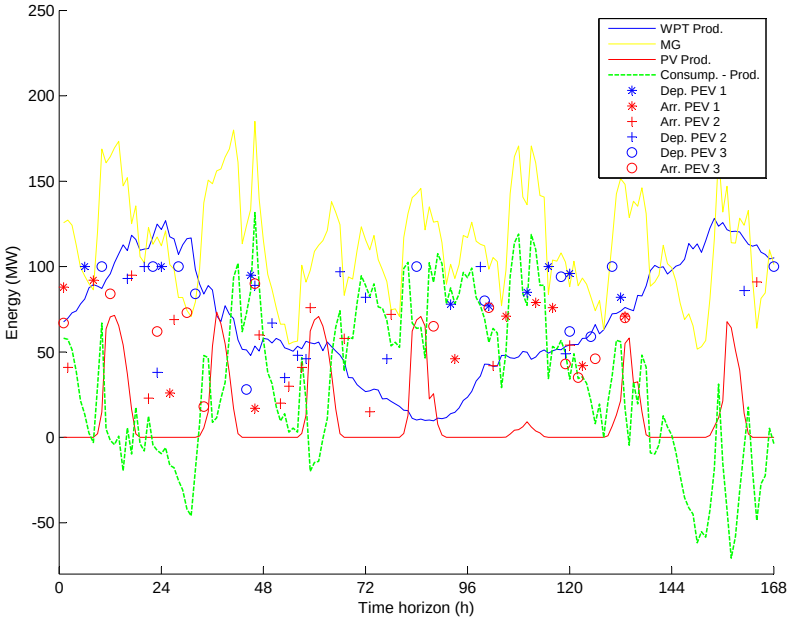

Figure 6.2: One week ahead forecasts

Figure 6.3: Historical microgrid data with hour sampling

Algorithm 6.1: Generate PEV

Input: Cardinality of the set of interval $|I|$

Output: PEV availability pev^{a}_{vi}, PEV arrival pev^{arr}_{vi}, PEV departure pev^{dep}_{vi}, PEV arrival SOC $pev^{SOC_{arr}}_{vi}$, PEV departure SOC $pev^{SOC_{dep}}_{vi}$

1 **for** $i \leftarrow 0$ ***to*** $|I|$ **do**
2 $pev^{a}_{vi} \leftarrow$ random binary $\in [true, false]$
3 **if** pev^{a}_{vi} *is true* **then**
4 $pev^{SOC_{arr}}_{vi} \leftarrow$ random SOC $\in [low, medium, much]$
5 $i' \leftarrow i +$ random available time $\in [short, medium, long]$
6 $pev^{a}_{vi,\ldots,i'} \leftarrow$ true
7 $i \leftarrow i'$
8 $pev^{dep}_{vi} \leftarrow true$
9 $pev^{SOC_{dep}}_{vi} \leftarrow pev^{a}_{vi} +$ random extra SOC $\in [low, medium, much]$
10 **end**
11 **end**
12 **return** pev^{a}_{vi}, pev^{arr}_{vi}, pev^{dep}_{vi}, $pev^{SOC_{arr}}_{vi}$, $pev^{SOC_{dep}}_{vi}$

In Line 2 of Algorithm 6.1, PEV receives a random status of arriving or not. If it is arriving, a random initial SOC, from different ranges of possible initial SOCs, is assigned in line 4. After defining the availability time at the SmartPark, line 5, the departure flag is set in line 8 and a random departure SOC, higher than arrival, is defined in line 9. In the model considered in this thesis, each vehicle is considered to demand energy from the grid and, thus, its departure SOC is always greater than its arrival SOC. A maximum allowed percentage of charging per interval is set to be 35%. Thus, any huge charging, higher than 35%, is expected by the PEV owner. Parameters are formally presented in Section 5.1.

Typical microgrid prices, also obtained from Hong, Wilson & Xie (Hong et al. 2014), are shown in Figure 6.4. This figure shows the probabilistic forecast of the prices. In this case, the medium quartile q_{50} is considered to be the real measured price. For simplicity, this data is repeated to the other days, when required by a longer energy storage planning.

6.1.1 Probabilistic forecasting problems

The probabilistic forecasts are obtained using the HFM described in Chapter 3. If it happens that the forecasts are far from the actual measured data, they are slightly ad-

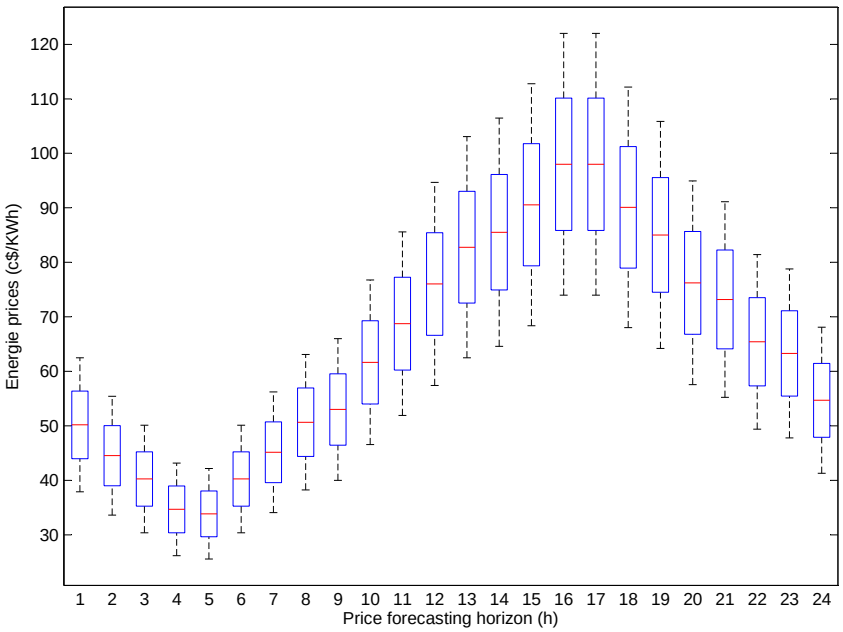

Figure 6.4: Probabilistic price forecasts

justed in order to provide a reasonable probabilistic forecast scenario to be, didactically, used here.

Figures 6.5a, 6.5b, 6.5c and 6.5d show the obtained probabilistic forecasts for the historical data introduced in Section 6.1. As can be verified, lower and upper quartiles (q_1 and q_{99}, respectively) were able to afford acceptable limits for each MG component time series forecast (prices (Figure 6.4), consumption (Figures 6.5a and 6.5b), solar (Figure 6.5c), total renewable energy production, solar + wind, (Figure 6.5d)). From intervals the forecast time horizons 105 to 115 the model did not have a good performance in forecasting solar PV production, thus, a small gap can be verified. Nevertheless, since the extreme scenario analyses handled here do not consider the relationship between the current measured values, the probabilistic forecast can still be considered precise.

6.2 Energy storage management over deterministic scenarios

The SPSMH algorithm was implemented in C++ in the framework OptFrame 2.0, already introduced in Section 3.4.1, runing with CPLEX 12.5.1.

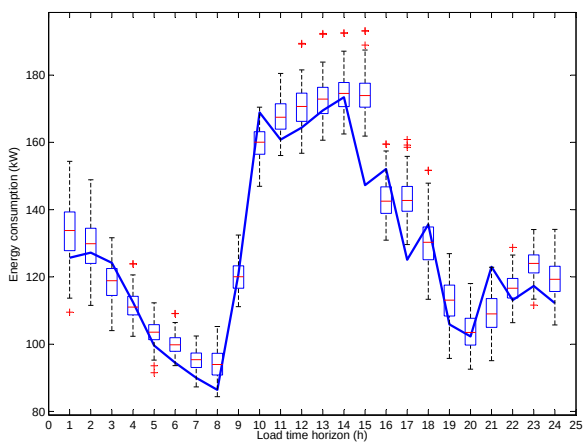

(a) Load consumption for one day ahead.

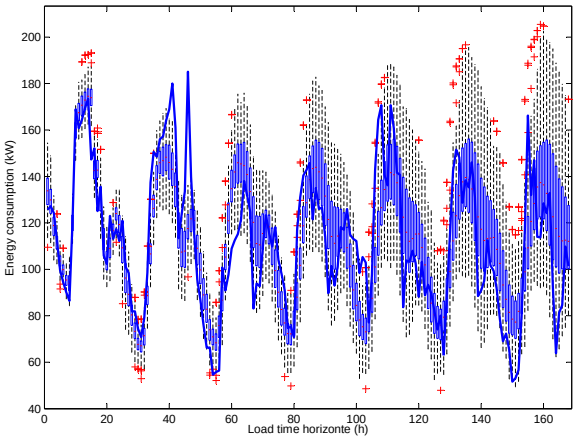

(b) Load consumption for one week ahead.

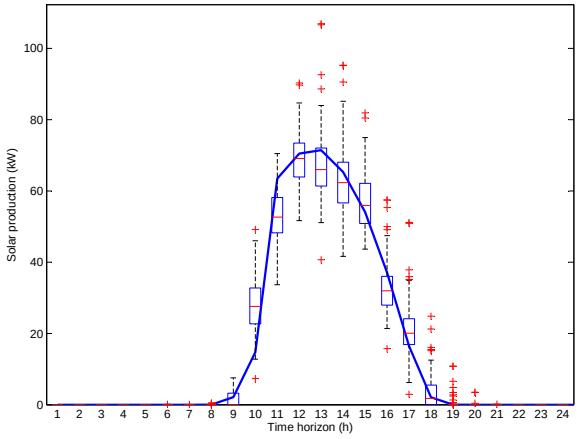

(c) Solar PV production for one day ahead.

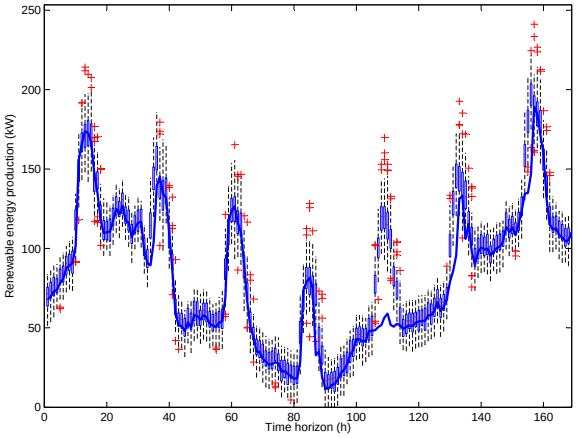

(d) Wind and solar generation for one week ahead.

Figure 6.5: Probabilistic forecasts

The tests were carried out on a DELL Inspiron Intel Core i7-3537U, 2.00 x 4 GHZ with 8GB of RAM, with operating system Ubuntu 12.04.3 precise, and compiled by g++ 4.6.3, using the Eclipse Kepler Release.

6.2.1 Initial results and first storage planing scenarios

This first batch of experiments seeks to analyze the behavior of the proposed model over the deterministic scenario presented in Section 6.1. Two different storage planning time horizons were evaluated, $k = 24$ and $k = 168$. Main grid prices of the first scenario were taken from the 11th quantile of the probabilistic forecast reported in Figure 6.4. The expected buying prices for the forecast horizon of $k = 168$ were taken from the medium

quartile, q_{50}, and repeated for each day. Selling prices were set to be 70% of the buying price for the first energy storage planning and 30% for the long-term. The number of discrete intervals $nIntervals$, which regulates the possible values for the objective functions weights (Section 5.3), was set to be 20 and 10, respectively for $k = 24$ and $k = 168$. Thus, 9260 and 1330 MILP models were solved (excluding the case where $\lambda_1, \lambda_2, \lambda_3$ are equal to 0), respecting a maximum optimization time limit of 60 seconds. For instance, the following set of possible values for the linear weightening were considered for the one-week ahead storage planning: $\Lambda_{k=168} = [0, 0.1, 0.2, 0.3, 0.4, 0.5, 0.6, 0.7, 0.8, 0.9, 1]$. As may be noticed, the number of possible values can be increased in large scale and real case applications by increasing the value of $nIntervals$.

Batteries characteristics are shown in Figure 6.6. Flywheel and CAES batteries were set to be able to discharge deeper than the Lithium-ion, 2% and 40% of maximum DoD, respectively. Possible rates of charge and discharge were generated according to 11 possibilities.

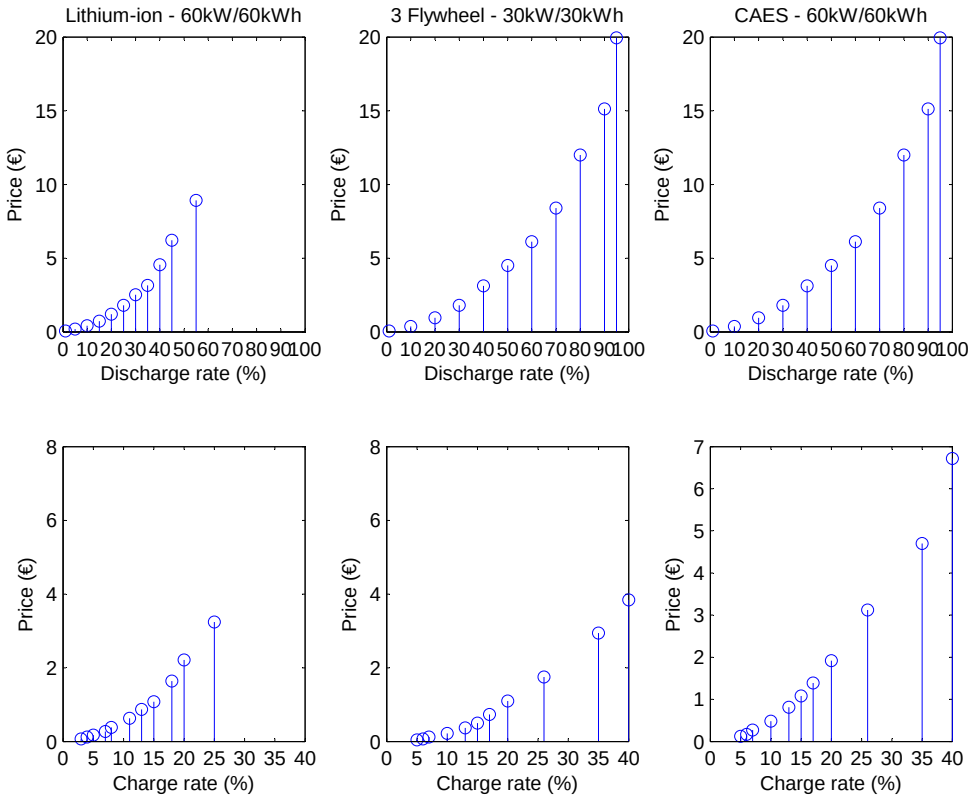

Figure 6.6: Batteries rate of charge, discharge and prices.

Figure 6.7 presents the obtained set of non-dominated solution for the first forecast time horizon, composed of 205 solutions.

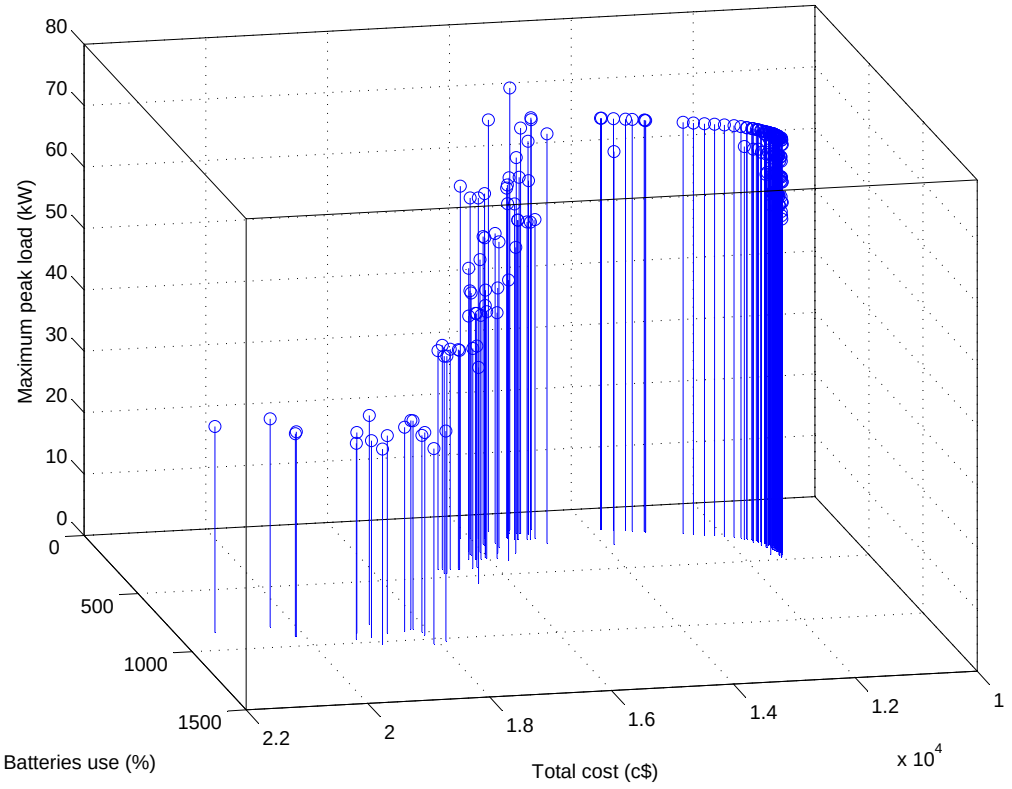

Figure 6.7: Pareto front for one day ahead with deterministic energy storage schedule.

The expected grid rate for the best solution of each objective function can be seen in Figures 6.8a and 6.8b. As can be verified, the optimization of each objective function resulted in different power dispatching strategies. The best total cost of the one-day ahead schedule was $ 112.92, with a total percentage of batteries use of 418% and maximum load of 67 kW. By saving batteries use, a solution with a slightly greater maximum peak load of 72 kW was obtained with a total cost of $ 152.61. The schedule which minimizes the maximum peak load schedule was able to minimize it in up to 31 kW, expecting a total cost of $ 189,13 and a total amount of batteries use equal to 1022 %. An analogous behavior was reported for the one week ahead storage planning.

6.2.2 Results considering the SPSMH with MIP start solutions

In the proposed approach, only the binary variables from the original MILP are stored, as well as the objective function values. Thus, the CPLEX restores each solution

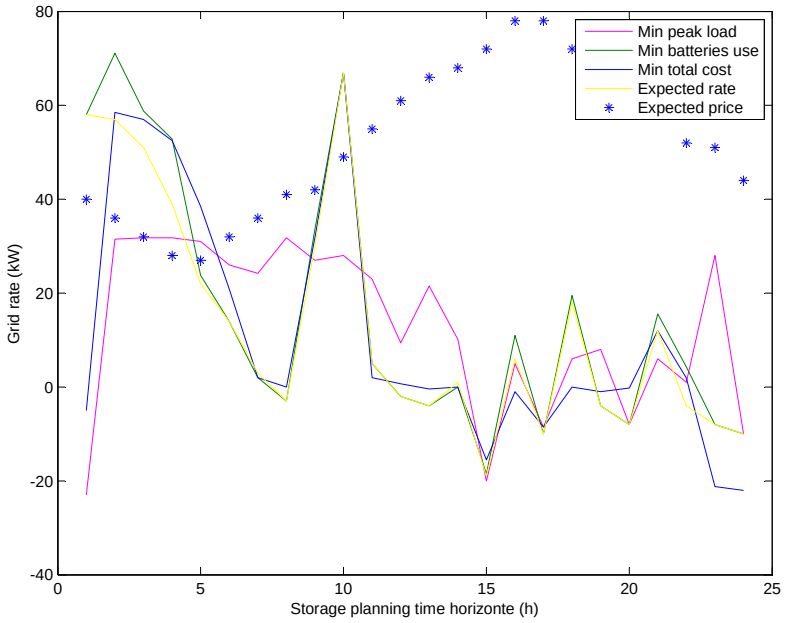

(a) One day ahead

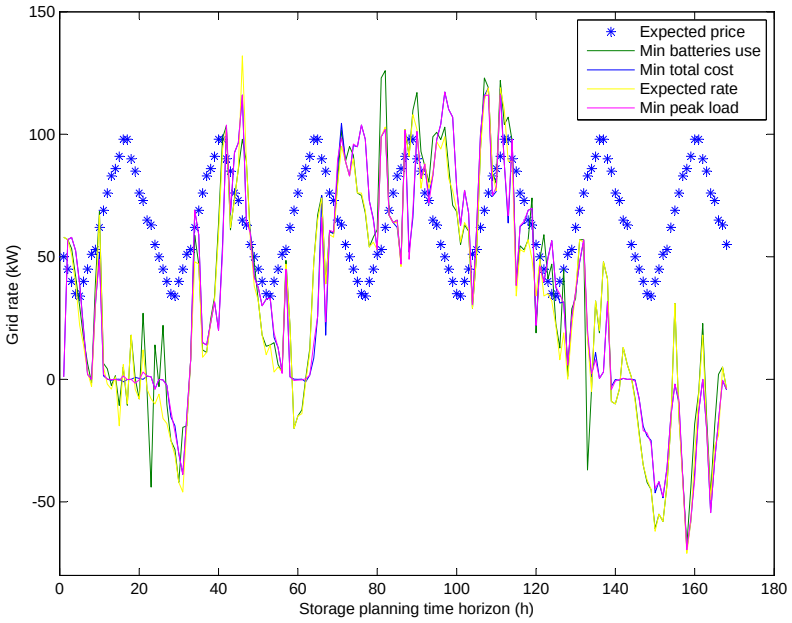

(b) One week ahead

Figure 6.8: Grid rate for deterministic power dispatching

and starts its search.

Generating new microgrid scenarios with PEVs

Load time series from two different small microgrid residential areas (one already considered in Section 6.1) and one commercial building, in a city of Zhejiang Province of China, provided by Nian Liu et al. (Liu et al. 2014), were considered here, as well as a microgrid house with high load fluctuation, extracted from the REDD dataset.

The cases of study described here comprise a small Wind Power Turbine (WPT) and Solar PV array. The last two have been adapted from time series of a WPT with 160 kW capacity and PV array with a total capacity of 80 kW, already described in Section 6.1. We design three scenarios: the case 1 is composed only with the REDD microgrid house (Figure 6.9); the second combined two different residential areas and loads from the house (Figure 6.10); and the case 3 combines the demand profiles from the commercial building and the microgrid household. Random arrivals are shown with asterisk points and their departures with circles. Different color represents different PEVs.

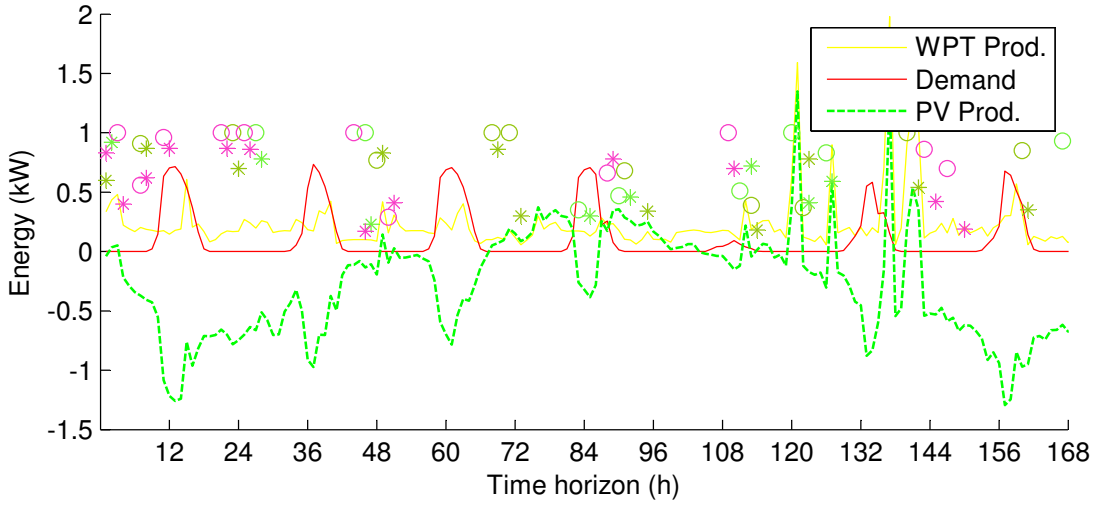

Figure 6.9: Microgrid household with two small sources of RER generation and 3 PEVs

We updated the prices described in Section 6.2 and included a SMES battery as another option for this new mini/microgrid scenarios. Figure 6.11 depicts the discharging prices that we assigned to the PEVs batteries. Four different energy storage systems were considered: CAES, Flywheels, Lithium-ion and SMES. Some studies in the literature have been discussing if rapid charging is really a point to be damaging batteries. Results in a particle accelerator, performed by Li et al. (Li et al. 2014), at the Department of

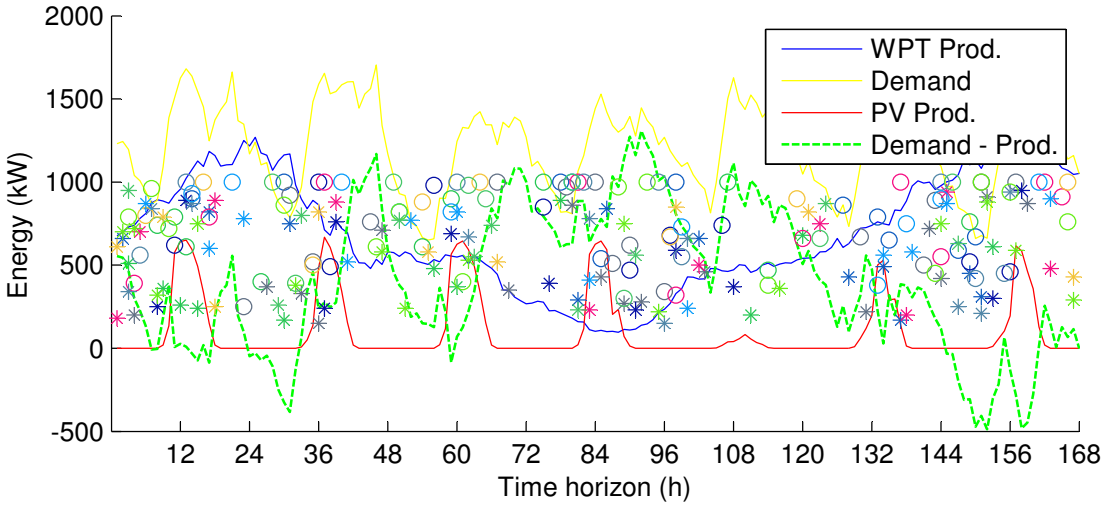

Figure 6.10: Residential microgrid area with two sources of RER generation and 10 PEVs

Energy of the SLAC National Accelerator Laboratory in Menlo Park, showed that more uniform charging, whether fast or slow, were the main causes of battery degradation. They found evidences that rapid charging and draining doesn't damage Lithium Ion Electrode as much as the literature used to think. In any case, our model is robust enough to be adjusted to any new information found by researchers. Since it is based on a discrete set of values associated to each charge or discharge cycle, the only thing that might be needed is to update those values.

We included some uncertainties over the batteries maximum rates of charge and discharge. They were generated at random according to the PEV maximum battery (20, 30, 60 or 70 kWh), also chosen at random. However, at least, 100 discretized points, were considered as possible rates for charging and discharging the PEVs batteries. They were uniformly generated from 0 until the maximum rate for each vehicle.

Scenarios were composed of different number of PEVs: 3, 10, 20, and 50. Forecasting horizons of 24 hours ahead were considered.

Matheuristic smart mechanism performance

The CPLEX matheuristic black-box has been set to proceed with its search with the maximum time of 5 seconds. Different numbers of weighted-sum MILP were generated for each scenario: 27, 64 and 125. Three variants were analyzed, one with sequential

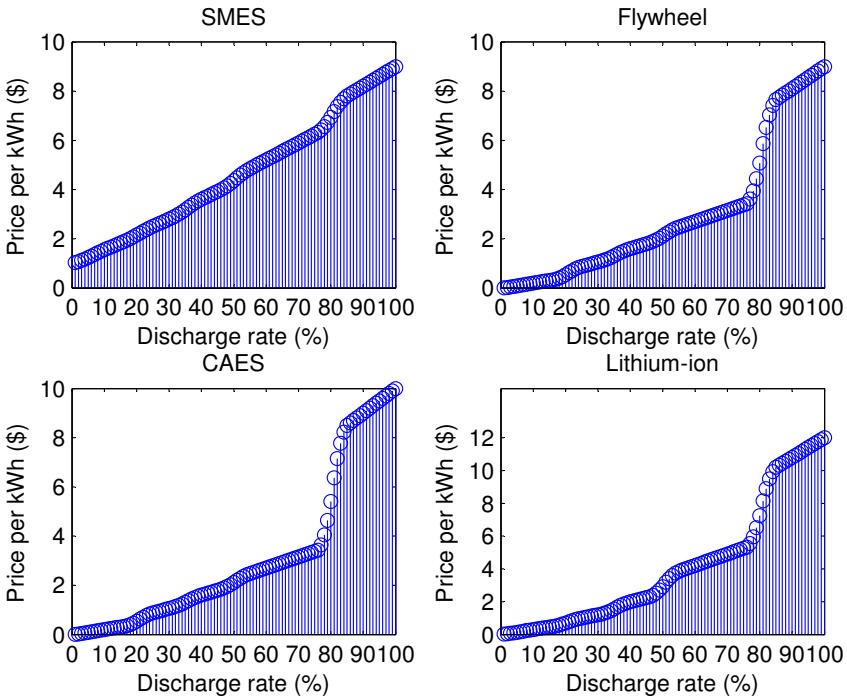

Figure 6.11: Batteries discharge prices according to the rate of discharge.

order of the weighted-sum MILP, SPSMH, another one with random order, namely SPSMH-R, and the last one was the same variant reported in Section 6.2.1, so-called SPSMH-without, which does not include the MIP start mechanism.

Obtained sets of non-dominated solutions were evaluated according to the Hypervolume (HV) and Coverage quality indicators (Zitzler & Thiele 1998), Diversity metric Δ (Deb et al. 2002) and Cardinality regarding a Pareto Front Reference (REF), composed with all obtained solution for each case. Hypervolume was calculated using the computational tool provided by Beume et al. (Beume et al. 2009).

As can be seen in Table 6.1, the Δ metric was reduced, resulting in better quality of the Pareto Fronts obtained by the SPSMH. The other quality indicators also reported better results when using the proposed initialization mechanisms.

Specially in problems with 20 and 50 PEVS, the SPSMH-without was almost not able to find any solution, in five seconds execution, to be added to the final Pareto Front. The idea of initializing the model with initial feasible solutions was very useful and could enhance the quality of the final set of non-dominated solutions. Further experiments should analyze the behavior of the method with higher computational times.

Table 6.1: Pareto fronts average values comparisons

Indicator of Quality	SPSMH-without	SPSMH	SPSMH-R
Cardinality	53,1	62,7	64,5
Coverage	0,1498	0,2525	0,2346
Δ	0,0236	0,0025	0,0026
HV	217,10	224,65	227,93

6.3 Energy storage management using probabilistic forecasts

In this second batch of experiments, two different scenarios, extracted from Table 5.1, were considered. The first one involves power dispatching based on the worst case scenario and on evaluating objective function $f_{objExtremeScenario}$ regarding the best case. The second scenario was designed to optimize energy storage considering the best case scenario while its performance over the worst case scenario was also evaluated by $f_{objExtremeScenario}$. Both Sharpe Ratio criteria ($f_{objSharpeRatioTotalCost}(s)$ and $f_{objSharpeRatioMaxLoad}(s)$) were evaluated for 20 different random scenarios.

Figures 6.14a and 6.14b present the obtained set of non-dominated solutions, composed of more than 4000 solutions, represented by parallel coordinates graphs, ordered with the tool provided by de Freitas et al. (2015). The latter introduced a polynomial algorithm for finding the best order of the objective functions, in order to provide more readable and understandable Pareto Fronts. In particular, Aggregation Trees are used for finding the best groups, regarding a new concept of harmony and conflict between objectives. The AT are depicted in Figures 6.12a and 6.12b.

Finally, polar graphs are also depicted, Figures 6.13a and 6.13b, in order to facilitate the visualization of the conflicts between the objectives.

As can be verified in the branches of the AT, considering the worst case scenario, the pairs of objective function and criteria $(3, 6)$ and criteria $(4, 5)$ the lowest conflict. It can concluded by verifying the first branches in the AT. This result makes sense and reinforces that by minimizing the max peak load, implicitly, its variability over the grid also decrease. On the other hand, when minimizing total costs and battery use, higher variability of grid peak load might be expected.

Moreover, in the worst case scenario, the robustness of the total cost (measured by

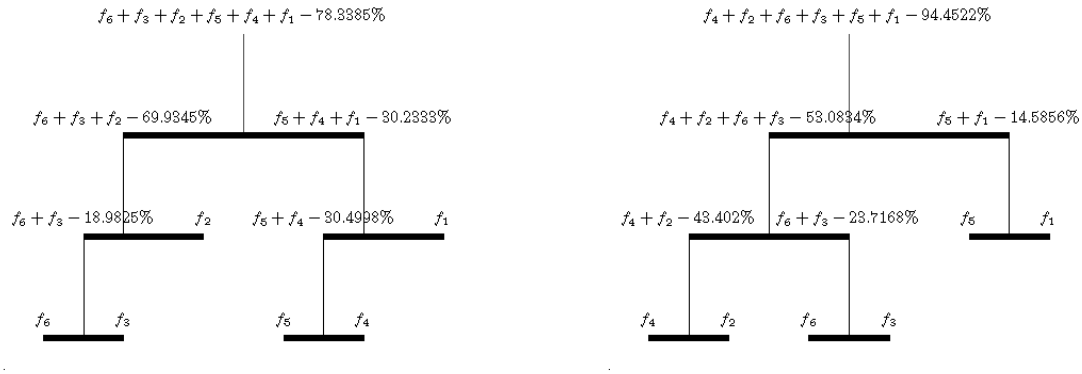

(a) Worst case storage planning. (b) Best case storage planning.

Figure 6.12: Aggregation tree

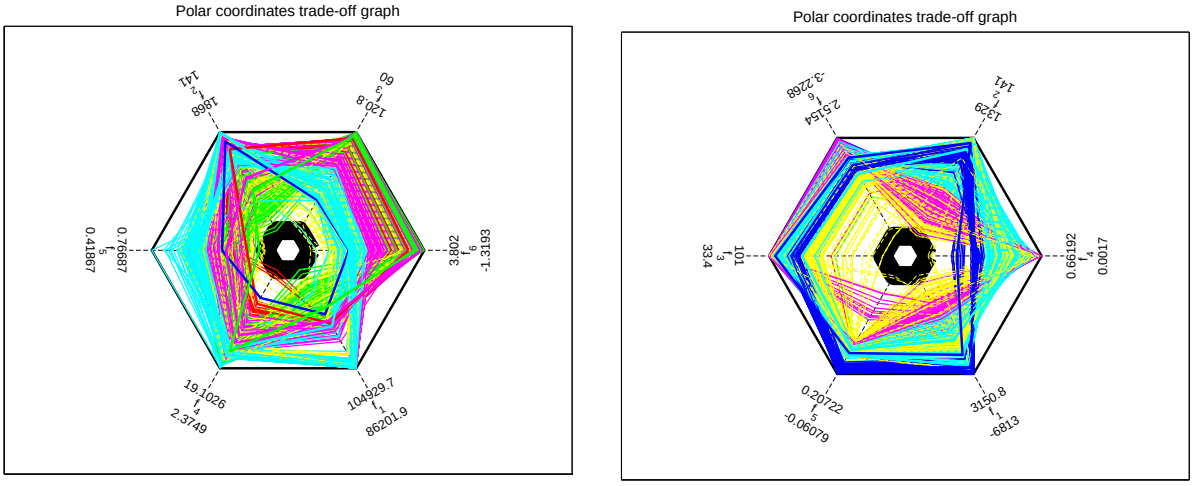

(a) Worst case storage planning. (b) Best case storage planning.

Figure 6.13: Polar graph

the criterion 4) can be seen in harmony with the volatility measured by criterion 5. Objectives $f_{objTotalCost}$ (1) and $f_{objBatteriesUse}(s)$ (2) present the highest conflict, clearly capturing the existing trade-off regarding the use of batteries. The latter fortify the benefit of using PEVs battery in order to assist mini/microgrid energy management, emphasizing how batteries can contribute for the RER integration. For the best case scenario, the pair of objective functions $(1, 2)$ kept showing largest conflict, information supported by looking at the last branches of the respective AT.

Since $f_{objSharpeRatioMaxLoad}(s)$ and $f_{objMaxPeakLoad}(s)$ are more harmonic storage schedules, it can also be concluded that the use of PEVs batteries promotes decrease of maximum peak load and its volatility over different possible scenarios. The use of PEVs batteries is also beneficial for reducing the difference between the expected total cost of the power dispatching and the one that might happen in extreme scenarios.

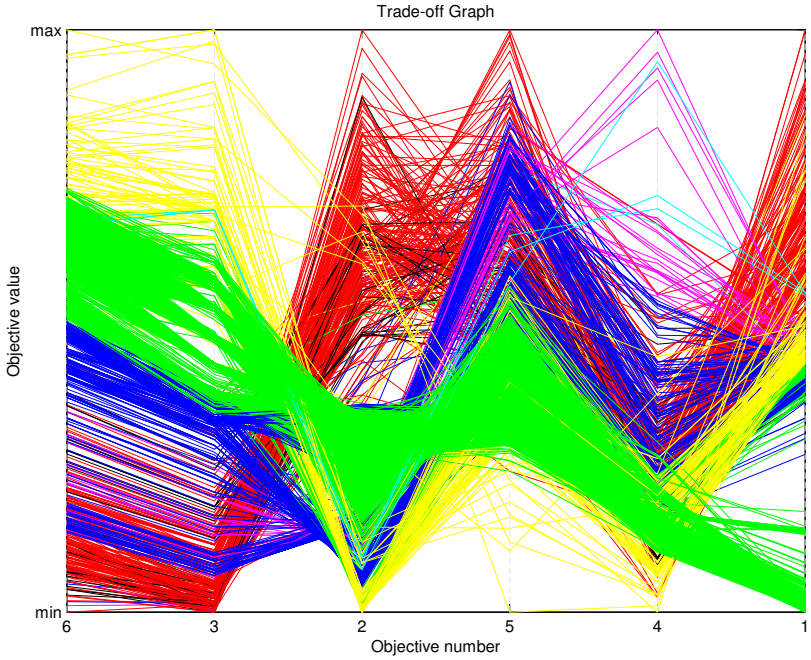

(a) Worst case

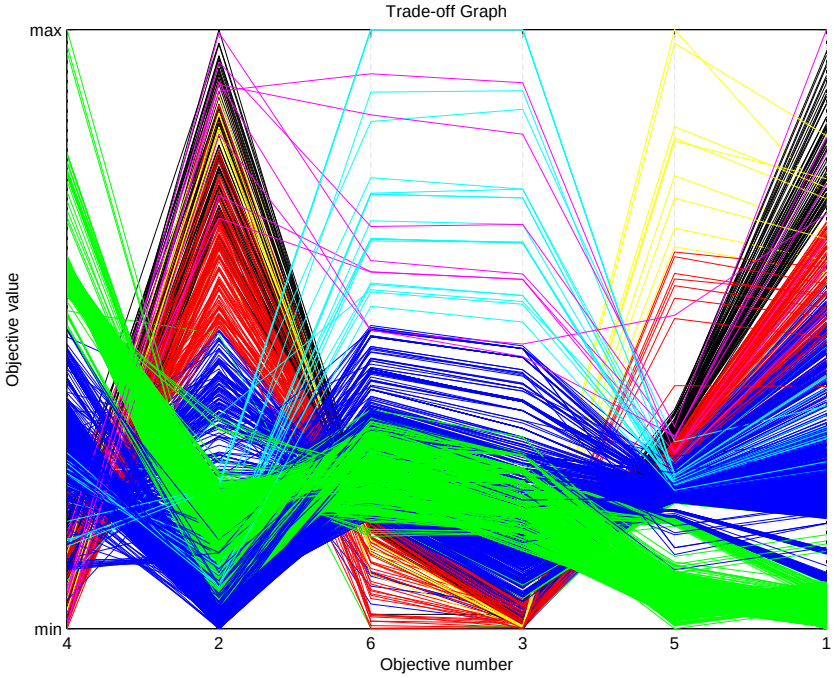

(b) Best case

Figure 6.14: Parallel coordinate plot

Chapter 7

Conclusions and future works

"A arte de prever involve a sabedoria do passado, vislumbrando-se o presente. Mas, a relatividade nos ensina que a recíproca do futuro também é verdadeira."

— Anonymous

7.1 Summary and final considerations

The main achieved goals, stated in the beginning of this thesis, are described below: (i) a detailed literature review related to the main topics addressed in this thesis was presented; (ii) a novel multi-objective energy storage power dispatching was introduced, analyzed and discussed; (iii) the development and design of a new hybrid forecasting model, with enough flexibility, able to be applied for forecasting different MG components; and, finally, (iv) a smart matheuristic black-box algorithm was used to solve the proposed MILP model.

In the Chapter 2, a literature review surrounding the SG technology, energy storage system and forecasting techniques was presented.

A novel Hybrid Forecasting Model (HFM) was introduced in Chapter 3. The model was applied to forecast different load forecasting problems of the SG environment. Probabilistic forecast were also achieved for two different forecasting problems: rainfall and wind power generation forecasting. While Chapter 4 described a novel self-adaptive ES for combinatorial optimization problems. In particular, the HFM was also calibrated using it.

Chapter 5 described the proposed multi-objective storage planing power dispatching, Optimization of different MG characteristics was proposed, such as: MG total costs, use of PEVs batteries, maximum MG system peak load, behavior in extreme and sets of different scenarios. Probabilistic forecasts were used in order to evaluate energy storage schedule in extreme scenarios and for optimizing schedules volatility. The well-known economic indicator Sharpe Ratio was applied for evaluating a new cost-to-variability index.

Finally, through computational experiments, Chapter 6, it was verified a reasonable potential of improving the use of self-generated energy, as well as reducing mini/micro-grid energy peak load by considering an ESS based on PEVs located at SmartParks. Trade-offs between the use of PEVs batteries, which are an important environment issue, were discussed. It is expected that the proposed model could be applied not only by MG users but also as a decision-making tool in order to assist smart-microgrid management.

7.2 Extensions

Entire code used in this research is, from this moment, available as example on the OptFrame website. Thus, it is expected that future researchers continue contributing to enhancing the proposed model, increasingly its efficiency and improving the tools and ideas presented in this thesis.

7.2.1 Extensions for the self-adaptive fuzzy model

The HFM could be adapted to tackle forecasting over different SG components, such as wind (Foley et al. 2012), solar (Bacher et al. 2009) forecasting, smart park storage forecasting (Saber & Venayagamoorthy 2010), among others. Finally, a parallel version of *GES* would be very useful to improve the performance of the model in problems with a huge amount of data. This approach could take advantage of *multi-core* technology and Graphics Processing Unit, which are already available in current machines and with easy abstraction for metaheuristic based algorithms.

It is proposed to develop a multi-objective version of the calibration algorithm GES, using different quality indicators (Hyndman & Koehler 2006) in order to obtain different forecasting models. It is suspected that, with this MO approach, different parts of the historical data could be learned. These non-dominated set of models could also be aggregated and analyzed as a probabilistic forecast, which has been receiving attention for load (Hong et al. 2014) and wind (Zhang et al. 2014) forecasting problems.

Current results were limited to only generate the probabilistic forecasts, thus, future efforts should try to evaluated the obtained probabilistic functions with well-known indicators, such as a Pinball Function (Gneiting 2011). This kind of comparison would complement the discussions and comparison with the literature.

7.2.2 Extensions for the multi-objective power disptaching problem

As future work the proposed model should be applied in other MG scenarios, including other renewable energy resources and a larger scenario with lower granularities. Those scenarios should include other RER and higher discretization levels (down to milliseconds), which would allow a more precise power dispatching. Since the model is mainly based on a MILP approach, it might be limited to handle real time scenarios, where decision making should be done as quick as possible. Thus, the development of a metaheuristic algorithm might provide a flexible tool to be applied over those cases.

The current model was limited and did not considered uncertainties over PEVs availability. Undoubtedly, PEVs users could be delayed or do not come to the SmartPark as expected. Thus, unexpected variations on the arriving and departuring time could be handle by a set of rules. The latter should prepare and analyze the impacts on the system whether a PEV does not come.

Other improvements and extensions in the MILP are also possible. The model may include a new set of parameters for controlling energy efficiency according to the way the battery is discharged. Basically, a new vector of parameters could contain the efficiency for each battery cycle (80% rate of discharge, in one hour, of a PEV battery with maximum capacity of 100kWh might provide only 72kWh, if battery efficiency is 90%).

References

Acharjee, P. (2013). Strategy and implementation of smart grids in india, *Energy Strategy Reviews* **1**(3): 193 – 204. Future Energy Systems and Market Integration of Wind Power. doi: http://dx.doi.org/10.1016/j.esr.2012.05.003.

Adhikari, R. (2015). A neural network based linear ensemble framework for time series forecasting, *Neurocomputing* **157**: 231 – 242. doi: http://dx.doi.org/10.1016/j.neucom.2015.01.012.

Administration., E. I. (2015). US Energy Information Administration, accessed on March, 2015, http://www.eia.doe.gov/emeu/aer/overview.html.

Aiex, R. M., Resende, M. G. C. & Ribeiro, C. C. (2002). Probability distribution of solution time in GRASP: An experimental investigation, *Journal of Heuristics* **8**: 343–373.

Aiex, R., Resende, M. & Ribeiro, C. (2007). Tttplots: a perl program to create time-to-target plots, *Optimization Letters* **1**: 355–366.

Al-Salem, A. (2004). Scheduling to minimize makespan on unrelated parallel machines with sequence dependent setup times, *Engineering Journal of the University of Qatar* **17**(1): 177–187.

Alemán-Nava, G. S., Casiano-Flores, V. H., Cárdenas-Chávez, D. L., Díaz-Chavez, R., Scarlat, N., Mahlknecht, J., Dallemand, J.-F. & Parra, R. (2014). Renewable energy research progress in mexico: A review, *Renewable and Sustainable Energy Reviews* **32**(0): 140 – 153. doi: http://dx.doi.org/10.1016/j.rser.2014.01.004.

Aler, R., Galván, I. M. & Valls, J. M. (2012). Applying evolution strategies to preprocessing EEG signals for brain-computer interfaces, *Information Sciences* **215**: 53 – 66. doi: http://dx.doi.org/10.1016/j.ins.2012.05.012.

Alvarez, E., Lopez, A., Gómez-Aleixandre, J. & de Abajo, N. (2009). On-line minimization of running costs, greenhouse gas emissions and the impact of distributed generation using microgrids on the electrical system, *Sustainable Alternative Energy (SAE), 2009 IEEE PES/IAS Conference on*, pp. 1–10. doi: 10.1109/SAE.2009.5534847.

Amjady, N., Keynia, F. & Zareipour, H. (2010). Short-term load forecast of microgrids by a new bilevel prediction strategy, *Smart Grid, IEEE Transactions on* **1**(3): 286–294.

Andersen, S. B. & Santos, I. F. (2012). Evolution strategies and multi-objective optimization of permanent magnet motor, *Applied Soft Computing* **12**(2): 778 – 792.

Bacher, P., Madsen, H. & Nielsen, H. A. (2009). Online short-term solar power forecasting, *Solar Energy* **83**(10): 1772 – 1783.

Batista, N., Melício, R., Matias, J. & Catalão, J. (2013). Photovoltaic and wind energy systems monitoring and building/home energy management using zigbee devices within a smart grid, *Energy* **49**(0): 306 – 315. doi: http://dx.doi.org/10.1016/j.energy.2012.11.002.

Bennett, J. C., Robertson, D. E., Shrestha, D. L., Wang, Q., Enever, D., Hapuarachchi, P. & Tuteja, N. K. (2014). A system for continuous hydrological ensemble forecasting (SCHEF) to lead times of 9 days, *Journal of Hydrology* . doi: http://dx.doi.org/10.1016/j.jhydrol.2014.08.010.

Bessa, R., Trindade, A., Silva, C. S. & Miranda, V. (2015). Probabilistic solar power forecasting in smart grids using distributed information, *International Journal of Electrical Power & Energy Systems* **72**: 16 – 23. The Special Issue for 18th Power Systems Computation Conference. doi: http://dx.doi.org/10.1016/j.ijepes.2015.02.006.

Beume, N., Fonseca, C., Lopez-Ibanez, M., Paquete, L. & Vahrenhold, J. (2009). On the complexity of computing the hypervolume indicator, *Evolutionary Computation, IEEE Transactions on* **13**(5): 1075 –1082. doi: 10.1109/TEVC.2009.2015575.

Beyer, H. G. & Schwefel, H. P. (2002a). Evolution strategies - a comprehensive introduction, *Natural Computing* **1**: 3–52.

Beyer, H. G. & Schwefel, H. P. (2002b). Evolution strategies - a comprehensive introduction, *Natural Computing* **1**: 3–52.

Brown, R. (2008). Impact of smart grid on distribution system design, *Power and Energy Society General Meeting - Conversion and Delivery of Electrical Energy in the 21st Century, 2008 IEEE*, pp. 1–4. doi: 10.1109/PES.2008.4596843.

Buzug, T. & Pfister, G. (1992). Optimal delay time and embedding dimension for delay-time coordinates by analysis of the global static and local dynamical behavior of strange attractors, *Phys. Rev. A* **45**: 7073–7084. doi: 10.1103/PhysRevA.45.7073.

Cai, J. & Thierauf, G. (1996). Evolution strategies for solving discrete optimization problems, *Advances in Engineering Software* **25**(2-3): 177 – 183. Computing in Civil and Structural Engineering.

Center, E. N. C. (2015). EirGrid National Control Center.
URL: *http://www.eirgrid.com/operations/systemperformancedata/systemdemand/*

Chakrabarty, A., Banerjee, S., Maity, S. & Chatterjee, A. (2013). Fuzzy model predictive control of non-linear processes using convolution models and foraging algorithms, *Measurement* **46**(4): 1616 – 1629. doi: 10.1016/j.measurement.2012.11.046.

Chaquet, J. M. & Carmona, E. J. (2012). Solving differential equations with fourier series and evolution strategies, *Applied Soft Computing* **12**(9): 3051 – 3062.

Chen, T. & Chen, H. (2009). Mixed-discrete structural optimization using a rank-niche evolution strategy, *Engineering Optimization* **41**(1): 39–58.

Chow, V. & Lai, C. W. (2015). Conditional sharpe ratios, *Finance Research Letters* **12**(0): 117 – 133. doi: http://dx.doi.org/10.1016/j.frl.2014.11.001.

Chuang, Y.-C., Chen, C.-T. & Hwang, C. (2015). A real-coded genetic algorithm with a direction-based crossover operator, *Information Sciences* **305**: 320 – 348. doi: http://dx.doi.org/10.1016/j.ins.2015.01.026.

Coelho, I. M., Munhoz, P. L. A., Haddad, M. N., Coelho, V. N., Silva, M. M., Souza, M. J. F. & Ochi, L. S. (2011a). A computational framework for combinatorial optimization problems, *VII ALIO/EURO Workshop on Applied Combinatorial Optimization*, Porto, pp. 51–54.

Coelho, I. M., Munhoz, P. L. A., Haddad, M. N., Coelho, V. N., Silva, M. M., Souza, M. J. F. & Ochi, L. S. (2011b). A computational framework for combinatorial optimization problems, *VII ALIO/EURO Workshop on Applied Combinatorial Optimization*, pp. 51–54.

Coelho, V., Grasas, A., Ramalhinho, H., Coelho, I., Souza, M. & Cruz, R. (2015). An ILS-based algorithm to solve a large-scale real heterogeneous fleet VRP with multi-trips and docking constraints, *European Journal of Operational Research* . doi: http://dx.doi.org/10.1016/j.ejor.2015.09.047.

Coelho, V., Guimaraes, F., Reis, A., Coelho, I., Coelho, B. & Souza, M. (2014a). A heuristic fuzzy algorithm bio-inspired by evolution strategies for energy forecasting problems, *Fuzzy Systems (FUZZ-IEEE), 2014 IEEE International Conference on*, pp. 338–345. doi: 10.1109/FUZZ-IEEE.2014.6891794.

Coelho, V. N., Coelho, I. M., Coelho, B. N., Cohen, M. W., Reis, A. J., Silva, S. M., Souza, M. J., Fleming, P. J. & Guimaraes, F. G. (2016). Multi-objective energy storage power dispatching using plug-in vehicles in a smart-microgrid, *Renewable Energy* **89**: 730 – 742. doi: http://dx.doi.org/10.1016/j.renene.2015.11.084.

Coelho, V. N., Coelho, I. M., Coelho, B. N., Reis, A. J., Enayatifar, R., Souza, M. J. & aes, F. G. G. (2016). A self-adaptive evolutionary fuzzy model for load forecasting problems on smart grid environment, *Applied Energy* **169**: 567 – 584. doi: http://dx.doi.org/10.1016/j.apenergy.2016.02.045.

Coelho, V. N., Guimaraes, F. G., Reis, A. J., Coelho, B. N., Coelho, I. M. & Souza, M. J. (2014b). A general variable neighborhood search heuristic for short term load forecasting in smart grids environment, *Power Systems Conference (PSC), 2014 Clemson University*, pp. 1–8.

Coelho, V. N., Souza, M. J. F., Coelho, I., Guimaraes, F. G., Lust, T. & Cruz, R. C. (2012). Multi-objective approaches for the open-pit-mining operational planning problem, *Electronic Notes in Discrete Mathematics* **39**: 233 – 240. doi: 10.1016/j.endm.2012.10.031.

Coelho, V. N., Souza, M. J. F., Coelho, I. M., aes, F. G. G., Lust, T. & Cruz, R. C. (2012). Multi-objective approaches for the open-pit mining operational planning problem, *Electronic Notes in Discrete Mathematics* **39**(0): 233 – 240.

Colson, C. & Nehrir, M. (2009). A review of challenges to real-time power management of microgrids, *Power Energy Society General Meeting, 2009. PES '09. IEEE*, pp. 1–8. doi: 10.1109/PES.2009.5275343.

Colson, C., Nehrir, M. & Wang, C. (2009). Ant colony optimization for microgrid multi-objective power management, *Power Systems Conference and Exposition, 2009. PSCE'09. IEEE/PES*, pp. 1–7.

Commission, E. (2006). Smart grids – vision and strategy for europe's electricity networks of the future, *Technical Report EUR 22040*, European Commission.

Comodi, G., Giantomassi, A., Severini, M., Squartini, S., Ferracuti, F., Fonti, A., Cesarini, D. N., Morodo, M. & Polonara, F. (2015). Multi-apartment residential microgrid with electrical and thermal storage devices: Experimental analysis and simulation of energy management strategies, *Applied Energy* **137**(0): 854 – 866. doi: http://dx.doi.org/10.1016/j.apenergy.2014.07.068.

Costa, F. P. (2005). *Applications of optimization techniques to open-pit-mining problems (in portuguese)*, Master's dissertation,

Costa, F. P., Souza, M. J. F. & Pinto, L. R. (2004). A model of dynamic allocation of trucks (in portuguese), *Revista Brasil Mineral* **231**: 26–31.

Costa, L. & Oliveira, P. (2001). Evolutionary algorithms approach to the solution of mixed integer non-linear programming problems, *Computers & Chemical Engineering* **25**(10): 257–266.

Cota, L. P., Haddad, M. N., Souza, M. J. . F. & Coelho, V. N. (2014). Airp: A heuristic algorithm for solving the unrelated parallel machine sheduling problem, *In Proceedings of the 2014 IEEE Congress on Evolutionary Computation (CEC 2014)* .

Cota, L. P., Haddad, M. N., Souza, M. J. F. & Martins, A. X. (2014). Um algoritmo heurístico para resolver o problema de sequenciamento em máquinas paralelas não-relacionadas com tempos de preparação dependentes da sequência, *In Proceedings of the 35th Congresso Nacional de Matemática Aplicada e Computacional* .

D'Amico, G., Petroni, F. & Prattico, F. (2014). Wind speed and energy forecasting at different time scales: A nonparametric approach, *Physica A: Statistical Mechanics and its Applications* **406**(0): 59 – 66.

Dávi, G. A., no Martín, E. C., Ruther, R. & Solano, J. (2016). Energy performance evaluation of a net plus-energy residential building with grid-connected photovoltaic system in Brazil, *Energy and Buildings* . doi: http://dx.doi.org/10.1016/j.enbuild.2016.03.058.

de Freitas, A. R. R., Fleming, P. J. & Guimarães, F. G. (2015). Aggregation trees for visualization and dimension reduction in many-objective optimization, *Information Sciences* **298**(0): 288 – 314. doi: http://dx.doi.org/10.1016/j.ins.2014.11.044.

Deb, K., Pratap, A., Agarwal, S. & Meyarivan, T. (2002). A fast and elitist multiobjective genetic algorithm: NSGA-II, *Evolutionary Computation, IEEE Transactions on* **6**(2): 182–197. doi: 10.1109/4235.996017.

Díaz, P. & Masó, J. (2013). Evolution of production and the efficient location of renewable energies. the case of china, *Energy Procedia* **40**(0): 15 – 24. European Geosciences Union General Assembly. doi: http://dx.doi.org/10.1016/j.egypro.2013.08.003.

Dimeas, A. & Hatziargyriou, N. (2005). Operation of a multiagent system for microgrid control, *Power Systems, IEEE Transactions on* **20**(3): 1447–1455. doi: 10.1109/TPWRS.2005.852060.

Dong, X., Nowak, M., Chen, P. & Lin, Y. (2015). Self-adaptive perturbation and multi-neighborhood search for iterated local search on the permutation flow shop problem, *Computers & Industrial Engineering* **87**: 176 – 185. doi: http://dx.doi.org/10.1016/j.cie.2015.04.030.

Drezga, I. & Rahman, S. (1998). Input variable selection for ANN-based short-term load forecasting, *Power Systems, IEEE Transactions on* **13**(4): 1238–1244. doi: 10.1109/59.736244.

Drezga, I. & Rahman, S. (1999). Short-term load forecasting with local ann predictors, *Power Systems, IEEE Transactions on* **14**(3): 844–850. doi: 10.1109/59.780894.

Ederer, N. (2015). Evaluating capital and operating cost efficiency of offshore wind farms: A DEA approach, *Renewable and Sustainable Energy Reviews* **42**: 1034 – 1046. doi: http://dx.doi.org/10.1016/j.rser.2014.10.071.

Ehm, W., Gneiting, T., Jordan, A. & Krüger, F. (2015). Of Quantiles and Expectiles: Consistent Scoring Functions, Choquet Representations, and Forecast Rankings, *ArXiv e-prints* .
URL: *http://adsabs.harvard.edu/abs/2015arXiv150308195E*

Ekanayake, J., Liyanage, K., Wu, J., Yokoyama, A. & Jenkins, N. (2012). *Smart grid: technology and applications*, John Wiley & Sons.

Ellabban, O., Abu-Rub, H. & Blaabjerg, F. (2014). Renewable energy resources: Current status, future prospects and their enabling technology, *Renewable and Sustainable Energy Reviews* **39**(0): 748 – 764. doi: http://dx.doi.org/10.1016/j.rser.2014.07.113.

Enayatifar, R., Sadaei, H. J., Abdullah, A. H. & Gani, A. (2013). Imperialist competitive algorithm combined with refined high-order weighted fuzzy time series (rhwfts-ica) for short term load forecasting, *Energy Conversion and Management* **76**(0): 1104 – 1116.

Fadaeenejad, M., Saberian, A., Fadaee, M., Radzi, M., Hizam, H. & AbKadir, M. (2014). The present and future of smart power grid in developing countries, *Renewable and Sustainable Energy Reviews* **29**(0): 828 – 834. doi: http://dx.doi.org/10.1016/j.rser.2013.08.072.

Farhangi, H. (2010). The path of the smart grid, *Power and Energy Magazine, IEEE* **8**(1): 18–28. doi: 10.1109/MPE.2009.934876.

Fathima, A. H. & Palanisamy, K. (2015). Optimization in microgrids with hybrid energy systems - a review, *Renewable and Sustainable Energy Reviews* **45**(0): 431 – 446. doi: http://dx.doi.org/10.1016/j.rser.2015.01.059.

Feo, T. A., Resende, M. G. C. & Smith, S. H. (1994). A greedy randomized adaptive search procedure for maximum independent set, *Operations Research* **42**: 860–878.

Foley, A. M., Leahy, P. G., Marvuglia, A. & McKeogh, E. J. (2012). Current methods and advances in forecasting of wind power generation, *Renewable Energy* **37**(1): 1 – 8.

Fossati, J. P., Galarza, A., Martín-Villate, A. & Fontán, L. (2015). A method for optimal sizing energy storage systems for microgrids, *Renewable Energy* **77**(0): 539 – 549. doi: http://dx.doi.org/10.1016/j.renene.2014.12.039.

Freitas, A. R. & Guimaraes, F. G. (2011). Originality and diversity in the artificial evolution of melodies, *Proceedings of the 13th annual Conference on Genetic and Evolutionary Computation*, New York.

French, M. N., Krajewski, W. F. & Cuykendall, R. R. (1992). Rainfall forecasting in space and time using a neural network, *Journal of Hydrology* **137**(1-4): 1 – 31. doi: http://dx.doi.org/10.1016/0022-1694(92)90046-X.

Gangui, Y., Yu, L., Gang, M., Yang, C., Junhui, L., Jigang, L. & Lei, M. (2012). The ultra-short term prediction of wind power based on chaotic time series, *Energy Procedia* **17, Part B**(0): 1490 – 1496. 2012 International Conference on Future Electrical Power and Energy System.

García-Villalobos, J., Zamora, I., Martín, J. S., Asensio, F. & Aperribay, V. (2014). Plug-in electric vehicles in electric distribution networks: A review of smart charging approaches, *Renewable and Sustainable Energy Reviews* **38**: 717 – 731. doi: http://dx.doi.org/10.1016/j.rser.2014.07.040.

Garey, M. & Johnson, D. (1979). Computers and intractability: A guide to the theory of np-completeness, *WH Freeman & Co., San Francisco* **174**.

Geiger, M. J. (2004). Randomised variable neighbourhood search for multi objective optimisation, *In Proceedings of the 4th EUME Workshop Design and Evaluation of Advanced Hybrid MetaHeuristics* **November 4**(Nottingham, United Kingdom,): 34–42.
URL: *http://arxiv.org/abs/0809.0271*

Glover, F. (1989). Tabu search-part i, *ORSA Journal on computing* **1**(3): 190–206.

Glover, F. (1996a). Tabu Search and adaptive memory programming - advances, applications and challenges, *in* R. Barr, R. Helgason & J. Kennington (eds), *Interfaces in Computer Sciences and Operations Research*, Kluwer Academic Publishers, pp. 1–75.

Glover, F. (1996b). Tabu search and adaptive memory programming - advances, applications and challenges, *in* R. S. Barr, R. V. Helgason & J. L. Kennington (eds), *Computing Tools for Modeling, Optimization and Simulation: Interfaces in Computer Science and Operations Research*, Kluwer Academic Publishers, pp. 1–75.

Gneiting, T. (2011). Quantiles as optimal point forecasts, *International Journal of Forecasting* **27**(2): 197–207.

Goodwin, P. & Lawton, R. (1999). On the asymmetry of the symmetric {MAPE}, *International Journal of Forecasting* **15**(4): 405 – 408. doi: http://dx.doi.org/10.1016/S0169-2070(99)00007-2.

Guimarães, I. F., Pantuza, G. & Souza, M. J. F. (2007). Computational simulation model for solutions validation of the open-pit-mining with dynamic trucks allocation (in

portuguese), *Anais do XIV Simpósio de Engenharia de Produção (SIMPEP)*, Vol. 1, Bauru/SP, pp. 1–11.

Gwangseob, K. & Ana, P. B. (2001). Quantitative flood forecasting using multisensor data and neural networks, *Journal of Hydrology* **246**(1): 45–62.

Haddad, M. N., Cota, L. P., Souza, M. J. F. & Maculan, N. (2014). Aiv: A heuristic algorithm based on iterated local search and variable neighborhood descent for solving the unrelated parallel machine scheduling problem with setup times, *In Proceedings of the 16th International Conference on Enterprise Information Systems (ICEIS 2014)* pp. 376–383. doi: 10.5220/0004884603760383.

Haddad, M. N., Cota, L. P., Souza, M. J. F. & Maculan, N. (2015). Solving the unrelated parallel machine scheduling problem with setup times by efficient algorithms based on iterated local search, *Lecture Notes in Enterprise Information Systems* **227**: 131–148. doi: 10.1007/978-3-319-22348-3_8.

Hall, S. & Foxon, T. J. (2014). Values in the smart grid: The co-evolving political economy of smart distribution, *Energy Policy* **74**(0): 600 – 609. doi: http://dx.doi.org/10.1016/j.enpol.2014.08.018.

Hansen, P., Brimberg, J., Urošević, D. & Mladenović, N. (2009). Solving large p-median clustering problems by primal–dual variable neighborhood search, *Data Mining and Knowledge Discovery* **19**(3): 351–375. doi: 10.1007/s10618-009-0135-4.

Hansen, P. & Mladenović, N. (2001). Variable neighborhood search: Principles and applications, *European Journal of Operational Research* **130**: 449–467.

Hansen, P., Mladenovic, N. & Pérez, J. A. M. (2008). Variable neighborhood search, *European Journal of Operational Research* **191**: 593–595.

Hasancebi, O. (2007). Discrete approaches in evolution strategies based optimum design of steel frames, *Structural Engineering and Mechanics* **26**(2): 191–210.

Herdy, M. (1992). Reproductive isolation as strategy parameter in hierarichally organized evolution strategies, *Parallel Problem Solving from Nature*, Vol. 2, Elsevier, Amsterdam, pp. 207 – 217.

Hernández, L., Baladrón, C., Aguiar, J. M., Carro, B., Sánchez-Esguevillas, A. & Lloret, J. (2014). Artificial neural networks for short-term load

forecasting in microgrids environment, *Energy* **75**: 252 – 264. doi: http://dx.doi.org/10.1016/j.energy.2014.07.065.

Hong, T. (2014). Energy forecasting: Past, present, future, *The International Journal of Applied Forecasting* **32**: 43–48.

Hong, T., Wilson, J. & Xie, J. (2014). Long term probabilistic load forecasting and normalization with hourly information, *Smart Grid, IEEE Transactions on* **5**(1): 456–462.

Hosny, M. I. & Mumford, C. L. (2010). *Parallel Problem Solving from Nature, PPSN XI: 11th International Conference, Kraków, Poland, September 11-15, 2010, Proceedings, Part II*, Springer Berlin Heidelberg, Berlin, Heidelberg, chapter Solving the One-Commodity Pickup and Delivery Problem Using an Adaptive Hybrid VNS/SA Approach, pp. 189–198. doi: 10.1007/978-3-642-15871-1_20.

Huarng, K. (2001). Heuristic models of fuzzy time series for forecasting, *Fuzzy Sets and Systems* **123**(3): 369 – 386.

Hyndman, R. (2014). Better acf and pacf plots, but no optimal linear prediction, *Electronic Journal of Statistics [E]* **8**(2): 2296–2300.

Hyndman, R. J. & Koehler, A. B. (2006). Another look at measures of forecast accuracy, *International Journal of Forecasting* **22**(4): 679 – 688. doi: http://dx.doi.org/10.1016/j.ijforecast.2006.03.001.

Hyndman, R. J., Koehler, A. B., Snyder, R. D. & Grose, S. (2002). A state space framework for automatic forecasting using exponential smoothing methods, *International Journal of Forecasting* **18**(3): 439 – 454. doi: http://dx.doi.org/10.1016/S0169-2070(01)00110-8.

Hyndman, R. & Khandakar, Y. (2008). Automatic time series forecasting: The forecast package for r, *Journal of Statistical Software* **27**(3): 1–22. doi: 10.18637/jss.v027.i03.

Islam, Z. & Gan, T. Y. (2015). Potential combined hydrologic impacts of climate change and el niño southern oscillation to south saskatchewan river basin, *Journal of Hydrology* **523**: 34 – 48. doi: http://dx.doi.org/10.1016/j.jhydrol.2015.01.043.

Javed, F., Arshad, N., Wallin, F., Vassileva, I. & Dahlquist, E. (2012). Forecasting for demand response in smart grids: An analysis on use of anthropologic and structural

data and short term multiple loads forecasting, *Applied Energy* **96**(0): 150 – 160. Smart Grids.

Johnson, D. S., Papadimitriou, C. H. & Yannakakis, M. (1988). How easy is local search?, *Journal of computer and system sciences* **37**(1): 79–100.

Kahrobaee, S., Rajabzadeh, R. A., Soh, L.-K. & Asgarpoor, S. (2014). Multiagent study of smart grid customers with neighborhood electricity trading, *Electric Power Systems Research* pp. 123 – 132. doi: http://dx.doi.org/10.1016/j.epsr.2014.02.013.

Kanchev, H., Lu, D., Francois, B. & Lazarov, V. (2010). Smart monitoring of a microgrid including gas turbines and a dispatched pv-based active generator for energy management and emissions reduction, *Innovative Smart Grid Technologies Conference Europe (ISGT Europe), 2010 IEEE PES*, pp. 1–8. doi: 10.1109/ISGTEUROPE.2010.5638875.

Kashan, A. H., Akbari, A. A. & Ostadi, B. (2015). Grouping evolution strategies: An effective approach for grouping problems, *Applied Mathematical Modelling* **39**(9): 2703 – 2720. doi: http://dx.doi.org/10.1016/j.apm.2014.11.001.

Kempton, W. & Tomić, J. (2005). Vehicle-to-grid power fundamentals: Calculating capacity and net revenue, *Journal of Power Sources* **144**(1): 268 – 279.

Khwaja, A., Naeem, M., Anpalagan, A., Venetsanopoulos, A. & Venkatesh, B. (2015). Improved short-term load forecasting using bagged neural networks, *Electric Power Systems Research* **125**: 109 – 115. doi: http://dx.doi.org/10.1016/j.epsr.2015.03.027.

Kirkpatrick, S. (1984). Optimization by simulated annealing: Quantitative studies, *Journal of statistical physics* **34**(5-6): 975–986.

Koprinska, I., Rana, M. & Agelidis, V. G. (2015). Correlation and instance based feature selection for electricity load forecasting, *Knowledge-Based Systems* **82**: 29 – 40. doi: http://dx.doi.org/10.1016/j.knosys.2015.02.017.

Kou, P., Liang, D., Gao, L. & Lou, J. (2015). Probabilistic electricity price forecasting with variational heteroscedastic gaussian process and active learning, *Energy Conversion and Management* **89**(0): 298 – 308. doi: http://dx.doi.org/10.1016/j.enconman.2014.10.003.

Krzysztofowicz, R. (1999). Bayesian theory of probabilistic forecasting via deterministic hydrologic model, *Water Resources Research* **35**(9): 2739–2750. doi: 10.1029/1999WR900099.

Lahouar, A. & Slama, J. B. H. (2015). Day-ahead load forecast using random forest and expert input selection, *Energy Conversion and Management* **103**: 1040 – 1051. doi: http://dx.doi.org/10.1016/j.enconman.2015.07.041.

Land, A. H. & Doig, A. G. (1960). An automatic method of solving discrete programming problems, *Econometrica: Journal of the Econometric Society* pp. 497–520.

Ledoit, O. & M., W. (2008). Robust performance hypothesis testing with the sharpe ratio, *Journal of Empirical Finance* **15**(5): 850 – 859. doi: http://dx.doi.org/10.1016/j.jempfin.2008.03.002.

Lee, Y.-S. & Tong, L.-I. (2011). Forecasting energy consumption using a grey model improved by incorporating genetic programming, *Energy Conversion and Management* **52**(1): 147 – 152. doi: 10.1016/j.enconman.2010.06.053.

Lee, Y.-S. & Tong, L.-I. (2012). Forecasting nonlinear time series of energy consumption using a hybrid dynamic model, *Applied Energy* **94**(0): 251 – 256. doi: 10.1016/j.apenergy.2012.01.063.

Levron, Y., Guerrero, J. & Beck, Y. (2013). Optimal power flow in microgrids with energy storage, *Power Systems, IEEE Transactions on* **28**(3): 3226–3234.

Li, J., Pardalos, P. M., Sun, H., Pei, J. & Zhang, Y. (2015). Iterated local search embedded adaptive neighborhood selection approach for the multi-depot vehicle routing problem with simultaneous deliveries and pickups, *Expert Systems with Applications* **42**(7): 3551 – 3561. doi: http://dx.doi.org/10.1016/j.eswa.2014.12.004.

Li, R., Emmerich, M. T. M., Eggermont, J., Bäck, T., Schütz, M., Dijkstra, J. & Reiber, J. H. C. (2013). Mixed integer evolution strategies for parameter optimization, *Evolutionary Computing* **21**(1): 29–64. doi: 10.1162/EVCO_a_00059.

Li, Y., El Gabaly, F., Ferguson, T. R., Smith, R. B., Bartelt, N. C., Sugar, J. D., Fenton, K. R., Cogswell, D. A., Kilcoyne, A. L. D., Tyliszczak, T., Bazant, M. Z. & Chueh, W. C. (2014). Current-induced transition from particle-by-particle to concurrent intercalation in phase-separating battery electrodes, *Nat Mater* **13**(12): 1149–1156. doi: http://dx.doi.org/10.1038/nmat4084.

Lidula, N. & Rajapakse, A. (2011). Microgrids research: A review of experimental microgrids and test systems, *Renewable and Sustainable Energy Reviews* **15**(1): 186 – 202. doi: http://dx.doi.org/10.1016/j.rser.2010.09.041.

Lin, C.-C., Yang, C.-H. & Shyua, J. Z. (2013). A comparison of innovation policy in the smart grid industry across the pacific: China and the {USA}, *Energy Policy* **57**(0): 119 – 132. doi: http://dx.doi.org/10.1016/j.enpol.2012.12.028.

Liu, N., Tang, Q., Zhang, J., Fan, W. & Liu, J. (2014). A hybrid forecasting model with parameter optimization for short-term load forecasting of micro-grids, *Applied Energy* **129**(0): 336 – 345.

Logenthiran, T., Srinivasan, D. & Wong, D. (2008). Multi-agent coordination for DER in microgrid, *Sustainable Energy Technologies, 2008. ICSET 2008. IEEE International Conference on*, pp. 77–82. doi: 10.1109/ICSET.2008.4746976.

Lourenço, H. R., Martin, O. C. & Stützle, T. (2003). Iterated local search, *in* F. Glover & G. Kochenberger (eds), *Handbook of Metaheuristics*, Kluwer Academic Publishers, Boston.

Lust, T. & Teghem, J. (2010). Two-phase pareto local search for the biobjective traveling salesman problem, *Journal of Heuristics* **16**: 475–510.

Lust, T., Teghem, J. & Tuyttens, D. (2011). Very large-scale neighborhood search for solving multiobjective combinatorial optimization problems, *in* R. Takahashi, K. Deb, E. Wanner & S. Greco (eds), *Evolutionary Multi-Criterion Optimization*, Vol. 6576 of *Lecture Notes in Computer Science*, Springer Berlin / Heidelberg, pp. 254–268.

Lutzenberger, J. A. (1980). *Fim do Futuro? Manifesto Ecológico Brasileiro*, 5, Editora Movimento, São Paulo.

Macedo, L. H., Franco, J. F., Rider, M. J. & Romero, R. (2014). Operação ótima de sistemas de armazenamento de energia em smart grids com fontes renováveis, *Anais do XX Congresso Brasileiro de Automática*, Belo Horizonte/MG.

Mahmood, A., Javaid, N., Zafar, A., Riaz, R. A., Ahmed, S. & Razzaq, S. (2014). Pakistan's overall energy potential assessment, comparison of lng, TAPI and IPI gas projects, *Renewable and Sustainable Energy Reviews* **31**(0): 182 – 193. doi: http://dx.doi.org/10.1016/j.rser.2013.11.047.

Makridakis, S. (1993). Accuracy measures: theoretical and practical concerns, *International Journal of Forecasting* **9**(4): 527 – 529. doi: http://dx.doi.org/10.1016/0169-2070(93)90079-3.

Manchester, S. C., Swan, L. G. & Groulx, D. (2015). Regenerative air energy storage for remote wind-diesel micro-grid communities, *Applied Energy* **137**(0): 490 – 500. doi: http://dx.doi.org/10.1016/j.apenergy.2014.06.070.

Mastorocostas, P., Theocharis, J. & Bakirtzis, A. (1999). Fuzzy modeling for short term load forecasting using the orthogonal least squares method, *Power Systems, IEEE Transactions on* **14**(1): 29–36. doi: 10.1109/59.744480.

McHenry, M. P. (2013). Technical and governance considerations for advanced metering infrastructure/smart meters: Technology, security, uncertainty, costs, benefits, and risks, *Energy Policy* **59**: 834 – 842. doi: http://dx.doi.org/10.1016/j.enpol.2013.04.048.

Mladenovic, N. & Hansen, P. (1997). A variable neighborhood search, *Computers and Operations Research* **24**: 1097–1100.

Mohammadi, S., Soleymani, S. & Mozafari, B. (2014). Scenario-based stochastic operation management of microgrid including wind, photovoltaic, micro-turbine, fuel cell and energy storage devices, *International Journal of Electrical Power & Energy Systems* **54**(0): 525 – 535. doi: http://dx.doi.org/10.1016/j.ijepes.2013.08.004.

Monacchi, A., Egarter, D., Elmenreich, W., D'Alessandro, S. & Tonello, A. M. (2014). Greend: An energy consumption dataset of households in italy and austria, *arXiv preprint arXiv:1405.3100* .

Monache, L. D. & Alessandrini, S. (2014). Chapter 12 - probabilistic wind and solar power predictions, *in* L. E. Jones (ed.), *Renewable Energy Integration*, Academic Press, Boston, pp. 149 – 158. doi: http://dx.doi.org/10.1016/B978-0-12-407910-6.00012-0.

Monteiro, C., Ramirez-Rosado, I. J. & Fernandez-Jimenez, L. A. (2013). Short-term forecasting model for electric power production of small-hydro power plants, *Renewable Energy* **50**: 387 – 394. doi: http://dx.doi.org/10.1016/j.renene.2012.06.061.

Muche, T. (2014). Optimal operation and forecasting policy for pump storage plants in day-ahead markets, *Applied Energy* **113**: 1089 – 1099. doi: http://dx.doi.org/10.1016/j.apenergy.2013.08.049.

Mwasilu, F., Justo, J. J., Kim, E.-K., Do, T. D. & Jung, J.-W. (2014). Electric vehicles and smart grid interaction: A review on vehicle to grid and renewable energy sources integration, *Renewable and Sustainable Energy Reviews* **34**: 501 – 516. doi: http://dx.doi.org/10.1016/j.rser.2014.03.031.

Nastos, P., Moustris, K., Larissi, I. & Paliatsos, A. (2013). Rain intensity forecast using artificial neural networks in athens, greece, *Atmospheric Research* **119**: 153 – 160. doi: http://dx.doi.org/10.1016/j.atmosres.2011.07.020.

Nguyen, C. & Flueck, A. (2012). Agent based restoration with distributed energy storage support in smart grids, *Smart Grid, IEEE Transactions on* **3**(2): 1029–1038. doi: 10.1109/TSG.2012.2186833.

Olivares, D., Mehrizi-Sani, A., Etemadi, A., Canizares, C., Iravani, R., Kazerani, M., Hajimiragha, A., Gomis-Bellmunt, O., Saeedifard, M., Palma-Behnke, R., Jimenez-Estevez, G. & Hatziargyriou, N. (2014a). Trends in microgrid control, *Smart Grid, IEEE Transactions on* **5**(4): 1905–1919. doi: 10.1109/TSG.2013.2295514.

Olivares, D., Mehrizi-Sani, A., Etemadi, A., Canizares, C., Iravani, R., Kazerani, M., Hajimiragha, A., Gomis-Bellmunt, O., Saeedifard, M., Palma-Behnke, R., Jimenez-Estevez, G. & Hatziargyriou, N. (2014b). Trends in microgrid control, *Smart Grid, IEEE Transactions on* **5**(4): 1905–1919. doi: 10.1109/TSG.2013.2295514.

Pahl-Wostl, C., Tábara, D., Bouwen, R., Craps, M., Dewulf, A., Mostert, E., Ridder, D. & Taillieu, T. (2008). The importance of social learning and culture for sustainable water management, *Ecological Economics* **64**(3): 484 – 495. doi: http://dx.doi.org/10.1016/j.ecolecon.2007.08.007.

Pao, H.-T. & Fu, H.-C. (2013). Renewable energy, non-renewable energy and economic growth in brazil, *Renewable and Sustainable Energy Reviews* **25**(0): 381 – 392. doi: http://dx.doi.org/10.1016/j.rser.2013.05.004.

Papadopoulos, P., Skarvelis-Kazakos, S., Grau, I., Cipcigan, L. & Jenkins, N. (2012). Electric vehicles' impact on british distribution networks, *Electrical Systems in Transportation, IET* **2**(3): 91–102. doi: 10.1049/iet-est.2011.0023.

Pascual, J., Barricarte, J., Sanchis, P. & Marroyo, L. (2015). Energy management strategy for a renewable-based residential microgrid with generation and demand forecasting, *Applied Energy* **158**: 12 – 25. doi: http://dx.doi.org/10.1016/j.apenergy.2015.08.040.

Pearson, K. (1905). The problem of the random walk, *Nature* **72**(1865): 294.

Pereira Jr., A. O., da Costa, R. C., Costa, C. V., Marreco, J. M. & La Rovere, E. L. (2013). Perspectives for the expansion of new renewable energy sources in brazil, *Renewable and Sustainable Energy Reviews* **23**(0): 49 – 59. doi: http://dx.doi.org/10.1016/j.rser.2013.02.020.

Pereira, M. G., Camacho, C. F., Freitas, M. A. V. & da Silva, N. F. (2012). The renewable energy market in brazil: Current status and potential, *Renewable and Sustainable Energy Reviews* **16**(6): 3786 – 3802. doi: http://dx.doi.org/10.1016/j.rser.2012.03.024.

Pisinger, D. & Ropke, S. (2010). Large neighborhood search, *Handbook of metaheuristics*, Springer, pp. 399–419.

Prado, R. S., Silva, R. C. P., Neto, O. M., aes, F. G. G., Sanches, D. S., ao Bosco A. London Jr., J. & Delbem, A. C. (2014). Differential evolution using ancestor tree for service restoration in power distribution systems, *Applied Soft Computing* **23**: 498 – 508. doi: http://dx.doi.org/10.1016/j.asoc.2014.06.005.

Qaurooni, D. & Akbarzadeh-T, M.-R. (2013). Course timetabling using evolutionary operators, *Applied Soft Computing* **13**(5): 2504 – 2514.

Rabadi, G., Moraga, R. J. & Al-Salem, A. (2006). Heuristics for the unrelated parallel machine scheduling problem with setup times, *Journal of Intelligent Manufacturing* **17**(1): 85–97.

Rajasekaran, S. (2006). Optimal mix for high performance concrete by evolution strategies combined with neural networks, *Indian Journal of Engineering and Materials Sciences* **13**(11): 7–17.

Raza, M. Q. & Khosravi, A. (2015). A review on artificial intelligence based load demand forecasting techniques for smart grid and buildings, *Renewable and Sustainable Energy Reviews* **50**: 1352 – 1372. doi: http://dx.doi.org/10.1016/j.rser.2015.04.065.

Reis, A. & Alves da Silva, A. (2005). Feature extraction via multiresolution analysis for short-term load forecasting, *Power Systems, IEEE Transactions on* **20**(1): 189–198.

Resende, M. G. C. & Ribeiro, C. C. (2010). Greedy randomized adaptive search procedures: Advances, hybridizations, and applications, *in* M. Gendreau & J. Potvin (eds), *Handbook of Metaheuristics*, 2 edn, Springer, New York, pp. 283–319.

Ribeiro, C. C. & Resende, M. G. C. (2011). Path-relinking intensification methods for stochastic local search algorithms, *Journal of Heuristics* pp. 1–22.

Ribeiro, C. C. & Rosseti, I. (2009). Exploiting run time distributions to compare sequential and parallel stochastic local search algorithms, *Proceedings of the VIII Metaheuristics International Conference*, Hamburg.

Ribeiro, P. F., Johnson, B. K., Crow, M. L., Arsoy, A. & Liu, Y. (2001). Energy storage systems for advanced power applications, *Proceedings of the IEEE* **89**(12): 1744–1756.

Rigo-Mariani, R., Sareni, B., Roboam, X. & Turpin, C. (2014). Optimal power dispatching strategies in smart-microgrids with storage, *Renewable and Sustainable Energy Reviews* **40**(0): 649 – 658. doi: http://dx.doi.org/10.1016/j.rser.2014.07.138.

Rogers, A., Ramchurn, S. D. & Jennings, N. R. (2012). Challenges for autonomous agents and multi-agent systems research, *Twenty-Sixth AAAI Conference on Artificial Intelligence (AAAI-12)*, Toronto, CA, pp. 2166–2172.

Romo, R. & Micheloud, O. (2015). Power quality of actual grids with plug-in electric vehicles in presence of renewables and micro-grids, *Renewable and Sustainable Energy Reviews* **46**(0): 189 – 200. doi: http://dx.doi.org/10.1016/j.rser.2015.02.014.

Saber, A. Y. & Venayagamoorthy, G. K. (2010). Intelligent unit commitment with vehicle-to-grid – a cost-emission optimization, *Journal of Power Sources* **195**(3): 898 – 911.

Saeys, Y., Inza, I. n. & Larrañaga, P. (2007). A review of feature selection techniques in bioinformatics, *Bioinformatics* **23**(19): 2507–2517. doi: 10.1093/bioinformatics/btm344.

Sathicq, M. B., Bauer, D. E. & Gómez, N. (2015). Influence of el niño southern oscillation phenomenon on coastal phytoplankton in a mixohaline ecosystem on the southeastern of south america: Río de la plata estuary, *Marine Pollution Bulletin* **98**(1-2): 26 – 33. doi: http://dx.doi.org/10.1016/j.marpolbul.2015.07.017.

Savage, L. J. (1971). Elicitation of personal probabilities and expectations, *Journal of the American Statistical Association* **66**(336): pp. 783–801.
URL: *http://www.jstor.org/stable/2284229*

Schneider, M., Stenger, A. & Hof, J. (2014). An adaptive vns algorithm for vehicle routing problems with intermediate stops, *OR Spectrum* **37**(2): 353–387. doi: 10.1007/s00291-014-0376-5.

Selakov, A., Cvijetinović, D., Milović, L., Mellon, S. & Bekut, D. (2014). Hybrid pso-svm method for short-term load forecasting during periods with significant temperature variations in city of burbank, *Applied Soft Computing* **16**: 80 – 88. doi: http://dx.doi.org/10.1016/j.asoc.2013.12.001.

Shapiro, S. S. & Wilk, M. B. (1964). *An analysis of variance test for normality(complete samples)*., PhD thesis, JSTOR.

Sharpe, W. F. (1994). The sharpe ratio, *The Journal of Portfolio Management* **21**(1): 49 – 58. doi: http://10.3905/jpm.1994.409501.

Solomon, S., Plattner, G.-K., Knutti, R. & Friedlingstein, P. (2009). Irreversible climate change due to carbon dioxide emissions, *Proceedings of the national academy of sciences* **106**(6): 1704–1709.

Song, Q. & Chissom, B. S. (1993). Fuzzy time series and its models, *Fuzzy Sets and Systems* **54**(3): 269 – 277. doi: http://dx.doi.org/10.1016/0165-0114(93)90372-O.

Souza, M. J. F., Coelho, I. M., Ribas, S., Santos, H. G. & Merschmann, L. H. C. (2010). A hybrid heuristic algorithm for the open-pit-mining operational planning problem, *European Journal of Operational Research, EJOR* **207**: 1041–1051.

Spiegelhalter, D. J. (2014). The future lies in uncertainty, *Science* **345**(6194): 264–265. doi: 10.1126/science.1251122.
URL: *http://www.sciencemag.org/content/345/6194/264.short*

Stadler, M., Cardoso, G., Mashayekh, S., Forget, T., DeForest, N., Agarwal, A. & Schonbein, A. (2016). Value streams in microgrids: A literature review, *Applied Energy* **162**: 980 – 989. doi: http://dx.doi.org/10.1016/j.apenergy.2015.10.081.

Sun, Z.-C., Chen, T.-H., Lian, K.-L., Kuo, C.-C., Cheng, I.-T., Chang, Y.-R. & Ho, Y.-H. (2013). Study on load forecasting of an actual micro-grid system in taiwan, *Industrial Electronics (ISIE), 2013 IEEE International Symposium on*, pp. 1–7.

Tabrizi, A. B., Whale, J., Lyons, T. & Urmee, T. (2015). Rooftop wind monitoring campaigns for small wind turbine applications: Effect of sampling rate and averaging period, *Renewable Energy* **77**: 320 – 330. doi: http://dx.doi.org/10.1016/j.renene.2014.12.037.

Tan, X., Li, Q. & Wang, H. (2013). Advances and trends of energy storage technology in microgrid, *International Journal of Electrical Power & Energy Systems* **44**(1): 179 – 191. doi: http://dx.doi.org/10.1016/j.ijepes.2012.07.015.

Tascikaraoglu, A. & Sanandaji, B. M. (2016). Short-term residential electric load forecasting: A compressive spatio-temporal approach, *Energy and Buildings* **111**: 380 – 392. doi: http://dx.doi.org/10.1016/j.enbuild.2015.11.068.

Taylor, J. & McSharry, P. (2007). Short-term load forecasting methods: An evaluation based on european data, *Power Systems, IEEE Transactions on* **22**(4): 2213–2219.

Tinador, P. (2008). Superconducting magnetic energy storage; status and perspective, *IEEE/CSC&ESAS European Superconductivity news forum*, number 3.

Tugcu, C. T., Ozturk, I. & Aslan, A. (2012). Renewable and non-renewable energy consumption and economic growth relationship revisited: Evidence from G7 countries, *Energy Economics* **34**(6): 1942 – 1950. doi: http://dx.doi.org/10.1016/j.eneco.2012.08.021.

Vallada, E. & Ruiz, R. (2011). A genetic algorithm for the unrelated parallel machine scheduling problem with sequence dependent setup times, *European Journal of Operational Research* **211**(3): 612–622.

Venayagamoorthy, G. & Chakravarty, P. (2014). Optimal fuzzy logic based coordination controller for improved transient stability of a smart grid, *Fuzzy Systems (FUZZ-IEEE), 2014 IEEE International Conference on*, pp. 346–353. doi: 10.1109/FUZZ-IEEE.2014.6891824.

Wai, R.-J., Chen, Y.-C. & Chang, Y.-R. (2011). Short-term load forecasting via fuzzy neural network with varied learning rates, *Fuzzy Systems (FUZZ), 2011 IEEE International Conference on*, pp. 2426–2431.

Wang, S., Yu, D. & Yu, J. (2015). A coordinated dispatching strategy for wind power rapid ramp events in power systems with high wind power penetration, *International Journal of Electrical Power & Energy Systems* **64**: 986 – 995. doi: http://dx.doi.org/10.1016/j.ijepes.2014.08.019.

Welsch, M., Bazilian, M., Howells, M., Divan, D., Elzinga, D., Strbac, G., Jones, L., Keane, A., Gielen, D., Balijepalli, V. M., Brew-Hammond, A. & Yumkella, K. (2013). Smart and just grids for sub-saharan africa: Exploring

options, *Renewable and Sustainable Energy Reviews* **20**(0): 336 – 352. doi: http://dx.doi.org/10.1016/j.rser.2012.11.004.

Weron, R. (2014). Electricity price forecasting: A review of the state-of-the-art with a look into the future, *International Journal of Forecasting* **30**(4): 1030 – 1081.

Xenias, D., Axon, C. J., Whitmarsh, L., Connor, P. M., Balta-Ozkan, N. & Spence, A. (2015). UK smart grid development: An expert assessment of the benefits, pitfalls and functions, *Renewable Energy* **81**(0): 89 – 102. doi: http://dx.doi.org/10.1016/j.renene.2015.03.016.

Xiao, Y., Kaku, I., Zhao, Q. & Zhang, R. (2011). A reduced variable neighborhood search algorithm for uncapacitated multilevel lot-sizing problems, *European Journal of Operational Research* **214**(2): 223 – 231. doi: http://dx.doi.org/10.1016/j.ejor.2011.04.015.

Yao, L., Zhang, A.-L. & Yang, H.-J. (2011). Discretion variable optimization design of prestressed steel truss with stress constrains, *Beijing Gongye Daxue Xuebao/Journal of Beijing University of Technology* **37**(3): 368–374.

Ying, K.-C., Lee, Z.-J. & Lin, S.-W. (2012). Makespan minimisation for scheduling unrelated parallel machines with setup times, *Journal of Intelligent Manufacturing* **23**(5): 1795–1803.

Yuan, J., Shen, J., Pan, L., Zhao, C. & Kang, J. (2014). Smart grids in china, *Renewable and Sustainable Energy Reviews* **37**(0): 896 – 906. doi: http://dx.doi.org/10.1016/j.rser.2014.05.051.

Zakeri, B. & Syri, S. (2015). Electrical energy storage systems: A comparative life cycle cost analysis, *Renewable and Sustainable Energy Reviews* **42**(0): 569 – 596. doi: http://dx.doi.org/10.1016/j.rser.2014.10.011.

Zamo, M., Mestre, O., Arbogast, P. & Pannekoucke, O. (2014). A benchmark of statistical regression methods for short-term forecasting of photovoltaic electricity production. part ii: Probabilistic forecast of daily production, *Solar Energy* **105**(0): 804 – 816. doi: http://dx.doi.org/10.1016/j.solener.2014.03.026.

Zhang, X., Huang, S., Hu, Y., Zhang, Y., Mahadevan, S. & Deng, Y. (2013). Solving 0-1 knapsack problems based on amoeboid organism algorithm, *Applied Mathematics and Computation* **219**(19): 9959 – 9970.

Zhang, Y., Wang, J. & Wang, X. (2014). Review on probabilistic forecasting of wind power generation, *Renewable and Sustainable Energy Reviews* **32**(0): 255 – 270. doi: http://dx.doi.org/10.1016/j.rser.2014.01.033.

Zhao, B., Xue, M., Zhang, X., Wang, C. & Zhao, J. (2015). An MAS based energy management system for a stand-alone microgrid at high altitude, *Applied Energy* **143**(0): 251 – 261. doi: http://dx.doi.org/10.1016/j.apenergy.2015.01.016.

Zheng, W.-D. & Cai, J.-D. (2010). A multi-agent system for distributed energy resources control in microgrid, *Critical Infrastructure (CRIS), 2010 5th International Conference on*, pp. 1–5. doi: 10.1109/CRIS.2010.5617485.

Zitzler, E. & Thiele, L. (1998). Multiobjective optimization using evolutionary algorithms - a comparative case study, *in* A. Eiben, T. Back, M. Schoenauer & H.-P. Schwefel (eds), *Parallel Problem Solving from Nature - PPSN V*, Vol. 1498 of *Lecture Notes in Computer Science*, Springer Berlin / Heidelberg, pp. 292–301.

Index